

Chapter 27: Rotational and Vibrational Spectroscopy

Calculate the equilibrium bond length and force constant for H^{35}Cl using infrared absorption.

Light absorption, emission, and scattering are the primary tools for molecular structure determination. Spectroscopically determined structure parameters include equilibrium bond lengths, angles, force constants, and bond dissociation energies. Spectroscopy and molecular structure calculations are complimentary tools for molecular structure determination. Molecular structure methods are compared and validated based on agreement with experimentally determined structure and bond strength measures; for examples see Tables 26.2.1 and 26.4.2. In addition, spectroscopic constants are used for the statistical mechanical calculation of thermodynamic parameters, which include internal energy, enthalpy, entropy, Gibbs energy, and equilibrium constants. For ideal-gas reactions, equilibrium constants are calculated more accurately from spectroscopic constants than possible using concentration measurements in the laboratory. Spectroscopic methods are also important tools for the determination of the concentration and distribution of chemical substances in the atmosphere, surface waters, marine environments, and interstellar space. The use of spectroscopic techniques for molecular structure determination is covered in the next three chapters. A subsequent chapter then discusses the use of spectroscopic constants to determine thermodynamic parameters.

We begin with an overview of spectroscopy, followed by a detailed discussion of rotational and vibrational techniques. A photon is a powerful probe of nature.

27.1 Spectroscopy in General: The Intensity of Spectroscopic Transitions

A spectrum is a plot of the light absorption or emission as a function of wave length, wave number, or frequency. The characteristic features of a light absorption or emission spectrum include the band positions, widths, and intensities. The band positions correspond to transitions between allowed quantum states of the system:

$$\Delta E = h\nu = hc/\lambda = hc\tilde{\nu} \quad \tilde{\nu} = \Delta E/hc \quad \nu = \tilde{\nu}c \quad (8.10.2, 23.2.7) \quad 27.1.1$$

The quantum states can be for rotation alone, for rotation and vibration, or for rotation, vibration, and electronic degrees of freedom (please review Section 2.4). In magnetic resonance spectroscopy, the quantum states involve intrinsic nuclear or electron spin transitions. The transition wave lengths or wave numbers are a “map” of the quantum states of the system. The widths of the transitions are determined by molecular motion and the intrinsic line width, Eq. 23.4.47. The intensity of the transitions is determined by the concentration, the population of the states involved in the transition, and the intrinsic absorption probability. Consider first the intensity a transition.

The absorbance of a sample is proportional to the concentration through the Beer-Lambert Law, Eq. 2.4.8: $A = \epsilon[c]$. The molar absorption coefficient, ϵ , is a function of temperature and a strong function of frequency or wave length, which is explicitly expressed as $\epsilon(\nu)$ or $\epsilon(\lambda)$. The molar absorption coefficient varies from zero to a maximum at the frequency or wave length of maximum absorption, ν_{max} or λ_{max} . The molar absorption coefficient is an intrinsic measure of the ability of a molecule to absorb light, independent of concentration, which is our focus in the following discussion.

Three processes are active in light absorption. Consider a two-level system with the number of molecules in the lower state N_0 at energy ε_0 and the number of molecules in the upper state N_1 at energy ε_1 , Figure 27.7.1. The absorption frequency and emission frequencies are given by $\Delta E = h\nu = \varepsilon_1 - \varepsilon_0$. The absorption of a photon promotes a molecule in the lower state into the upper state by a second-order kinetic process. The rate of absorption is proportional to the number of molecules in the lower state, the **Einstein absorption coefficient** $B_{1\leftarrow 0}$, and the radiation energy density $\rho(\nu)$: rate = $B_{1\leftarrow 0} \rho(\nu) N_0$. The absorption coefficient $B_{1\leftarrow 0}$ is the probability of light absorption per molecule. Analogous to chemical kinetics, $B_{1\leftarrow 0}$ is the rate constant for absorption. The **radiation energy density**, $\rho(\nu)$, plays the role of the concentration of the light energy in a narrow band of frequencies near ν . The radiation energy density is proportional to the square of the electric field strength and has units of joule seconds per unit volume, J s m^{-3} . The upper state loses population through **stimulated emission** and **spontaneous emission**. In stimulated emission, the incident light interacts with the excited molecule and causes the emission of an additional photon, returning the molecule to the lower state. The incident light is not absorbed. The rate of stimulated emission is proportional to the number of molecules in the upper state, the **Einstein stimulated emission coefficient** $B_{1\rightarrow 0}$, and the radiation energy density $\rho(\nu)$: rate = $B_{1\rightarrow 0} \rho(\nu) N_1$. Spontaneous emission occurs in the presence and absence of incident light and depopulates the excited state with the emission of a photon. Fluorescence and phosphorescence are examples of spontaneous emission. The rate of spontaneous emission is inversely proportional to the spontaneous emission lifetime, τ_{sp} . The rate of spontaneous emission is proportional to the number of molecules in the upper state and the **Einstein spontaneous emission coefficient**, $A_{1\rightarrow 0} = 1/\tau_{\text{sp}}$. The net absorption rate is given by the net change in population of the excited state, balancing the three coupled kinetic processes:

$$\frac{dN_1}{dt} = \underbrace{B_{1\leftarrow 0} \rho(\nu) N_0}_{\text{absorption}} - \underbrace{B_{1\rightarrow 0} \rho(\nu) N_1}_{\text{stimulated emission}} - \underbrace{A_{1\rightarrow 0} N_1}_{\text{spontaneous emission}} \quad 27.1.2$$

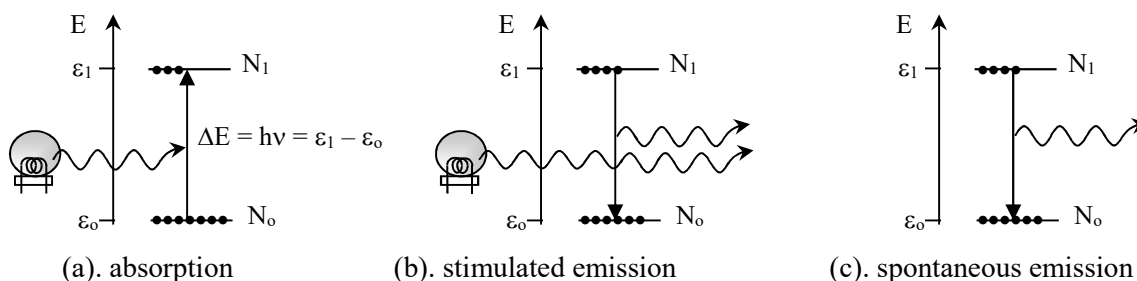


Figure 27.1.1: Light absorption, stimulated emission, and spontaneous emission are first-order kinetic processes. The rate of energy absorption is the net effect of the three processes.

By convention, an absorption transition is given as upper \leftarrow lower, while an emission transition is given as upper \rightarrow lower. We will show in the Section 27.9 that the Einstein coefficients for absorption and stimulated emission are equal: $B_{1\leftarrow 0} = B_{1\rightarrow 0}$. For many experiments the rate of spontaneous emission is small compared to the rate of stimulated emission, giving the net rate of absorption as proportional to the population difference, from Eq. 27.1.2:

$$\text{net rate} = \frac{dN_1}{dt} \cong B_{1 \leftarrow 0} \rho(\nu) [N_0 - N_1] \quad (\text{spontaneous} \ll \text{stimulated}) \quad 27.1.3$$

In other words, light causes transitions in both directions. Absorption and spontaneous emission are always in competition, with the net result determined by the population difference. At equilibrium, the populations are given by the Boltzmann distribution at ambient temperature T . At the start of an experiment, the population is at thermal equilibrium and the absorption intensity is maximal. After the external light source, with sufficient intensity, has been on for a long period, the population of the two-levels equalizes, $N_1 = N_0$. No net absorption results. The state with equal populations and vanishing absorption is said to be **saturated**.

The molar absorption coefficient, $\epsilon(\nu)$ at the absorption frequency ν , is proportional to the rate of energy absorption and correspondingly, the population difference of the initial and final states of the transition, Eq. 27.1.3. The population difference, at equilibrium, is given by the Boltzmann distribution, Eqs. 8.10-4-8.10.8. For convenience, the energy scale is shifted so that the initial level is defined as zero energy and the final state is at energy $\Delta\epsilon = \epsilon_1 - \epsilon_0 = h\nu$:

$$\epsilon(\nu) \propto N_0 - N_1 \propto p_0 - p_1 \propto \frac{N}{q} \left(e^{-0/kT} - e^{-\Delta\epsilon/kT} \right) \propto 1 - e^{-\Delta\epsilon/kT} \quad (\text{equilibrium}) \quad 27.1.4$$

where p_0 and p_1 are the probabilities of occupation of the two levels, N is the total number of molecules, q is the probability-normalization constant (partition function), k is Boltzmann's constant, T is the absolute temperature, and kT is the available thermal kinetic energy per molecule. At room temperature, $kT = 207.2 \text{ cm}^{-1}$ or $RT \cong 2.5 \text{ kJ mol}^{-1}$. Transitions with larger $\Delta\epsilon$ compared to kT have greater intensity. Nuclear magnetic resonance transitions are in the radio-frequency region near 100 MHz or $\sim 0.0033 \text{ cm}^{-1}$. Rotational transitions occur over a broad range in the microwave region near 10 GHz or $\sim 0.33 \text{ cm}^{-1}$. Fundamental vibrational transitions are in the mid- and far-infrared region, 4000-30 cm^{-1} . Electronic transitions are in the UV-visible region, roughly from 900-100 nm, with 300 nm corresponding to 33,000 cm^{-1} . As a consequence the population differences are greatest in the UV-visible and smallest for NMR, Figure 27.1.2. NMR is an insensitive technique requiring high concentrations, typically in the $\sim 0.1 \text{ M}$ range, while typical concentrations for UV-visible spectroscopy are in the 10^{-5} M range.

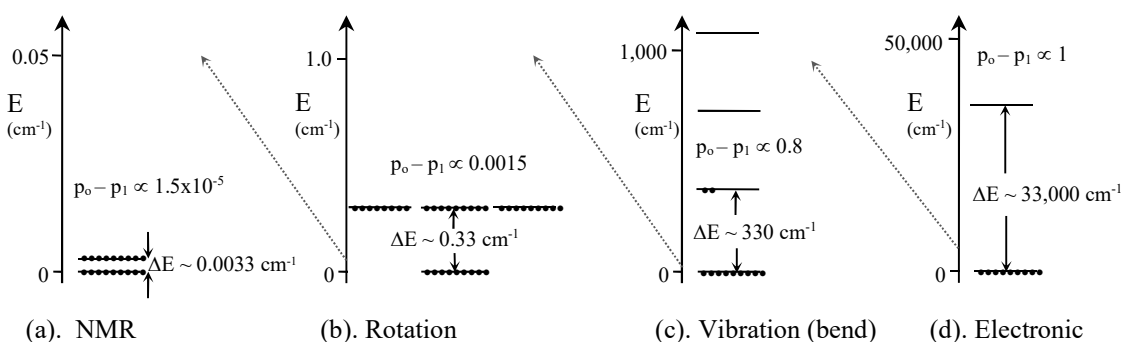


Figure 27.1.2: Spectroscopic transitions with large energy differences have large population differences and give intense absorption bands. Probability differences, $p_0 - p_1$, are given at room temperature, $kT = 207.2 \text{ cm}^{-1}$. The NMR population difference is only 15 in 1 million.

Selection Rules Predict the Occurrence of Transitions: After having accounted for concentration and population differences, the intrinsic probability of photon absorption by a transition between quantum states is related to the ability of a molecule to interact with the electric field of light. The interaction is represented by the $B_{1 \leftarrow 0} \rho(\nu)$ and $B_{1 \rightarrow 0} \rho(\nu)$ factors in Eq. 27.1.2. For the oscillating electric field of light to interact with the molecule, the molecule must present an oscillating electric field resulting from the motion under study. When the frequency of the oscillating electric field of the light is equal to the frequency of the oscillating electric field caused by the molecule, energy can be exchanged between light field and the molecule. Consider the absorption of a photon by a rotating molecule. To present an oscillating electric field upon rotation, a molecule must have a permanent dipole moment. Molecules such as HCl, CO, and CHCl_3 give rotational absorption spectra, while symmetrical molecules such as O_2 , N_2 , and CCl_4 do not. The permanent dipole moment of a molecule is given by the expectation value of the electric **dipole moment operator**:

$$\hat{\mu} = \hat{\mu}_{\text{el}} + \hat{\mu}_{\text{nuclei}} = - \sum_{i=1}^n e \hat{r}_i + \sum_{j=1}^m q_j \hat{r}_j \quad 27.1.5$$

electrons *nuclei*

where the sums are taken over the coordinates of each of the n -electrons, \hat{r}_i , and each of the m -nuclei, \hat{r}_j . The charge on each nucleus j is $q_j = Z_j e$. The permanent dipole moment is then:

$$\langle \hat{\mu} \rangle = \int \Psi_{\text{el}}^* (\hat{\mu}_{\text{el}} + \hat{\mu}_{\text{nuclei}}) \Psi_{\text{el}} d\tau \quad 27.1.6$$

where Ψ_{el} is the electronic wave function of the molecule. The requirement of a dipole moment for rotational absorption spectroscopy is an example of a **selection rule**. Each form of spectroscopy has a corresponding selection rule.

The Transition Dipole Moment Involves the Initial and Final States: The intensity of an absorption or emission transition from the initial state Ψ_i to the final state Ψ_j is proportional to the square of the **transition dipole moment**. The transition dipole moment, μ_{tr} , is:

$$\mu_{\text{tr}} = \langle \hat{\mu} \rangle = \int \Psi_j^* \hat{\mu} \Psi_i d\tau \quad (j \leftarrow i) \quad 27.1.7$$

Using the Born-Oppenheimer approximation, the wave functions are the products of the molecular orbital, vibrational, and rotational wave functions: $\Psi_i = \Psi_{\text{el},i} \Psi_{\text{vib},i} \Psi_{\text{rot},i}$. Specifically for a diatomic molecule, the vibrational wave functions in the harmonic approximation are given by Eq. 24.2.18, $\chi_{\nu}(\mathbf{R}) = N_{\nu} H_{\nu} e^{-1/2 \alpha^2 (\mathbf{R} - \mathbf{R}_0)^2}$. The rotational wave functions in the rigid-rotor approximation are given by the spherical harmonics, $Y_{J,m_j}(\theta, \phi)$, Table 24.5.1, giving:

$$\mu_{\text{tr}} = \langle \hat{\mu} \rangle = \int [\Psi_{\text{el},j} \chi_{\nu'}(\mathbf{R}) Y_{J',m_{j'}}(\theta, \phi)]^* \hat{\mu} \Psi_{\text{el},i} \chi_{\nu''}(\mathbf{R}) Y_{J'',m_{j''}}(\theta, \phi) d\tau \quad 27.1.8$$

where the initial quantum numbers for vibration and rotation are ν'' and J'' and the final quantum numbers are ν' and J' . Transitions with a non-zero transition dipole moment are called **allowed** transitions. A vanishing transition dipole moment gives a **forbidden** transition. Selection rules allow us to determine if the transition dipole moment is non-zero.

For rotational spectroscopy, the initial and final electronic and vibrational states are identical, $\Psi_{\text{el},j} = \Psi_{\text{el},i}$ and $\nu' = \nu''$. The requirement of a non-vanishing transition dipole moment reduces to the restriction of a non-zero permanent dipole moment, Eq. 27.1.6. The selection rule based on the presentation of an oscillating electric field is called the **gross** selection rule. Eq. 27.1.7 also

gives rise to **specific** selection rules, which are based on the conservation of angular momentum. Photons carry unit angular momentum with projection $m_S = \pm 1$. To conserve angular momentum upon absorption of a photon, the angular momentum of the molecule must change in compensation. The specific selection rule for rotational spectroscopy is $\Delta J = \pm 1$. Different forms of spectroscopy have different selection rules.

For vibrational spectroscopy, the initial and final electronic states are identical, $\Psi_{el,j} = \Psi_{el,i}$. For a diatomic molecule, the integral in Eq. 27.1.7 involves integration over the internuclear distance, R . However, the electronic and vibrational wave functions both depend on the internuclear separation. To complete the integral, we expand the dipole moment in a power series around the equilibrium internuclear bond length, R_e :

$$\vec{\mu} = \vec{\mu}(R_e) + \left. \frac{d\vec{\mu}}{dR} \right|_{R_e} (R - R_e) + \frac{1}{2} \left. \frac{d^2\vec{\mu}}{dR^2} \right|_{R_e} (R - R_e)^2 + \dots \quad (\text{vibration, diatomic}) \quad 27.1.9$$

The derivatives are evaluated at the equilibrium internuclear distance. The first term is the dipole moment at the equilibrium internuclear positions. The transition dipole moment then separates into a corresponding series of terms:

$$\vec{\mu}_{tr} = \vec{\mu}(R_e) \int \chi_{v'} \chi_{v''} dR + \left. \frac{d\vec{\mu}}{dR} \right|_{R_e} \int \chi_{v'} (R - R_e) \chi_{v''} dR + \dots \quad (\text{vibration, diatomic}) \quad 27.1.10$$

The first term is zero because the vibrational wave functions are orthogonal. The first derivative of $\vec{\mu}$ gives the dominant contribution to the transition intensity. The final result is that for absorption of a photon the dipole moment of the molecule must change with changing internuclear separation:

$$\left. \frac{d\vec{\mu}}{dR} \right|_{R_e} \neq 0 \quad (\text{vibration, dipole allowed}) \quad 27.1.11$$

Vibrational absorption-transitions occur in the infrared region of the spectrum. Homonuclear diatomics, such as O_2 , N_2 , and Cl_2 , cannot have a changing dipole moment and are transparent in the infrared. Heteronuclear diatomics, such as CO and NO , have a dipole allowed stretching transition and are correspondingly **IR-active**, allowed. In polyatomic molecules, some vibration normal modes fulfill the gross selection rule and some do not. For polyatomics, the R in Eqs. 27.1.9-27.1.11 is replaced by the progress of the normal mode, Eq. 8.11.32. For symmetric, linear triatomics, such as CO_2 , the asymmetric stretch and the two degenerate bends have a changing dipole moment and are IR-active. However, the symmetric stretch of symmetrical linear molecules is **IR-inactive**, forbidden, Figure 27.1.3a. The albedo of the earth is increased by the absorption and reemission of infrared light by the asymmetric stretch and bending vibrations of CO_2 in the atmosphere. For bent triatomics, all normal modes are infrared active, Figure 27.1.3b. Water is also a greenhouse gas.

Evaluation of the integral $\int \chi_{v'} (R - R_e) \chi_{v''} dR$, in Eq. 27.1.10, gives that for purely harmonic potentials only transitions between adjacent vibrational levels are allowed, $\Delta v = \pm 1$. As for the specific selection rule, most molecules have singlet ground states with no net angular momentum, for which the rule remains the same as for rotational spectroscopy, $\Delta J = \pm 1$. In other words, to conserve angular momentum the rotational state must change along with the vibrational state. For molecules with a coupled state that has net angular momentum, e.g. ${}^2\Pi$, the specific selection rule is $\Delta J = 0, \pm 1$.

For electronic spectroscopy, the transition dipole moment requires that the dipole moment of the molecule must change in the electronic transition between the initial state i and the final state f . For electronic spectra the transition dipole moment places no restrictions on the vibrational or rotational transitions, except that the specific selection rule requires the conservation of angular momentum. For a common case of transitions between singlet electronic states with no net orbital angular momentum, $\Delta J = \pm 1$. For transitions that involve non-zero total angular momentum, then $\Delta J = 0, \pm 1$. We investigate electronic spectroscopy in detail in the next chapter.

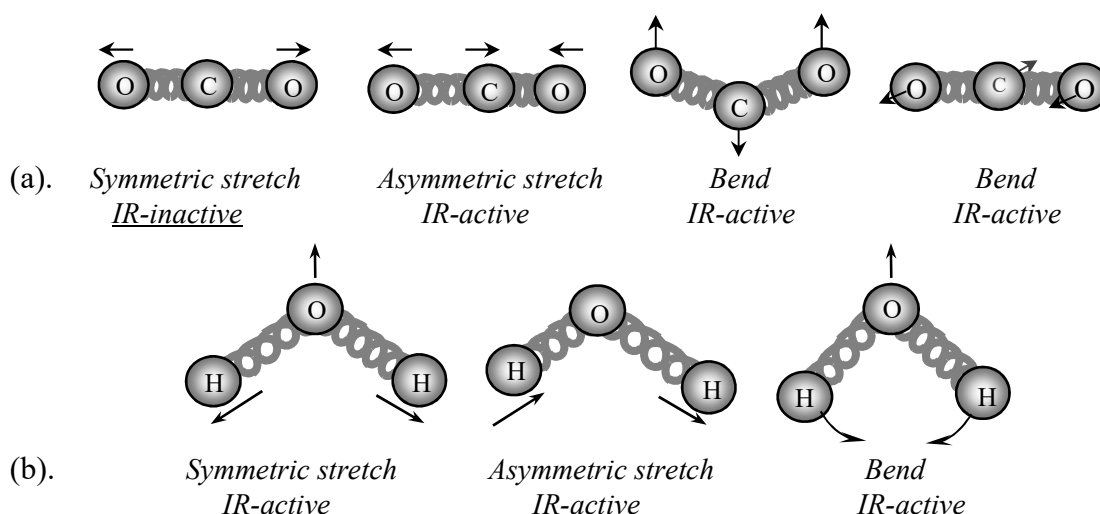


Figure 27.1.3: The gross selection rule for vibrational absorption is a changing dipole moment with internuclear separation. (a). The symmetric stretch for CO_2 is IR-inactive. (b). All normal modes of bent triatomics are IR-active; for example H_2O , SO_2 , and NO_2 .

In summary, the presence or absence of spectroscopic transitions is a probe of molecular symmetry. On the other hand, the width of spectroscopic transitions is a sensitive probe of molecular motion.

27.2 The Width of Spectroscopic Transitions

Intrinsic Lifetime Broadening is Determined from the Heisenberg Uncertainty: Intrinsic lifetime broadening is always active in spectroscopic transitions, Eqs. 23.4.45-23.4.48. The lifetime of the stationary state of the molecule is determined by the interaction of the isolated molecule with the surrounding light field. The shorter the lifetime, the broader the transition, as dictated by the Heisenberg Uncertainty Principle, $\delta E \delta t \geq \hbar/2$. However, broadening caused by molecular motion usually dominates the line width.

Motion Contributes to the Width of Spectral Transitions: In low pressure gases, the **Doppler effect** is the principal broadening mechanism. The Doppler effect is familiar as the change in pitch of a train whistle upon passing the listener, Figure 27.2.1. As a train approaches, the sound waves reach the listener with higher frequency and the pitch is higher than the stationary source. Each successive portion of the wave is produced closer to the listener and requires less time to reach the listener, compared to previous portions of the wave. As the train recedes, the sound

waves reach the listener with lower frequency and the pitch is lower. The shift in frequency is determined by the ratio of the source velocity, v_{source} , to the wave propagation velocity, v :

$$v_{\text{obs}} = (1 \pm v_{\text{source}}/v) v_0 \quad (+ \text{ for approaching, } - \text{ for receding}) \quad 27.2.1$$

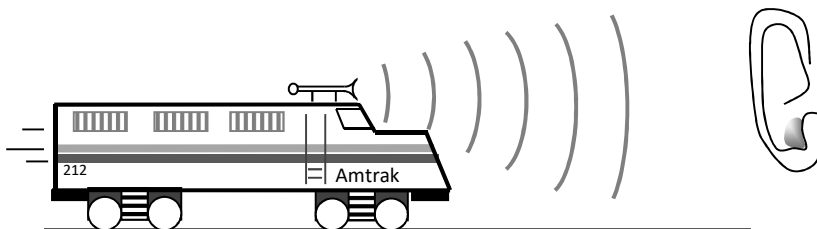


Figure 27.2.1: A sound source moving towards the observer has a higher pitch than the stationary source.

In a gas, the molecules move with a distribution of molecular velocities. The observed line-width is the average over the motions of the molecules along the direction of wave propagation. The direction of propagation is assigned to the x-direction for convenience. The appropriate average is the root-mean-square speed in the x-direction, $\bar{v}_{x,\text{rms}}$. The rms speed and the full-width at half-maximum of a transition caused by the Doppler effect, Δv_D , are:

$$\bar{v}_{x,\text{rms}} = \sqrt{\frac{kT}{m}} \quad \Delta v_D = 2 \left(\frac{v_0}{c} \right) \sqrt{\frac{2kT \ln(2)}{m}} \quad 27.2.2$$

where v_0 is the frequency of the stationary source, c is the speed of light, T is the absolute temperature, and m is the molecular mass in kg molecule^{-1} . High temperatures increase spectral broadening.

Exercise 27.2.1: Doppler Broadening

Calculate the Doppler line width of the vibrational transition of CO_2 for the asymmetric stretch at 2565 cm^{-1} at room temperature.

Answer: The mass of CO_2 is $m = (44.0 \text{ g mol}^{-1}/N_A)(1 \text{ kg}/1000 \text{ g}) = 7.307 \times 10^{-26} \text{ kg}$. The line width from Eq. 27.2.2 is converted to cm^{-1} with $\tilde{\nu} = \nu/c$. The square-root factor is proportional to the rms speed in m s^{-1} so the units of c in Eq. 27.2.2 are in m s^{-1} :

$$\begin{aligned} \Delta \tilde{\nu}_D &= 2 \left(\frac{\tilde{\nu}_0}{c} \right) \sqrt{\frac{2kT \ln(2)}{m}} = 2 \left(\frac{2565 \text{ cm}^{-1}}{2.998 \times 10^8 \text{ m s}^{-1}} \right) \sqrt{\frac{2(1.381 \times 10^{-23} \text{ J K}^{-1})(298.2 \text{ K}) \ln(2)}{7.307 \times 10^{-26} \text{ kg}}} \\ &= 0.00478 \text{ cm}^{-1} \end{aligned}$$

Doppler broadening is a limiting factor for very high resolution rotational and vibrational spectroscopy, but not normal laboratory applications. Several techniques have been developed to acquire spectra with minimal Doppler broadening.

For medium and high pressure gases and for liquids, molecular collisions are the principal broadening mechanism. Collisions shorten the lifetime of the excited state. The relationship of transition width to the excited state lifetime is once again governed by the Heisenberg Uncertainty Principle, $\delta E \delta t \geq \hbar/2$. The higher the pressure of a gas, the more frequent the collisions, the shorter the lifetime of the states, and the broader the transition. Assuming a gas-phase two-state system, the full width at half maximum for the transition is approximately $\Delta\nu_C = 1/(\pi T_2)$, where T_2 is the average time between collisions. The average time between collisions is inversely proportional to the pressure, P , giving the transition width caused by collisions as:

$$\Delta\nu_C \cong b P \quad \text{(two-states) } 27.2.3$$

where b is the pressure-broadening coefficient, which is often roughly approximated as 10 MHz torr⁻¹ or equivalently 0.25 cm⁻¹ bar⁻¹. In other words, working at ambient pressure limits the spectroscopic resolution to about 1/4-wave number. Because collisions in liquids and solutions are much more frequent than gases, transitions in liquids and solutions are much broader than the gas phase. As a consequence most high resolution spectroscopic structure determination is done with low pressure gases. High resolution spectroscopy is also commonly based on Fourier transform techniques, rather than instruments with a scanned grating or a scanned frequency source. Fourier methods are generally the most efficient means of acquiring high resolution spectra.

27.3 Fourier Transform Methods

Fourier Transform Based Spectroscopy Gives a Multiplex Advantage: Single detector spectrophotometers that generate spectra by rotating a grating or moving a slit are potentially high resolution, but the scanning process is usually quite slow, Figure 2.4.1. Instead, a Fourier transform based method is usually used to acquire spectra, typically in less time than is possible in high resolution scanning instruments. Fourier transform, **FT**, instruments maintain high resolution and have excellent absolute wave number and frequency accuracy. The speed of FT based instruments allows multiple spectra to be averaged to improve the signal-to-noise ratio. The signal-to-noise ratio in a spectrum improves as the square root of the number of scans that are averaged: $s/n \propto \sqrt{N_{\text{scans}}}$. The time advantage results because FT methods acquire data on all frequency components in the spectrum simultaneously, instead of one frequency at a time. This favorable attribute is called the **multiplex advantage**. Instruments based on mechanically scanning a monochromator or frequency source are called **continuous wave**, or **cw**, instruments. FT methods are used in pulsed and interferometer based instruments. Pulsed FT-measurements are used in NMR, ESR, microwave, and ultra-fast IR and UV/Visible spectroscopy. Interferometer based instruments are widely used in infrared, Raman, and UV/Visible measurements. To simplify our discussion, we first discuss pulsed spectroscopy.

Pulsed measurements can be easily demonstrated. Simply bang your fist on the table at which you are sitting (not that you have ever thought of doing so while studying PChem). The response of the table is to ring and buzz; the response contains all the component resonant frequencies of the parts of the table and anything lying on the table. Your ear converts the sound waves into signals to your brain that give the pitch and amplitude of all the frequency components of the sound. You hear all the resonant frequencies of the table simultaneously. Fourier transforms allow absorption and emission measurements to emulate the same process. Joseph Fourier (1768-1830) proved that any function of time, $f(t)$, can be approximated arbitrarily well by a series of cosines and sines of a range of frequencies.

We first consider a periodic function. The lowest possible frequency component of a periodic function is $\nu_0 = 1/L$, where L is the period, Figure 27.3.1a. The function is then decomposed as a Fourier series with frequency components that are integer multiples of the lowest frequency ν_0 :

$$f(t) = \sum_{n=0}^{\infty} A_n \cos(2\pi n\nu_0 t) + \sum_{n=0}^{\infty} B_n \sin(2\pi n\nu_0 t) \quad \nu_0 = 1/L \quad 27.3.1$$

The amount or amplitude of each frequency component, $n\nu_0$, is given by the **Fourier coefficients**, A_n and B_n . The cosine terms are used for functions that have large amplitude at time zero, and the sine terms are used for functions that have zero amplitude at time zero. The Fourier coefficients are calculated as integrals over one period of the function:

$$A_n = 2 \int_0^L f(t) \cos(2\pi n\nu_0 t) dt \quad B_n = 2 \int_0^L f(t) \sin(2\pi n\nu_0 t) dt \quad 27.3.2$$

An example function $f(t)$ with period L is shown at the bottom of Figure 27.3.1a. The function is a possible combination of three different frequency components at 1, 2, and 3 kHz. The **spectrum** of the function corresponds to the plot of the Fourier coefficients as a function of the frequency. The spectra of several examples are shown in Figure 27.3.1b as histograms. In laboratory applications, the frequency components are closely spaced and so numerous that the corresponding spectrum is drawn as a series of points that are connected by a smooth curve; you don't normally notice that the spectrum is not continuous. In our example, we only have three possible frequencies, but in NMR the number of frequencies is often 16,384 or as many as 65,536, so the spectrum appears as a smooth curve.

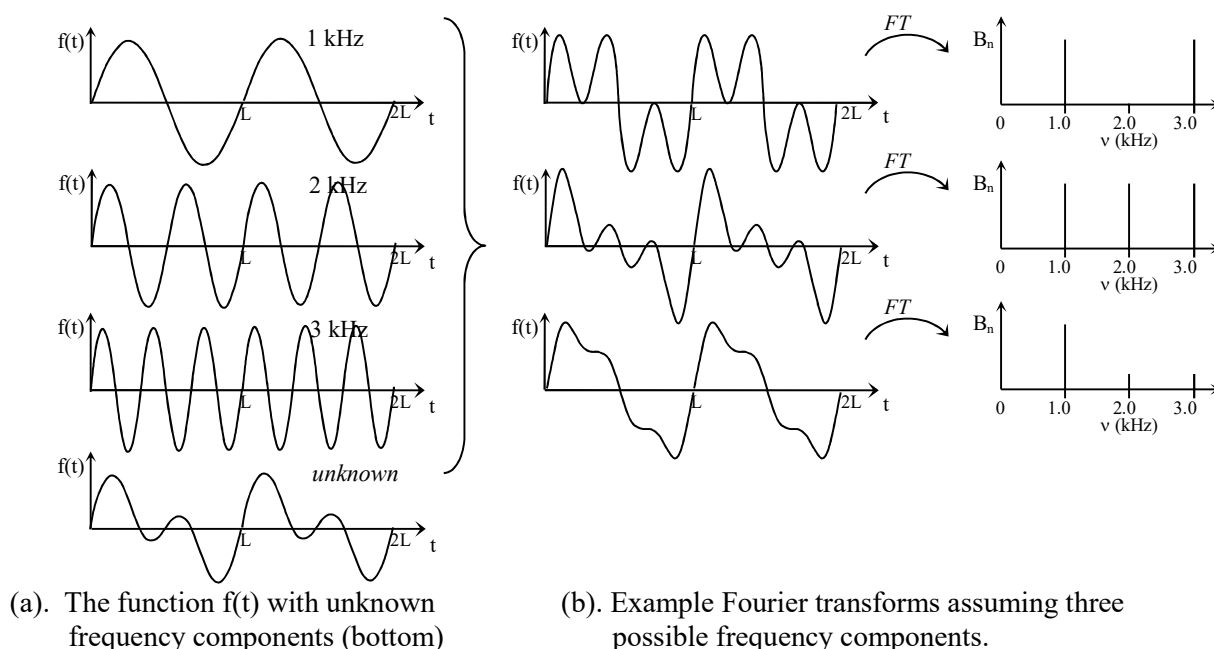


Figure 27.3.1: An arbitrary function can be decomposed into a sum of sine and cosine waves. (a). The function $f(t)$ is a sum of possible components at 1, 2, and 3 kHz. (b). Example Fourier transforms of three component frequencies. A typical NMR spectrum has 16,384 possible component frequencies, which taken together are shown as a continuous plot, instead of a histogram.

FT techniques are so important that we should carefully discuss how Eqs. 27.3.2 work. Consider the unknown example function $f(t)$ at the bottom of Figure 27.3.1a; what are the component frequencies and amplitudes? The unknown function and the three possible component frequencies are superimposed in Figure 27.3.2a. Since the function begins at zero amplitude, only sine-transform terms are needed. Next $f(t)$ and each possible sine wave are multiplied together, point-by-point across the time interval of one period, Figure 27.3.2b. The Fourier coefficients are the integrals of the product across one period of the function, Figure 27.3.2c. You can visualize the integrals by finding the successive sum of all the data points from time zero to time L . In this example the integrals for the components at 1 kHz and 2 kHz are large, but the integral at 3 kHz is zero. In other words, there are two lines in the spectrum of $f(t)$, one line at 1 kHz and one line at 2 kHz. Our examples so far have used **discrete** Fourier transforms; that is, transforms evaluated at regularly spaced intervals, $n\nu_0$. Laboratory instruments use discrete Fourier transforms. Analytical evaluation of Fourier transforms is often easier on a continuous range of frequencies.

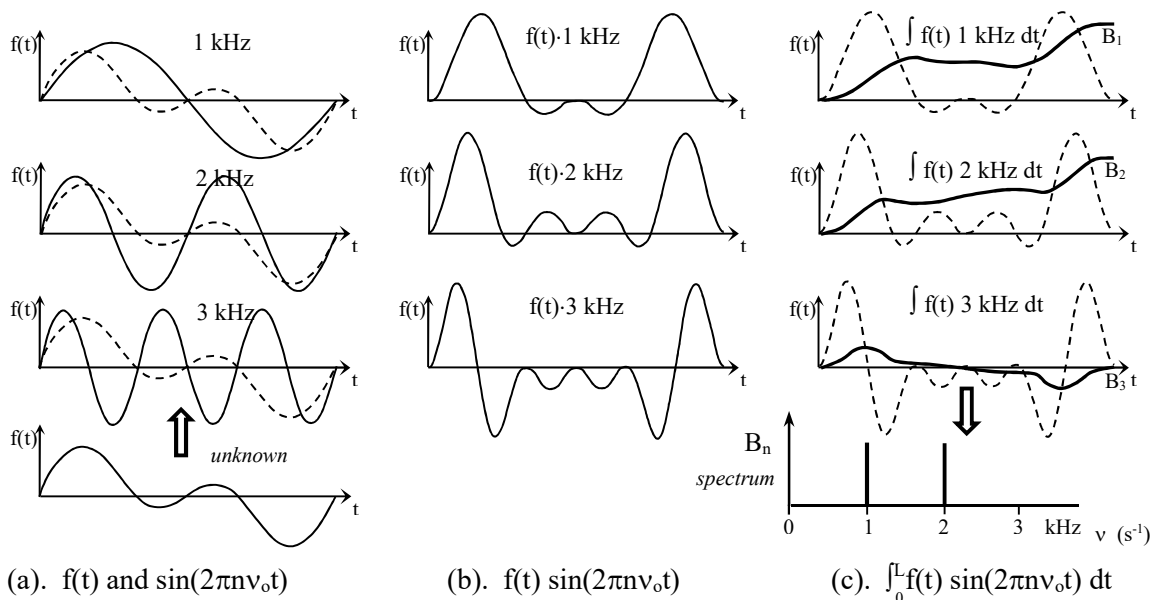


Figure 27.3.2: Formation of Fourier integrals. (a). The function to be transformed, $f(t)$, and pure sine waves are superimposed. (b). The function and the sine wave for each component frequency are multiplied, time-point-by-time-point. (c). The Fourier integral is the successive sum of the product data points. The Fourier coefficients at 1 kHz and 2 kHz are large, while the coefficient at 3 kHz is zero. The original function has two component frequencies.

To do a Fourier transform over a continuous range of frequencies, we relax the restriction of having a periodic function. Let the period of the function to be transformed go to infinity, $L \rightarrow \infty$. The lowest possible frequency then approaches zero: $\nu_0 = 1/L \rightarrow 0$. Then the frequencies that appear in the Fourier sums become a continuous variable ν : $2\pi n\nu_0 t \rightarrow 2\pi\nu t$. The Fourier sums and coefficients become continuous functions of the frequency:

$$f(t) = \int_0^{\infty} A(\nu) \cos(2\pi\nu t) d\nu + \int_0^{\infty} B(\nu) \sin(2\pi\nu t) d\nu \quad 27.3.3$$

$$A(\nu) = 2 \int_0^{\infty} f(t) \cos(2\pi\nu t) dt \quad B(\nu) = 2 \int_0^{\infty} f(t) \sin(2\pi\nu t) dt \quad 27.3.4$$

A simple example is useful at this point. Consider a short impulse, like banging your fist on the table. How can a short pulse excite all the resonant frequencies in the table? The impulse is modeled as a rectangular pulse of length t_p , Figure 27.3.3. For a rectangular pulse, the function is constant over the short time interval: $f(t) = 1$ for $t = 0$ to t_p and $f(t) = 0$ thereafter. Because the function is zero for $t > t_p$ the integration limits can be shortened and with $f(t) = 1$ for short times:

$$A(\nu) = 2 \int_0^{t_p} \cos(2\pi\nu t) dt \quad B(\nu) = 2 \int_0^{t_p} \sin(2\pi\nu t) dt \quad (\text{impulse}) \quad 27.3.5$$

The definite integrals are evaluated at the beginning and end of the pulse:

$$A(\nu) = 2 \left. \frac{\sin(2\pi\nu t)}{2\pi\nu} \right|_0^{t_p} \quad B(\nu) = 2 \left. \frac{-\cos(2\pi\nu t)}{2\pi\nu} \right|_0^{t_p} \quad 27.3.6$$

$$A(\nu) = 2 \frac{\sin(2\pi\nu t_p)}{2\pi\nu} \quad B(\nu) = 2 \frac{1 - \cos(2\pi\nu t_p)}{2\pi\nu} \quad 27.3.7$$

The full-width of the frequency response to the first zeros, Figure 27.3.3, is the inverse of the pulse width: $1/t_p$. This relationship is a reflection of the Uncertainty Principle, Section 27.2. The pulse is composed of a wide range of frequencies; the shorter the pulse, the broader is the range of frequencies. These frequency components are able to excite corresponding resonances in the table. In general if the function to be transformed is real and starts at a maximum, the cosine-transform $A(\nu)$ coefficients correspond to the absorption or emission spectrum of the transformed function. The sine-transform $B(\nu)$ coefficients then correspond to the **dispersion spectrum**. Spectroscopic experiments always have two corresponding responses, absorption and dispersion. The dispersive response is related to the index of refraction. A plot of the index of refraction of a sample as a function of frequency is proportional to the dispersive response, $B(\nu)$.

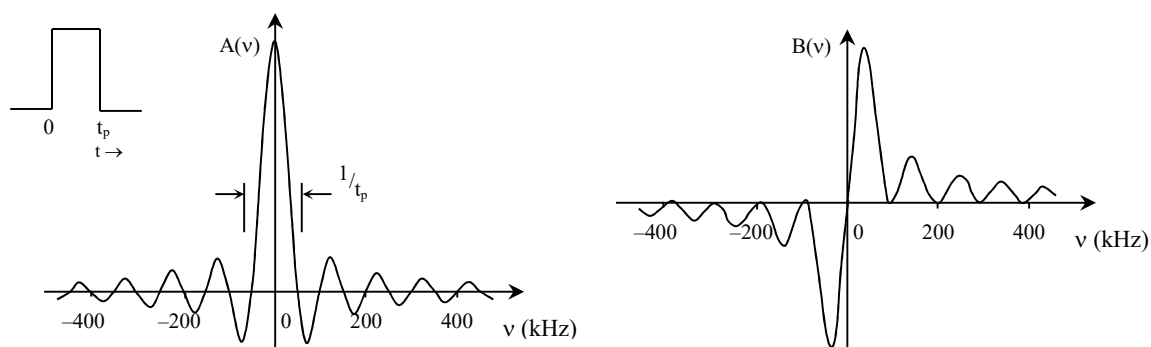


Figure 27.3.3: A short impulse has a wide frequency range. The Fourier transform of a rectangular pulse of width δ gives a $\sin(2\pi\nu\delta)/2\pi\nu$ absorptive line shape with width to the first nulls of $1/\delta$. The cosine transform gives the absorption spectrum $A(\nu)$, while the sine transform gives the dispersive spectrum $B(\nu)$.

In some experiments we focus on the absorption or emission spectrum, in others we focus on the dispersive response, such as optical rotatory dispersion. In pulsed NMR, ESR, and microwave

experiments both the absorptive and dispersive responses are always determined; however, only the absorptive response is typically displayed. For such cases the Euler Identity is conveniently used to combine the cosine and sine-transforms: $e^{i2\pi\nu t} = \cos(2\pi\nu t) + i \sin(2\pi\nu t)$. The Fourier expansion of the function to be transformed is then a single integral that includes both the sine and cosine terms:

$$f(t) = \int_{-\infty}^{\infty} g(\nu) e^{i2\pi\nu t} d\nu \quad 27.3.8$$

where $g(\nu)$ takes the role of the discrete Fourier coefficients, which is given by the transform:

$$g(\nu) = 2 \int_0^{\infty} f(t) e^{-i2\pi\nu t} dt \quad 27.3.9$$

The Fourier transform $g(\nu)$ is a complex function with:

$$\text{Absorption or Emission} = \text{Re}[g(\nu)] \quad \text{Dispersion} = \text{Im}[g(\nu)] \quad 27.3.10$$

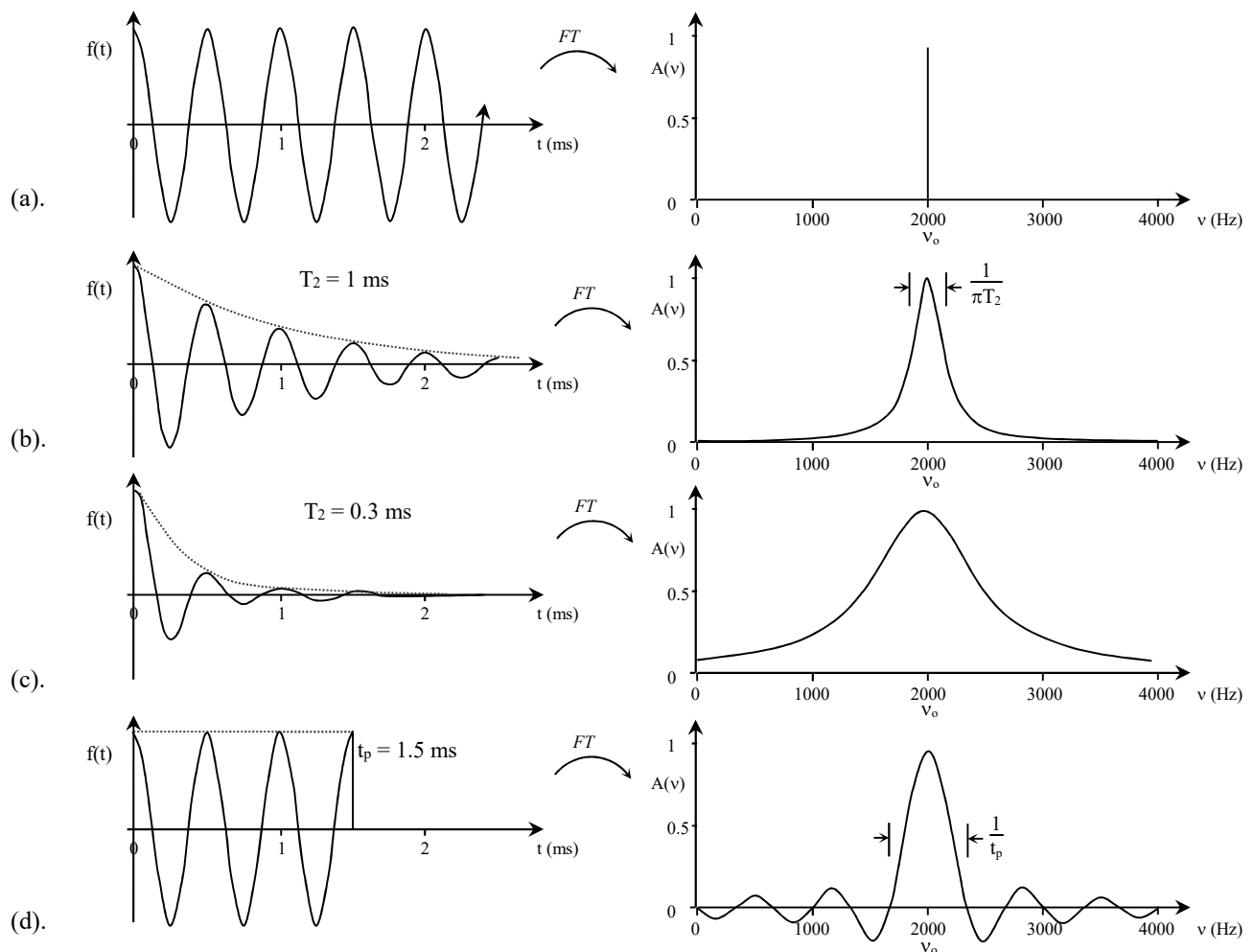


Figure 27.3.4: (a). A continuous sine wave has a very narrow frequency distribution. (b). Multiplication by e^{-t/T_2} gives a Lorentzian line with $\text{FWHM} = 1/\pi T_2$. (c). A shorter T_2 gives a broader line. (d). Multiplication by a rectangular function gives a $\sin(2\pi\nu t_p)/2\pi\nu$ line shape. Each example wave is centered at $\nu_0 = 2000$ Hz.

An intuitive understanding of Fourier transforms is helpful, since Fourier methods occur so often in theoretical and experimental practice. In our examples, the function to be transformed is in the **time-domain**. The Fourier transform gives the absorption or emission spectrum, which is in the **frequency-domain**. The units invert upon Fourier transformation: in this case from seconds to seconds⁻¹. A continuous cosine at frequency ν_0 gives a sharp, single-frequency Fourier transform, Figure 27.3.4a. Multiplication of the cosine wave by an exponentially decreasing function of time e^{-t/T_2} gives a transient response with lifetime of T_2 . The FT of an exponentially damped cosine gives a **Lorentzian line shape** centered on ν_0 , Figure 27.3.4b:

$$f(t) = e^{-t/T_2} \cos(2\pi\nu_0 t) \quad A(\nu) = \text{Re}[g(\nu)] = \frac{1}{\pi} \left(\frac{T_2}{1 + 4\pi^2 T_2^2 (\nu - \nu_0)^2} \right) \quad 27.3.11$$

The full-width at half-maximum is given by $\text{FWHM} = 1/\pi T_2$. As the lifetime T_2 decreases, the transient becomes shorter, and the line width increases, Figure 27.3.4c. The relationship between the lifetime and lineshape is a quantitative expression of the Uncertainty Principle, as discussed in Section 27.2. Lorentzian line shapes are commonly encountered in spectroscopy, especially solution NMR. Finally, consider a single-frequency cosine that has been multiplied by a rectangular function of width t_p . The Fourier transform of the rectangular impulse in Figure 27.3.3 is translated so that the line is centered about the center-frequency ν_0 instead of $\nu = 0$, Figure 27.3.4d.

Fourier transforms are widely used outside of chemistry and physics, including time-series analysis of the price fluctuations of stock-markets, population fluctuations of species in a given ecological setting, and frequency analysis of earth quakes and musical instruments. Having completed our general survey of the attributes of all forms of spectroscopy, we begin our discussion of molecular structure determination with rotational spectroscopy in low pressure gases. As we encounter new types of spectroscopy, we will usually discuss diatomic molecules in some detail and then discuss the additional attributes of the spectra of polyatomic molecules.

27.4 Rotational spectroscopy

Selection Rules Require a Permanent Dipole Moment: In rotational spectroscopy, interaction with light causes the angular momentum of the molecule to increase or decrease. The classical analogy is that molecules rotate faster after absorption of light. The principle interaction in microwave cooking is the excitation of molecular rotation of water molecules in the food. However, low-pressure gas phase spectroscopy is required to achieve sufficiently narrow transition widths to resolve molecular information. Selection rules require a permanent dipole moment for the appearance of a rotational absorption spectrum. The change in rotational quantum number is restricted to $\Delta J = \pm 1$ in absorption or emission, respectively. We begin with diatomic molecules.

The Rotational Constant Gives the Bond Length: The energies of the rotational states of a diatomic molecule in the rigid-rotor approximation are given by Eqs. 24.5.40-24.5.43, in joules and cm^{-1} respectively:

$$E_J = \tilde{B}_0 h c J(J + 1) \quad \tilde{F}_J = \frac{E_J}{h c} = \tilde{B}_0 J(J + 1) \quad (24.5.41-24.5.42) \quad 27.4.1$$

where \tilde{B}_o is the **rotational constant** in terms of the observed equilibrium bond length R_o , I is the moment of inertia, and μ is the reduced mass in kg:

$$\tilde{B}_o = \frac{\hbar}{4\pi I c} \quad I = \sum_{i=1}^n m_i r_i^2 = \mu R_o^2 \quad \mu = \frac{m_1 m_2}{m_1 + m_2} \quad (24.4.3, 24.4.10) \quad 27.4.2$$

A distinction between R_e and R_o must be made. The equilibrium bond length R_e is the bond length at the minimum of the potential energy curve, Figure 26.1.1. The observed equilibrium bond length R_o is the vibrationally averaged bond length in the $\nu = 0$ vibrational state. For anharmonic potentials, the vibrational wave function has a higher probability at the outer turning point compared to the inner turning point; classically speaking, the molecule spends “more time” at the outer turning point than the inner turning point. As a result $R_o > R_e$; however, the difference between the two is small, especially for low lying vibrations. Eqs. 27.4.2 are applicable to both types of bond lengths; R_e is evaluated from \tilde{B}_e , without vibrational averaging, and is directly comparable to molecular structure calculations. R_o is evaluated from \tilde{B}_o and is the value determined experimentally using rotational spectroscopy. The “o” subscript indicates the constant is determined in the $\nu = 0$ vibrational level. To be precise, the vibrational averaging for \tilde{B}_o is proportional to the expectation value $\langle 1/R^2 \rangle$, since $\tilde{B} = \hbar/4\pi m R^2 c$.

The energy level in wave numbers is called the **rotational term**, \tilde{F}_J , Figure 27.4.1. The connection between rotational spectroscopy and molecular structure is the dependence on equilibrium bond length. Given the angular momentum quantum number J , the allowed projections of the angular momentum on the z-axis are $m_J = 0, \pm 1, \dots, \pm J$, with a degeneracy of $g_J = 2J + 1$.

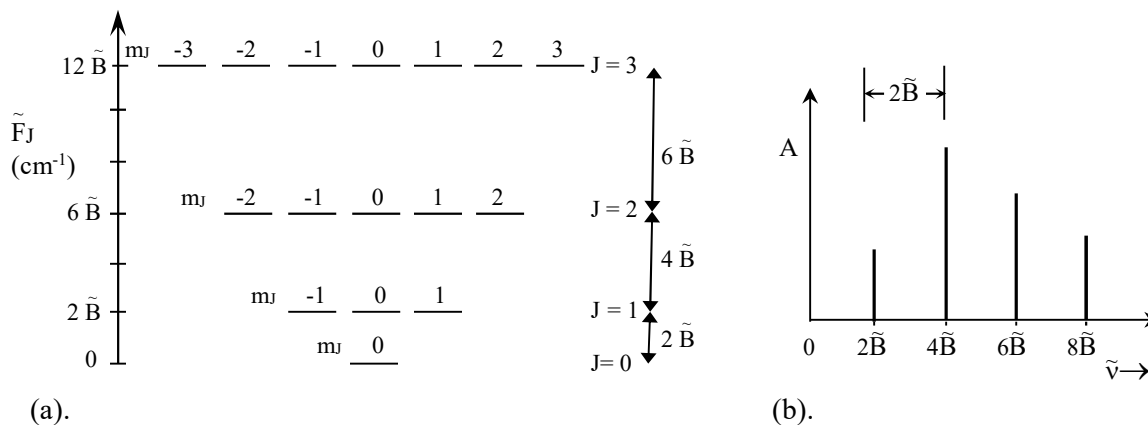


Figure 27.4.1: (a). Energy levels for the rigid rotor diverge with increasing J . (b). The rotational absorption spectrum has equally spaced lines.

By convention the upper level in a transition is listed as J' and the lower level as J'' , giving the transition as $J' \leftarrow J''$ for absorption and $J' \rightarrow J''$ for emission. Given the quantum number of the lower state J'' , the upper state quantum number is $J' = J'' + 1$ and the energy difference between adjacent energy levels in absorption is:

$$\Delta E = E_{J''+1} - E_{J''} = \tilde{B}hc[(J''+1)(J''+1 + 1) - J''(J''+1)] = 2\tilde{B}hc(J'' + 1) \quad (24.5.43)$$

$$\Delta\tilde{F} = \tilde{F}_{J''+1} - \tilde{F}_{J''} = \tilde{B}[(J''+1)(J''+1 + 1) - J''(J''+1)] = 2\tilde{B}(J'' + 1) \quad (J'': \text{lower level}) \quad 27.4.3$$

in joules and wave numbers, respectively. Equivalently, given the quantum number of the upper state J' , the quantum number for the lower state is $J'' = J' - 1$ and the energy difference between adjacent energy levels is:

$$\Delta E = E_{J'} - E_{J'-1} = \tilde{B}hc[J'(J'+1) - (J'-1)(J'-1 + 1)] = 2\tilde{B}hcJ' \quad (24.5.43)$$

$$\Delta\tilde{F} = \tilde{F}_{J'} - \tilde{F}_{J'-1} = \tilde{B}[J'(J' + 1) - (J'-1)(J'-1 + 1)] = 2\tilde{B}J' \quad (J': \text{upper level}) \quad 27.4.4$$

The resulting spectrum is a series of equally spaced lines, Figure 27.4.1b. The spacing between adjacent transitions is $2\tilde{B}$. Rotational spectroscopy for low-lying J transitions occurs in the microwave and terahertz region of the electromagnetic spectrum. Direct digital frequency synthesis in the microwave region allows transition frequencies to be determined with up to 12 significant figures, making microwave spectroscopy the most accurate method of molecular structure determination. The precision of microwave spectroscopy allows the confident detection of chemical species in interstellar space, making microwave spectroscopy an important tool in astronomy, Table 27.4.1.

Table 27.4.1: Molecules Detected in Interstellar and Circumstellar Space.¹

Number of Atoms	Examples
2	CH CH ⁺ C ₂ CN CO CP CS CSi H ₂ HCl AlCl AlF KCl NO NS NaCl OH PN SO SO ⁺ SiO SiS
3	HCN HNC HCO HCO ⁺ HCS ⁺ C ₂ H OCS C ₂ O C ₂ S SiC ₂ H ₃ ⁺ NH ₂ H ₂ O H ₂ S N ₂ H ⁺ HNO CO ₂ N ₂ O SO ₂
4	HCNH ⁺ HNCO HNCS HOCO ⁺ HC ₂ N H ₂ CN H ₂ CO H ₂ CS HC ₂ H C ₃ H C ₃ N C ₃ O C ₃ S NH ₃ H ₃ O ⁺ SiC ₃
5	HCOOH H ₂ CNH H ₂ NCN CH ₄ CH ₂ CN H ₂ C ₂ O HC ₃ N C ₃ H ₂ C ₄ H C ₄ Si SiH ₄ CHO ₂ H H ₂ C ₃ C ₅ H ₃ CO ⁺
6	HCONH ₂ CH ₃ OH CH ₃ SH CH ₃ CN CH ₃ NC C ₂ H ₄ H ₂ C ₄ C ₅ H C ₅ N HC ₃ HO HC ₃ NH ⁺
7-8	NH ₂ CH ₃ HCOCH ₃ CH ₂ CHCN CH ₃ C ₂ H HC ₅ N C ₆ H HCOOCH ₃ CH ₃ CO ₂ H CH ₃ C ₃ N C ₇ H H ₂ C ₆
9-13	CH ₃ CH ₂ OH (CH ₃) ₂ O CH ₃ CH ₂ CN CH ₃ C ₄ H HC ₇ N HC ₄ CH ₃ CH ₃ C ₅ N (CH ₃) ₂ CO HC ₉ N C ₆ H ₆ HC ₁₁ N

In low-pressure gases, the resolution is routinely sufficient to resolve different series of peaks for molecules with different specific isotopes. Molecules with identical formulas but different isotopic substitution are called **isotopomers**. For example, the rotational constants for H³⁵Cl and H³⁷Cl are 10.440 cm⁻¹ and 10.424 cm⁻¹, respectively. The microwave spectrum of HCl appears as a series of doublets, with the intensities of the peaks for H³⁵Cl and H³⁷Cl in the ratio of the isotopic abundances, roughly 2:1 for H³⁵Cl:H³⁷Cl (see the HCl IR vibrational spectrum for an example of isotope splitting). Assuming that the bond length is identical for molecules with different isotopic substitution is an excellent assumption. The reduced masses then determine the difference in rotational constants using Eq. 27.4.2 for isotopomer 1 and isotopomer 2:

$$\frac{\tilde{B}_2}{\tilde{B}_1} = \frac{\frac{\hbar}{4\pi\mu_2 R_{\text{dc}}^2}}{\frac{\hbar}{4\pi\mu_1 R_{\text{dc}}^2}} = \frac{\mu_1}{\mu_2} \quad 27.4.5$$

For example, for H³⁵Cl and H³⁷Cl, the reduced masses are:

$$\mu_{\text{H}^{35}\text{Cl}} = \frac{(1.007825)(34.968853)}{1.007825+34.968853} (\text{g mol}^{-1}) \frac{1}{N_A} (1\text{kg}/1000 \text{ g}) = 1.62665 \times 10^{-27} \text{ kg}$$

$$\mu_{\text{H}^{37}\text{Cl}} = \frac{(1.007825)(36.965903)}{1.007825+36.965903} (\text{g mol}^{-1}) \frac{1}{N_A} (1\text{kg}/1000 \text{ g}) = 1.62912 \times 10^{-27} \text{ kg} \quad 27.4.6$$

giving the ratio of the rotational constants:

$$\tilde{B}_{\text{H}^{37}\text{Cl}}/\tilde{B}_{\text{H}^{35}\text{Cl}} = \mu_{\text{H}^{35}\text{Cl}}/\mu_{\text{H}^{37}\text{Cl}} = 1.62665 \times 10^{-27} \text{ kg}/1.62912 \times 10^{-27} \text{ kg} = 0.99849 \quad 27.4.7$$

The agreement with the experimental ratio of 0.99847 validates the assumption of equal bond lengths for H^{35}Cl and H^{37}Cl .

Example 27.4.1: Molecular Structure and Rotational spectroscopy

The spacing between rotational transitions for H^{35}Cl is 20.880 cm^{-1} . Determine the equilibrium bond length, R_0 .

Answer: The rotational constant is $\tilde{B} = 20.880 \text{ cm}^{-1}/2 = 10.440 \text{ cm}^{-1}$. The reduced mass for H^{35}Cl is given in Eqs. 27.4.6. For units, the \tilde{B} value can be converted to m^{-1} and then $c = 2.99792 \times 10^8 \text{ m s}^{-1}$:

$$\tilde{B} = 10.440 \text{ cm}^{-1} (100 \text{ cm}/1 \text{ m}) = 1044.0 \text{ m}^{-1}$$

$$\text{with Eq. 27.4.2: } I = \hbar/(4\pi\tilde{B}c) = 1.05457266 \times 10^{-34} \text{ J s}/[4\pi(1044.0 \text{ m}^{-1})(2.997925 \times 10^8 \text{ m s}^{-1})]$$

$$= 2.68135 \times 10^{-47} \text{ kg m}^2$$

Alternatively, keeping \tilde{B} in cm^{-1} and the speed of light in cm s^{-1} for the $\tilde{B}c$ product:

$$\text{with Eq. 27.4.2: } I = \hbar/(4\pi\tilde{B}c) = 1.05457266 \times 10^{-34} \text{ J s}/[4\pi(10.440 \text{ cm}^{-1})(2.997925 \times 10^{10} \text{ cm s}^{-1})]$$

$$= 2.68135 \times 10^{-47} \text{ kg m}^2$$

$$\text{with Eq. 27.4.2: } R_0 = (I/\mu)^{1/2} = 1.28389 \times 10^{-10} \text{ m} = 1.2840 \text{ \AA}$$

Centrifugal Distortion Decreases the Energy Level Spacing: Upon closer inspection, the spacing decreases by a small amount between adjacent transitions in rotational spectra. The cause is **centrifugal distortion**. Centrifugal distortion results in the breakdown of the rigid rotor approximation. The classical analogy is as the molecule rotates faster, the bond stretches slightly, which decreases the effective rotational constant. The bond between two atoms acts more like a spring than a rigid rod. To account for centrifugal distortion, the rotational energy is expanded in a power series in $J(J+1)$:

$$\tilde{F}_J = \tilde{B}_e J(J+1) - \tilde{D}_e [J(J+1)]^2 \quad 27.4.8$$

where \tilde{D}_e is the centrifugal distortion constant, which you should be careful to avoid confusing with the bond dissociation energies \tilde{D}_e or \tilde{D}_0 , which are much larger in magnitude. The sign in Eq. 27.4.8 is given as a negative so that \tilde{D}_e can be tabulated as a positive number. For H^{35}Cl the centrifugal distortion constant is quite small $\tilde{D}_e = 0.00053 \text{ cm}^{-1}$. A model has been developed to give an estimate of the centrifugal distortion:

$$\tilde{D}_e = \frac{4\tilde{B}_e^3}{\tilde{\nu}_0^2} \quad (\text{centrifugal distortion}) \quad 27.4.9$$

where $\tilde{\nu}_0$ is the fundamental vibration frequency. As the vibration frequency increases, the bond becomes stronger and more difficult to stretch, decreasing centrifugal distortion. For example, for H^{35}Cl , $\tilde{\nu}_0 = 2886 \text{ cm}^{-1}$ and the model estimate is quite good, $\tilde{D}_e = 4(10.44 \text{ cm}^{-1})^3 / (2886 \text{ cm}^{-1})^2 = 0.00055 \text{ cm}^{-1}$. The effects of centrifugal distortion are well within the resolution of current instruments but are often neglected under practical circumstances. Now that we understand rotational spectroscopy of diatomic molecules, we next discuss the changes in the theory necessary to study polyatomic molecules.

The rotational spectra of linear polyatomics are identical to diatomics and follow Eqs. 27.4.4 or 27.4.8 depending on the desired accuracy. The moment of inertia just includes more atoms. However, the rotational spectra for a linear polyatomic only gives one experimental value, \tilde{B}_e . How can rotational spectroscopy find the structure of linear polyatomics, which have more than one bond length? Consider $\text{O}=\text{C}=\text{S}$ as an example. The moment of inertia of a linear triatomic with atom masses m_1 , m_2 and m_3 , and bond lengths R_{12} and R_{23} , is:

$$\begin{array}{c} \textcircled{m_1} \text{---} R_{12} \text{---} \textcircled{m_2} \text{---} R_{23} \text{---} \textcircled{m_3} \end{array} \quad I = \left(\frac{m_1 m_3}{m} \right) (R_{12} + R_{23})^2 + \left(\frac{m_2}{m} \right) (m_1 R_{12}^2 + m_3 R_{23}^2) \quad 27.4.10$$

The rotational constants of molecules with different isotopic substitution are determined and the unique masses and rotational constants are used to write two simultaneous equations in two unknowns. The two unknowns are the bond lengths R_{12} and R_{23} . The rotational constant for $^{16}\text{O}=\text{C}=\text{S}$ is $\tilde{B}_e = 0.202864 \text{ cm}^{-1}$ and for $^{16}\text{O}=\text{C}=\text{S}$ is $\tilde{B}_e = 0.197910 \text{ cm}^{-1}$. The two simultaneous equations are solved using successive approximations to give $R_{\text{CO}} = 1.165 \text{ \AA}$ and $R_{\text{CS}} = 1.558 \text{ \AA}$. For more complex molecules, multiple isotopomers must be studied to unravel the complete molecular structure. For this example, the rotational constants for $^{16}\text{O}=\text{C}=\text{S}$ and $^{16}\text{O}=\text{C}=\text{S}$ are also known. For extension to non-linear polyatomics, we first need to separate types of molecules by symmetry to discuss the appearance of the rotational spectra.

Non-Linear Polyatomic Molecules Have Three Moments of Inertia: Non-linear polyatomic molecules can be classified into three classes based on their symmetry. We consider the moments of inertia about three orthogonal axes, I_{xx} , I_{yy} , and I_{zz} . The formula that was introduced for linear molecules, Eq. 24.4.3, must be extended. For example, the moment of inertia around the z-axis is determined by the square of the perpendicular distance of the atomic positions from the z-axis, $r_{z,i}^2 = (x_i^2 + y_i^2)$, Figure 27.4.2. The moments of inertia are given as a symmetric matrix with components given by the sums over all atoms, using Eq. 24.5.18:

$$\begin{array}{ll} I_{xx} = \sum m_i (y_i^2 + z_i^2) & I_{xy} = \sum m_i x_i y_i \\ I_{yy} = \sum m_i (x_i^2 + z_i^2) & I_{xz} = \sum m_i x_i z_i \\ I_{zz} = \sum m_i (x_i^2 + y_i^2) & I_{yz} = \sum m_i y_i z_i \end{array} \quad 27.4.11$$

The distances are with respect to the center of mass. The I_{xy} , I_{xz} , and I_{yz} components are reduced to zero by rotating the coordinate axis to a special set of axes, the **principal axes**. In the principal coordinates frame of reference, the moment of inertia of a molecule is completely represented by I_{xx} , I_{yy} , and I_{zz} . The principal axes usually correspond to axes with highest rotational symmetry.

Mathematically, the coordinate rotation is accomplished by matrix diagonalization; I_{xx} , I_{yy} , and I_{zz} are the eigenvalues of the moment of inertia matrix.

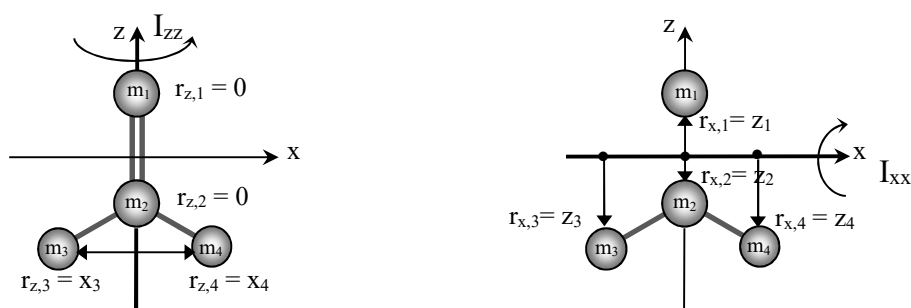


Figure 27.4.2: The moments of inertia are based on the perpendicular distance of the atom from the x , y , and z -axes. Illustrated are rotations about the z - and x -axes of a planar molecule that is oriented in the x - z plane (e.g. formaldehyde, $\text{CH}_2=\text{O}$). The distances simplify since all $y_i = 0$; then $r_{z,i}^2 = (x_i^2 + y_i^2)$ gives $r_{z,i} = x_i$.

Molecules are categorized on the basis of their three moments of inertia.

1. Spherical tops: A spherical top has identical moments of inertia about three orthogonal axes, $I_{xx} = I_{yy} = I_{zz}$. Examples of symmetric tops include methane, carbon tetrachloride, and SF_6 . For example, methane has three equivalent, mutually perpendicular two-fold rotation axes, Figures 26.7.3 and 27.4.3. Spherical tops cannot have a dipole moment, so they are invisible to the absorption of light in rotational spectroscopy. However, rotational transitions for spherical tops are observed in vibration-rotation and electronic spectroscopy, Section 27.6.

2. Symmetric tops: Symmetric tops have two equal moments of inertia. Examples include methyl chloride, chloroform, ammonia, phosphene, benzene, and cyclohexane. By convention, we align the molecule-fixed z -axis with the **figure axis**, which gives the principal coordinates frame. The figure-axis is the rotational axis of highest symmetry. For example, the figure axis for methylchloride is collinear with the C–Cl bond, which is a three-fold rotation axis, Figure 27.4.3. With this convention, for a symmetric top the moments of inertia about the x - and y -axis are identical and denoted I_{\perp} , since the x - and y -axes are perpendicular to the figure-axis. The moment of inertia around the z -axis is unique and denoted I_{\parallel} , since the z -axis is chosen parallel to the figure-axis:

$$I_{yy} = I_{xx} = I_{\perp} \quad I_{zz} = I_{\parallel} \quad (\text{symmetric top}) \quad 27.4.12$$

The two moments of inertia give two experimentally determined rotational constants, expressed in wave numbers as:

$$\tilde{B} = \frac{\hbar}{4\pi I_{\perp} c} \quad \tilde{A} = \frac{\hbar}{4\pi I_{\parallel} c} \quad (\text{symmetric top}) \quad 27.4.13$$

The \tilde{B} constant is for rotation perpendicular to the z -axis and is analogous to the rotational constant of diatomic molecules. The \tilde{A} constant is for rotation around the z -axis.

3. Asymmetric tops: The moments of inertia are each unique for an asymmetric top: $I_{xx} \neq I_{yy} \neq I_{zz}$. Of course, there are many examples of asymmetric tops including such simple molecules as dichloromethane, ethylene, and formaldehyde.

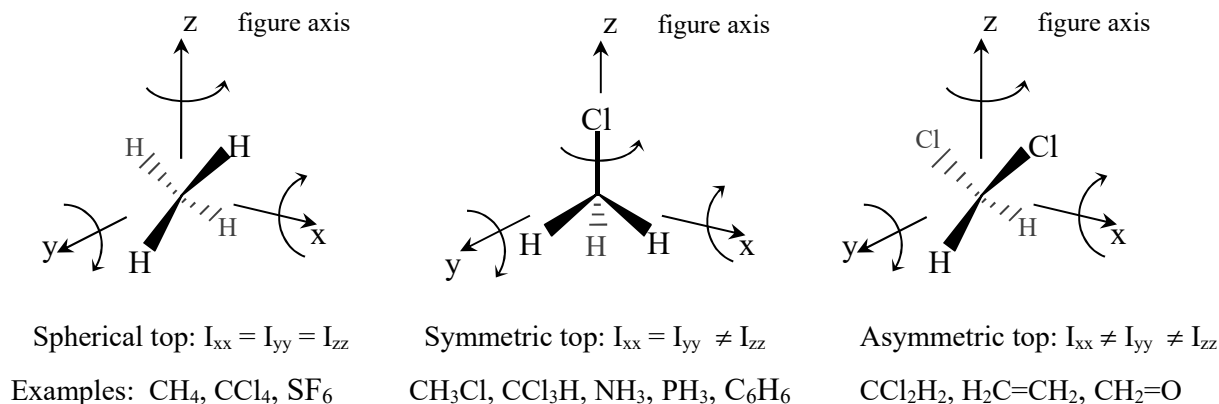


Figure 27.4.3: Polyatomic molecules are categorized as spherical tops, symmetric tops, and asymmetric tops. Symmetric tops have two equal moments of inertia. The z-axis, or figure axis, is the rotational axis of highest symmetry. See Figure 26.7.3 to clarify the axes choices.

The three moments of inertia give three experimentally determined rotational constants:

$$\tilde{A} = \frac{\hbar}{4\pi I_{zz}} \quad \tilde{B} = \frac{\hbar}{4\pi I_{xx}} \quad \tilde{C} = \frac{\hbar}{4\pi I_{yy}} \quad (\text{asymmetric top}) \quad 27.4.14$$

The spectra for asymmetric tops are quite complicated and are beyond the scope of this text. Fortunately, the spectra for symmetric tops are essentially the same as for diatomic molecules. We next discuss symmetric tops in detail.

We first develop the classical model for a rotating molecule, and then substitute quantum mechanical results for the classical angular momenta. In general the energy of a rotating molecule is the sum of the rotational energy about the x-, y-, and z-axes:

$$E = \frac{J_x^2}{2I_{xx}} + \frac{J_y^2}{2I_{yy}} + \frac{J_z^2}{2I_{zz}} \quad 27.4.15$$

The square of the total angular momentum is the sum of the components: $J^2 = J_x^2 + J_y^2 + J_z^2$. For a spherical top, $I_{xx} = I_{yy} = I_{zz} = I$, and Eq. 27.4.15 reduces to the same form as a diatomic molecule:

$$E = \frac{J^2}{2I} \quad (\text{spherical top}) \quad 27.4.16$$

The square of the total angular momentum is determined by the quantum number J , and the projection of the total angular momentum on a laboratory-fixed axis is also quantized with quantum number m_J :

$$J^2 = \hbar^2 J(J+1) \quad J_z = m_J \hbar \quad m_J = 0, \pm 1, \pm 2, \dots, \pm J \quad (\text{spherical top}) \quad 27.4.17$$

The rotational transitions are a set of equally or nearly equally spaced lines, as given by Eqs. 27.4.4 or 27.4.8, respectively. However, because of the lack of a dipole moment, spherical tops give no pure rotational spectra.

Symmetric Tops and Diatomics Have Analogous Spectra: For a symmetric top, using Eqs. 27.4.13 and 27.4.12, the classical rotational energy of a symmetric top is:

$$\Delta K = 0 \quad \Delta J = \pm 1 \quad (\text{symmetric top}) \quad 27.4.23$$

A dipole-allowed transition ending in the level with quantum number J' and beginning in level $J'' = J' - 1$ is at wave number:

$$\begin{aligned} \tilde{\nu}_J &= \tilde{F}_{J,K} - \tilde{F}_{J-1,K} = \tilde{B}J(J+1) - \tilde{B}(J-1)(J-1+1) \\ &= 2\tilde{B}J' \end{aligned} \quad (J': \text{upper level, symmetric top}) \quad 27.4.24$$

The terms in \tilde{A} cancel because K cannot change. The allowed absorption transitions for symmetric tops are the same as for diatomics, Eq. 27.4.4.

The K and m_J quantum numbers should be distinguished. The K quantum number determines the type of rotation, spinning or tumbling. The m_J quantum number determines the projection of the total angular momentum on a laboratory-fixed axis. Consider a spinning molecule with unit angular momentum, which is one with $J = K = 1$. In Figure 27.4.5, the lab z -axis is labeled Z to distinguish the lab-fixed axis from the molecule-fixed figure-axis z . The lab-fixed Z -axis is established by an external electric field oriented in the Z -direction. As m_J changes, the orientation of the rotation axis changes, but the molecule continues to spin around the figure-axis in the same way. For $J = 1$, the possible projections of the angular momentum have quantum numbers $m_J = -1, 0, +1$. For $J = K$ and $m_J = +1$, a figure skater is spinning on their skate blades. For $m_J = 0$, a figure skater is rolling on the ice. For $m_J = -1$ a figure skater is spinning on their head.

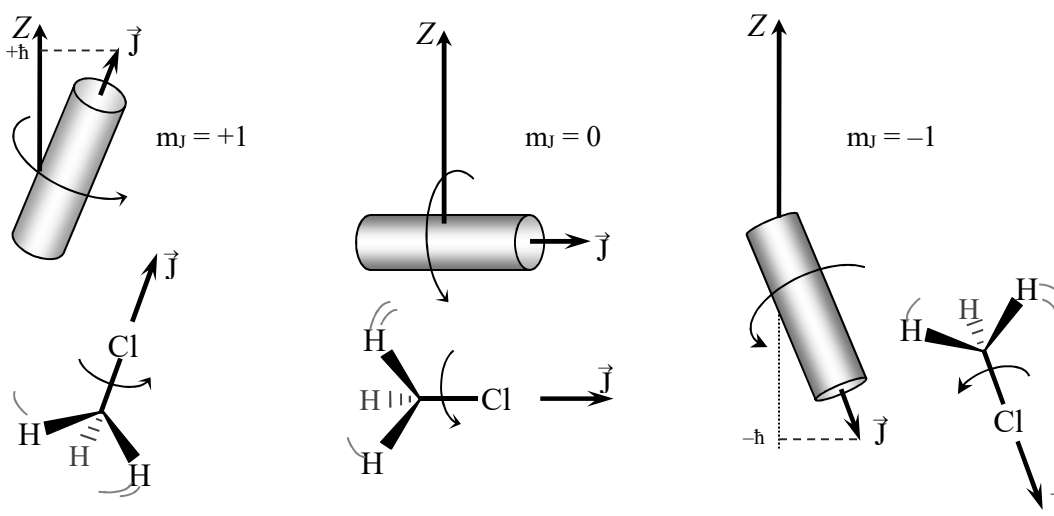


Figure 27.4.5: The K -quantum number determines the type of rotation, spinning or tumbling. The m_J quantum number determines the orientation of the rotation relative to a fixed laboratory axis. The example shown is for $J = K = 1$ and $m_J = -1, 0$, and $+1$. The molecule is spinning about the figure-axis in each case.

Pulsed Microwave Spectroscopy Uses the Multiplex Advantage: Rotational spectra cover a broad frequency range in the microwave and terahertz regions of the electromagnetic spectrum, depending on the moments of inertia of the molecule and the J'' of the initial state. The most

efficient method for acquisition of microwave spectra is by pulsed spectroscopy. Unlike NMR spectroscopy, the bandwidth of a short microwave pulse is not sufficient to cover a significant fraction of the necessary frequency range, as in Figure 27.3.4d. To circumvent the bandwidth limitations, the frequency is very rapidly scanned during the pulse, instead of using a constant frequency. Such pulses are called **chirped pulses**, and are formed using very rapid direct digital synthesis techniques, Figure 27.4.6. Other than the need for chirped excitation pulses, NMR and microwave spectroscopy are analogous; the response of the system after the excitation pulse is Fourier transformed to obtain the absorption spectrum.

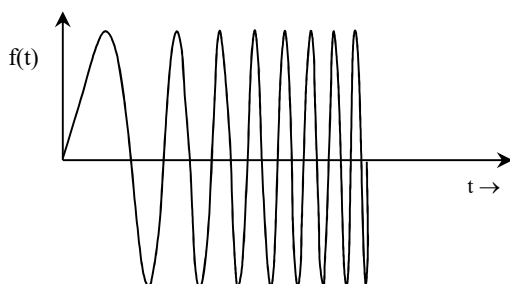


Figure 27.4.6: A chirped excitation pulse is used to achieve broad excitation bandwidth in Fourier transform microwave spectroscopy.

Example 27.4.2: *Molecular Structure from Rotational spectroscopy*

The rotational constant about the z-axis in formaldehyde is 9.41004 cm^{-1} (282.106 GHz). Calculate the H-C-H bond angle in formaldehyde. Assume a typical C-H bond length of 1.07 \AA .

Answer: Reference to Figure 27.4.2 shows that $x_4 = -x_3 = R_{\text{CH}} \sin(\theta/2)$, where θ is the H-C-H bond angle and R_{CH} is the C-H bond length. The C- and O-atoms do not contribute to the moment of inertia, because they lie on the z-axis. Since all the y_i coordinates are zero, the moment of inertia of formaldehyde about the z-axis is then:

$$I_{zz} = \sum m_i(x_i^2 + y_i^2) = \sum m_i x_i^2 = 2 m_{\text{H}} [R_{\text{CH}} \sin(\theta/2)]^2 \quad 27.4.25$$

The mass of the H-atom is $1.67353 \times 10^{-27} \text{ kg}$. The moment of inertia is given by Eq. 27.4.2:

$$\begin{aligned} I_{zz} &= \hbar/(4\pi\tilde{A}c) = 1.05457266 \times 10^{-34} \text{ J s} / [4\pi(9.41004 \text{ cm}^{-1})(2.997925 \times 10^{10} \text{ cm s}^{-1})] \\ I_{zz} &= 2.97478 \times 10^{-47} \text{ kg m}^2 = 2 m_{\text{H}} [R_{\text{CH}} \sin(\theta/2)]^2 \\ &= 2(1.67353 \times 10^{-27} \text{ kg}) [1.07 \times 10^{-10} \text{ m} \sin(\theta/2)]^2 \end{aligned}$$

Solving for the bond angle gives $\sin(\theta/2) = 0.881071$ or 123.5° .

27.5 Vibrational Absorption Spectroscopy

IR Selection Rules Require a Changing Dipole Moment: Infrared absorption spectroscopy requires that the dipole moment of the molecule change as a function of the internuclear distance for stretching vibrations or bond angle for bending vibrations. Homonuclear diatomics are the only molecules that do not have an infrared active vibrational mode. For polyatomic molecules some normal modes are infrared active and some are not, depending on the symmetry of the

molecule. Infrared absorption spectroscopy is a rich source of information on molecule structure and the strengths of chemical bonds.

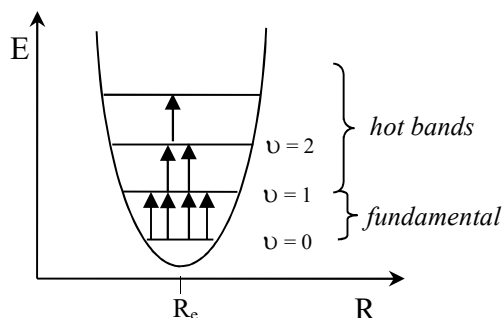


Figure 27.5.1: For a harmonic oscillator, only transitions between adjacent levels are allowed, $\Delta v = \pm 1$. Small numbers of molecules have excited initial vibrational quantum numbers, which result in “hot band” transitions.

Diatomic Molecules: Vibrations of molecules can be approximated as harmonic oscillators, Eqs. 24.2.15-24.3.16. In the harmonic approximation, the vibrational energy of a diatomic molecule or the vibrational energy of a normal mode of a polyatomic molecule is a linear function of the vibrational quantum number, v :

$$E_v = hv_0(v + \frac{1}{2}) = \hbar\omega_0(v + \frac{1}{2}) \quad (\text{harmonic}) \quad (24.2.15) \quad 27.5.1$$

where v_0 is the observed fundamental vibration frequency in cycles per second and ω_0 in radians per second. The spectroscopic absorption occurs in the infrared region of the spectrum, where wave numbers in cm^{-1} are the convenient energy units. The energy in wave numbers is called the **vibrational term**, \tilde{G}_v :

$$\tilde{G}_v = E/hc = \tilde{\nu}_0(v + \frac{1}{2}) \quad \tilde{\nu}_0 = \frac{\nu_0}{c} \quad \text{in cm}^{-1} \quad (\text{harmonic}) \quad 27.5.2$$

For a harmonic oscillator, only transitions between adjacent levels are allowed, $\Delta v = \pm 1$:

$$\Delta E = E_{v+1} - E_v = hv_0 \quad \Delta\tilde{G} = \tilde{G}_{v+1} - \tilde{G}_v = \tilde{\nu}_0 \quad (\text{harmonic}) \quad (24.2.16) \quad 27.5.3$$

Transitions beginning in different initial v states occur at the same frequency:

$$\nu_0 = \frac{1}{2\pi} \sqrt{\frac{k}{\mu}} \quad \omega_0 = 2\pi\nu_0 = \sqrt{\frac{k}{\mu}} \quad \tilde{\nu}_0 = \frac{1}{2\pi c} \sqrt{\frac{k}{\mu}} \quad 27.5.4$$

with k the force constant of the bond or normal mode and μ the reduced mass, Eq. 27.4.2. The harmonic potential is $V = \frac{1}{2}k(R - R_0)^2$. For careful work in the laboratory a more realistic vibrational potential energy function is required.

Anharmonicity Decreases the Energy Level Spacing: The experimentally determined energy levels for molecules show that the vibrational energy levels are not equally spaced. In real molecules, vibrational energy differences decrease with increasing v . The energy difference between adjacent states approaches zero at the dissociation limit, Figure 27.5.2a. The deviation

of the potential energy function from purely harmonic form is called **anharmonicity**. To account for anharmonicity, the energy of the vibrating molecule is expressed in a power series expansion:

$$E_v = h\nu_e(v + \frac{1}{2}) - h\chi_e\nu_e(v + \frac{1}{2})^2 + h\gamma_e\nu_e(v + \frac{1}{2})^3 + \dots \quad 27.5.5$$

where ν_e is the fundamental vibration frequency for small displacements about the equilibrium bond length, χ_e is the **anharmonicity**, and γ_e is the **second anharmonicity** constant, Table 27.6.1. One effect of anharmonicity is appearance of overtones. Overtones are weak $\Delta v = \pm 2$, $\Delta v = \pm 3$, and higher quantum number transitions. The intensity of each progressive overtone decreases by a factor of 10-20. Higher overtones are usually difficult to observe. If the potential is purely harmonic, the overtones occur at integer multiples of the fundamental vibration frequency, $\Delta v \nu_e$. Anharmonicity causes the overtones to fall at wave numbers less than integer multiples, because adjacent energy levels are not equally spaced, Figure 27.5.2b. For example, for H^{35}Cl the first overtone occurs at 5668.0 cm^{-1} instead of $2(2885.9) = 5771.8 \text{ cm}^{-1}$.

The anharmonicity is a useful experimental parameter that characterizes the shape of the vibrational potential. The full anharmonic potential is accurately determined in the Born-Oppenheimer approximation using advanced, correlated molecular structure methods for a series of fixed bond lengths, R . The anharmonicity of the theoretical potential energy curve, determined by curve fitting, can be compared to the experimental anharmonicity. However, for practical applications, a simple closed-form analytical function that approximates the vibrational potential energy function is useful.

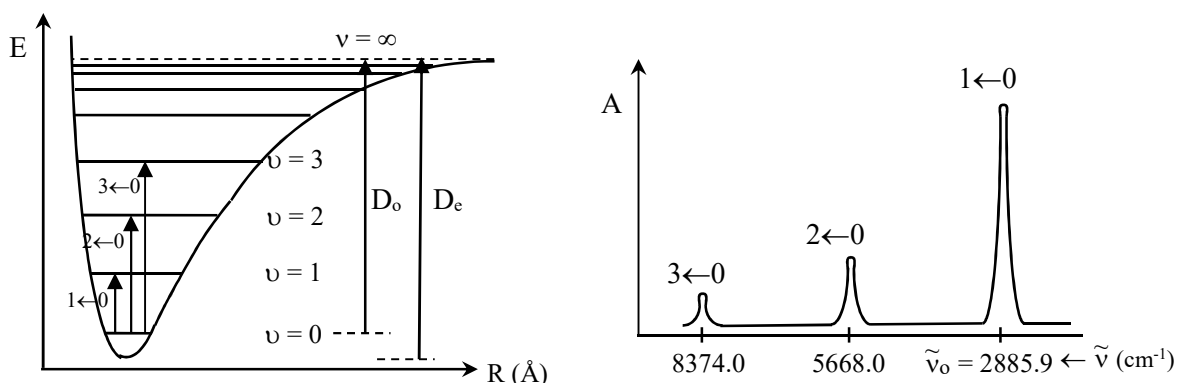


Figure 27.5.2: (a). For anharmonic potentials, the spacing between vibrational energy levels approaches zero at the dissociation limit. The equilibrium dissociation energy, D_e , is the energy at the dissociation limit with respect to the bottom of the potential energy well. The experimentally determined dissociation energy, D_0 , is referenced to the zero point energy. (b). Anharmonic potentials produce overtones in vibrational spectra.

The harmonic potential is a poor representation of the vibrational potential energy of a molecule, especially for large displacements (see also Eq. 8.8.20). Harmonic potentials don't allow for molecular dissociation; a purely harmonic bond cannot break. The **Morse Potential** is one commonly used functional form that approximates the vibrational potential energy in real molecules:

$$V = D_e [1 - e^{-a(R-R_e)}]^2 \quad (\text{Morse}) \quad 27.5.6$$

where D_e is the dissociation energy from the bottom of the potential well, R_e is the equilibrium bond length, and a is a constant that determines the steepness of the potential energy well:

$$a = \omega_e \left(\frac{\mu}{2D_e} \right)^{1/2} \quad (\text{Morse}) \quad 27.5.7$$

One important advantage of the Morse potential is that, rigorously, only the first two terms in Eq. 27.5.5 are required to give the exact energy of each vibrational level:

$$E_v = h\nu_e(v + 1/2) - h\chi_e\nu_e(v + 1/2)^2 \quad \text{or} \quad \tilde{G}_v = \tilde{\nu}_e(v + 1/2) - \chi_e\tilde{\nu}_e(v + 1/2)^2 \quad (\text{Morse}) \quad 27.5.8$$

The first equation is in joules and the second in wave number, cm^{-1} , units. The transition energy for adjacent levels, with the initial, lower vibrational quantum number v is:

$$E_{v+1} - E_v = h\nu_e(v+1+1/2) - h\chi_e\nu_e(v+1+1/2)^2 - h\nu_e(v+1/2) + h\chi_e\nu_e(v+1/2)^2 \quad (v+1 \leftarrow v) \quad 27.5.9$$

In algebraic manipulations, it is helpful to rearrange $(v+1+1/2)$ to give $((v+1/2)+1)$, so that $((v+1/2)+1)^2 = (v+1/2)^2 + 2(v+1/2) + 1$. Cancellation of terms in Eq. 27.5.9 then gives:

$$\Delta E_v = h\nu_e - h\chi_e\nu_e 2(v+1) \quad \text{or} \quad \Delta \tilde{G}_v = \tilde{\nu}_e - \chi_e\tilde{\nu}_e 2(v+1) \quad (v+1 \leftarrow v) \quad 27.5.10$$

By comparison of Eqs. 27.5.10 with Eqs. 27.5.1-27.5.3, the observed fundamental vibration frequency, $1 \leftarrow 0$, is for $v = 0$:

$$\nu_0 = \Delta E_0/h = \nu_e - 2\chi_e\nu_e \quad \text{or} \quad \tilde{\nu}_0 = \tilde{\nu}_e - 2\chi_e\tilde{\nu}_e \quad (\text{Morse}) \quad 27.5.11$$

Even the fundamental vibration frequency is decreased by anharmonicity. The zero point energies are given by Eqs. 27.5.8 with $v = 0$. The dissociation energies are then related by:

$$D_e = D_0 + 1/2 h\nu_e - 1/4 \chi_e h\nu_e \quad \text{or} \quad \tilde{D}_e = \tilde{D}_0 + 1/2 \tilde{\nu}_e - 1/4 \tilde{\nu}_e \chi_e \quad (\text{Morse}) \quad 27.5.12$$

The relationship between χ_e and \tilde{D}_e is determined by finding the vibrational quantum number at the convergence limit, v_{cl} . This quantum number corresponds to the value for which the energy level spacing between adjacent vibrational energy states is zero, from Eq. 27.5.10:

$$\Delta E = h\nu_e - h\chi_e\nu_e 2(v_{cl} + 1) = 0 \quad \text{or} \quad \Delta \tilde{G}_v = \tilde{\nu}_e - \chi_e\tilde{\nu}_e 2(v_{cl} + 1) = 0 \quad (\text{Morse}) \quad 27.5.13$$

Cancelling the common factor of $h\nu_e$ and rearranging gives $\chi_e 2(v_{cl} + 1) = 1$. Solving for the convergence limit:

$$v_{cl} + 1 = \frac{1}{2\chi_e} \quad \text{for the upper level} \quad \text{or} \quad v_{cl} = \frac{1}{2\chi_e} - 1 \quad \text{for the lower level} \quad 27.5.14$$

Substitution of the last equation into Eq. 27.5.8 gives the dissociation energy as equal to the vibrational energy at the convergence limit:

$$\tilde{D}_e = \tilde{G}_{v_{cl}+1} = \tilde{\nu}_e [(v_{cl}+1) + 1/2] - \chi_e\tilde{\nu}_e [(v_{cl}+1) + 1/2]^2 \quad (\text{Morse}) \quad 27.5.15$$

Substitution of Eq. 27.5.14 for $v_{cl}+1$ gives:

$$\tilde{D}_e = \frac{\tilde{\nu}_e}{2\chi_e} + \frac{\tilde{\nu}_e}{2} - \frac{\chi_e\tilde{\nu}_e}{4} (1/\chi_e + 1)^2 = \frac{\tilde{\nu}_e}{2\chi_e} + \frac{\tilde{\nu}_e}{2} - \frac{\chi_e\tilde{\nu}_e}{4} \left(\frac{1}{\chi_e^2} + \frac{2}{\chi_e} + 1 \right) \quad (\text{Morse}) \quad 27.5.16$$

Cancelling factors simplifies the previous expression to give:

$$\tilde{D}_e = \frac{\tilde{\nu}_e}{2\chi_e} + \frac{\tilde{\nu}_e}{2} - \left(\frac{\tilde{\nu}_e}{4\chi_e} + \frac{\tilde{\nu}_e}{2} + \frac{\chi_e\tilde{\nu}_e}{4} \right) = \frac{\tilde{\nu}_e}{4\chi_e} - \frac{\chi_e\tilde{\nu}_e}{4} \cong \frac{\tilde{\nu}_e}{4\chi_e} \quad (\text{Morse}) \quad 27.5.17$$

The final approximation is valid since the anharmonicity, χ_e , is usually a small fraction of the vibration frequency. This last expression allows the estimation of the bond dissociation energy for the molecule from the anharmonicity. The bond dissociation energy is, of course, one of the most fundamental measures of bond strength. Solving the last expression for the anharmonicity and using Eq. 27.5.7 also gives the relationship of the Morse a -coefficient to the anharmonicity:

$$\chi_e\tilde{\nu}_e = \frac{\tilde{\nu}_e^2}{4\tilde{D}_e} \quad \text{and} \quad \chi_e\tilde{\nu}_e = \frac{a^2\hbar}{8\pi^2\mu c} \quad (\text{Morse}) \quad 27.5.18$$

These relationships among the anharmonicity, bond dissociation energy, and Morse a -parameter are central in the determination of bond energies and potential energy surfaces. The application of these relationships require an accurate method for the experimental determination of the anharmonicity. Consider the adjacent differences in the wave numbers of the transitions in Figure 27.5.2 as shown in Figure 27.5.3. The difference $\Delta\tilde{\nu}_1 = \tilde{\nu}(2\leftarrow 0) - \tilde{\nu}(1\leftarrow 0)$ is between the first overtone and the fundamental, while $\Delta\tilde{\nu}_2 = \tilde{\nu}(3\leftarrow 0) - \tilde{\nu}(2\leftarrow 0)$ is between the second overtone and the first overtone. For example, the adjacent difference for the first overtone $\Delta\tilde{\nu}_1$ is equivalent to direct transition $2\leftarrow 1$, and the adjacent difference for the second overtone $\Delta\tilde{\nu}_2$ is equivalent to direct transition $3\leftarrow 2$. The general result is: $\Delta\tilde{\nu}_v = \Delta\tilde{G}_v$.

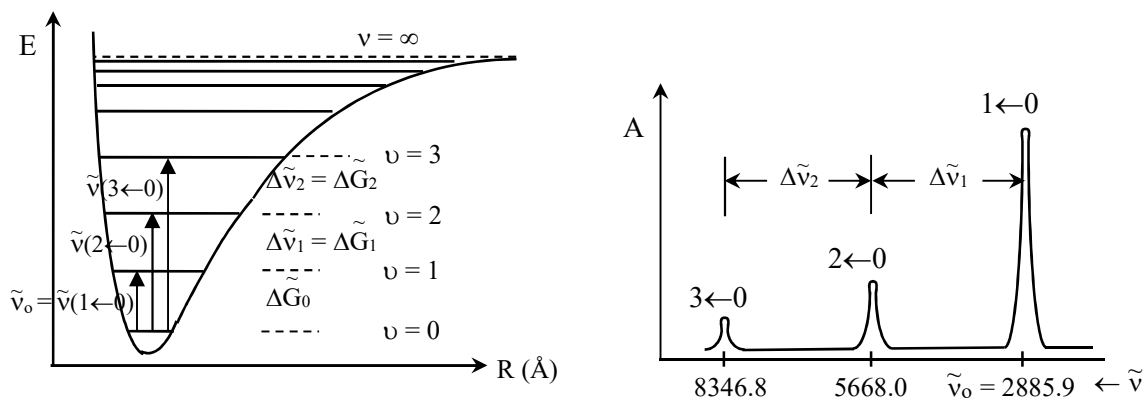


Figure 27.5.3: Adjacent wave number differences between transitions.

The wave numbers of the direct transitions are given by Eq. 27.5.10 resulting in the adjacent differences:

$$\Delta\tilde{\nu}_v = \Delta\tilde{G}_v = \tilde{\nu}_e - \chi_e\tilde{\nu}_e 2(v+1) = (\tilde{\nu}_e - 2\chi_e\tilde{\nu}_e) - 2\chi_e\tilde{\nu}_e v \quad (\text{Morse, } v:\text{overtone}) \quad 27.5.19$$

Substitution of the fundamental transition, Eq. 27.5.11, for the term in parentheses gives:

$$\Delta\tilde{\nu}_v = \tilde{\nu}_0 - 2\chi_e\tilde{\nu}_e v \quad (\text{Morse, } v:\text{overtone}) \quad 27.5.20$$

A plot of the adjacent wave number differences is a linear function of the vibrational quantum number of the lower overtone state with slope, $-2\chi_e\tilde{\nu}_e$. The intercept is the observed fundamental vibration frequency. A plot based on Eq. 27.5.20 is called a **Birge-Sponer** plot,

Figure 27.5.4. The dissociation energy is then given by Eqs. 27.5.18. Alternatively, if only the first overtone is known a rough estimate of the anharmonicity can be made from:

$$\Delta\tilde{\nu}_1 = \tilde{\nu}_0 - 2\chi_e\tilde{\nu}_e \quad \text{giving} \quad \chi_e\tilde{\nu}_e = (\tilde{\nu}_0 - \Delta\tilde{\nu}_1)/2 \quad (\text{Morse}) \quad 27.5.21$$

Example 27.5.1: Anharmonicity

Determine $\tilde{\nu}_e$, the force constant, anharmonicity, zero point energy, and the bond dissociation energies, \tilde{D}_e and \tilde{D}_0 , for H^{35}Cl . The fundamental and overtones for H^{35}Cl are 2885.98, 5667.98, 8346.78, 10922.83, and 13396.32 cm^{-1} .

Answer: A spreadsheet to calculate the adjacent wave number differences and corresponding Birge-Sponer plot are shown below:

ν	$\tilde{\nu}_{\nu \leftarrow 0}$ (cm^{-1})	$\Delta\tilde{\nu}_\nu$ (cm^{-1})
1	2885.98	2782.00
2	5667.98	2678.80
3	8346.78	2576.05
4	10922.83	2473.49
5	13396.32	

slope	-102.828	2884.655	intercept
\pm	0.102849	0.281665	\pm
r^2	0.999998	0.229978	$s(y)$
F	999583.8	2	df
ss_{reg}	52867.99	0.10578	ss_{resid}

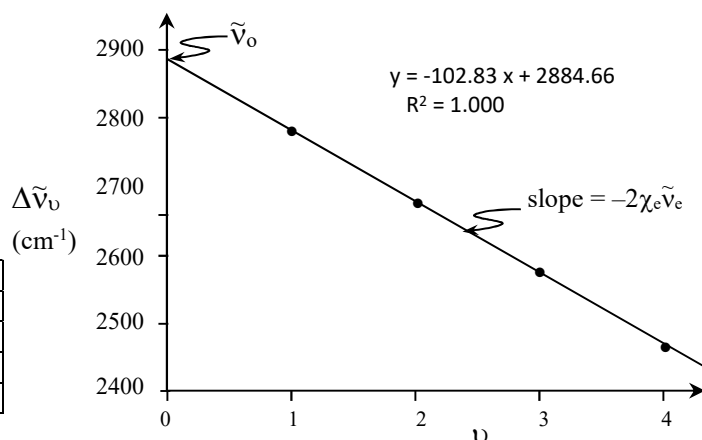


Figure 27.5.4: Birge-Sponer plot for H^{35}Cl with slope $= -2\chi_e\tilde{\nu}_e$.

The curve fit gives the anharmonicity as $\chi_e\tilde{\nu}_e = 51.41 \pm 0.05 \text{ cm}^{-1}$. The difference between the intercept and the experimental fundamental of 2885.98 cm^{-1} is caused by deviations from the Morse potential form and experimental error. Many researchers include the fundamental in the curve fit for $\nu = 0$ to improve the agreement. The final spectroscopic constants are:

with Eq. 27.5.11: $\tilde{\nu}_e = \tilde{\nu}_0 + 2\chi_e\tilde{\nu}_e = 2885.98 \text{ cm}^{-1} + 2(51.41) \text{ cm}^{-1} = 2988.81 \text{ cm}^{-1}$

with Eq. 27.5.4: $\tilde{k} = 4\pi^2c^2\tilde{\nu}_e^2\mu = 4\pi^2(2.99792 \times 10^{10} \text{ cm s}^{-1})^2(2988.81 \text{ cm}^{-1})^2(1.62668 \times 10^{-27} \text{ kg})$
 $\tilde{k} = 515.6 \text{ N m}^{-1}$

with Eq. 27.5.8: $\text{ZPE} = \tilde{G}_0 = \frac{1}{2}\tilde{\nu}_e - \frac{1}{4}\tilde{\nu}_e\chi_e = \frac{1}{2}(2988.81 \text{ cm}^{-1}) - \frac{1}{4}(51.41 \text{ cm}^{-1}) = 1481.55 \text{ cm}^{-1}$

with Eq. 27.5.18: $\tilde{D}_e = \tilde{\nu}_e^2/4\chi_e\tilde{\nu}_e = (2988.81 \text{ cm}^{-1})^2/(4(51.41 \text{ cm}^{-1}))$

$$\tilde{D}_e = 43,436 \text{ cm}^{-1} = 5.385 \text{ eV} = 519.6 \text{ kJ mol}^{-1}$$

with Eq. 27.5.12: $\tilde{D}_0 = \tilde{D}_e - \text{ZPE} = 43,436 \text{ cm}^{-1} - 1481.55 \text{ cm}^{-1} = 41955. \text{ cm}^{-1}$

$$\tilde{D}_0 = 5.202 \text{ eV} = 501.9 \text{ kJ mol}^{-1}$$

The literature values are $\tilde{\nu}_e = 2990.925 \text{ cm}^{-1}$, $\chi_e \tilde{\nu}_e = 52.800 \text{ cm}^{-1}$ and $\tilde{D}_0 = 4.430 \text{ eV} = 427.4 \text{ kJ mol}^{-1}$, Table 27.6.1. The literature values include the second anharmonicity correction giving greater accuracy.

Normal Modes Describe Vibrations for Polyatomic Molecules: Except for low frequency torsions, the normal modes of polyatomic molecules are adequately approximated by harmonic potentials. Instead of a single bond length or angle, a normal mode vibration progresses as a function of the normal coordinate of the mode, which includes multiple bond lengths and angles, Eq. 8.11.32. The derivative in Eq. 27.1.10 is with respect to the normal mode displacement.

Anharmonicity Causes Vibrational Modes to Interact: The most important effect of anharmonicity for polyatomic molecules is the appearance of overtones and sum and difference bands. For two normal mode fundamental vibrations, $\tilde{\nu}_1$ and $\tilde{\nu}_2$, the sum transition occurs at $\tilde{\nu}_1 + \tilde{\nu}_2$ and the difference band at $|\tilde{\nu}_1 - \tilde{\nu}_2|$. If they occur, overtone, sum, and difference transitions are usually much less intense than dipole allowed fundamentals. Sum and difference bands, taken together are called **combination bands** or just **combinations**.

Rotation and vibration transitions occur simultaneously. In the gas phase, fundamental, overtone, sum, and difference bands all display rotational fine structure. While microwave spectrometers are not common, rotational information is available from vibrational spectra.

27.6 Rotational-Vibrational Spectroscopy

Rotational Constants Are Available from Vibrational Spectra: The selection rules for vibrational spectroscopy of diatomics in singlet electronic states with no net orbital angular momentum are $\Delta v = \pm 1$ and $\Delta J = \pm 1$. The result is that vibration and rotation transitions occur simultaneously in gas phase spectroscopy. Vibrational transitions are a series of closely spaced lines instead of a single transition, Figures 27.6.1, 27.6.2. The set of lines differ in the change in rotation of the molecule and are called the **rotational fine-structure**.

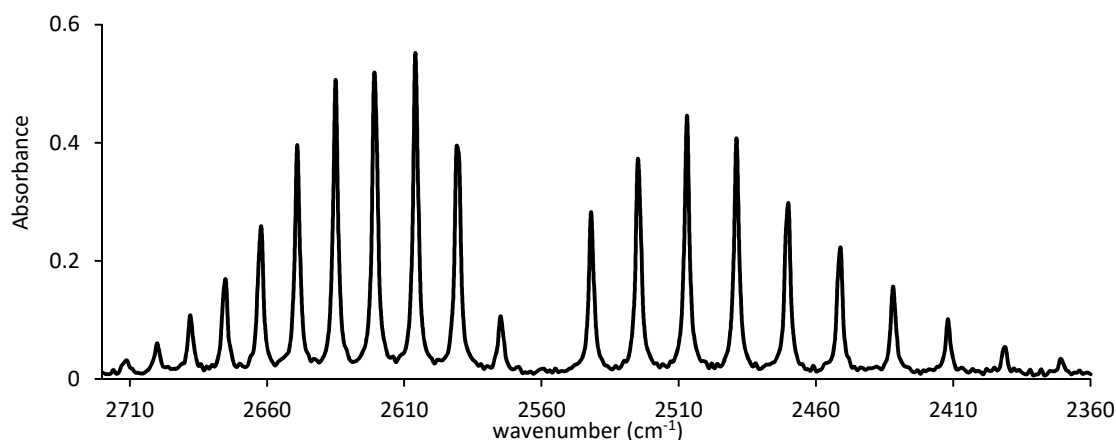


Figure 27.6.1: Rotation-vibration spectrum of HBr gas.

Consider a transition from an initial vibration-rotation state given by the quantum numbers v'', J'' to a final rotation-vibration state v', J' , giving the transition $v', J' \leftarrow v'', J''$, Figure 27.5.3. The

fundamental vibration transition is from the $\nu'' = 0$ to $\nu' = 1$ levels. Most molecules are found in their lowest energy vibration state, $\nu'' = 0$.

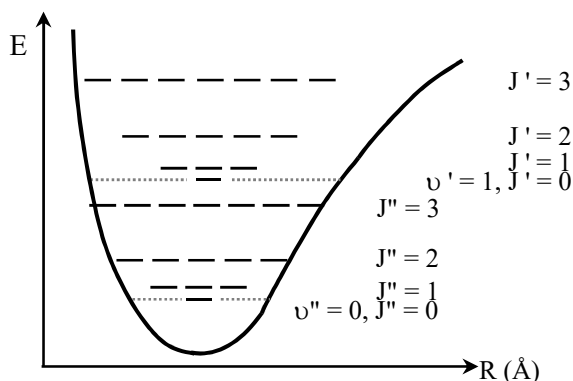


Figure 27.6.2: Rotation-vibration levels in a diatomic molecule. The spacing between the rotational levels is exaggerated for clarity.

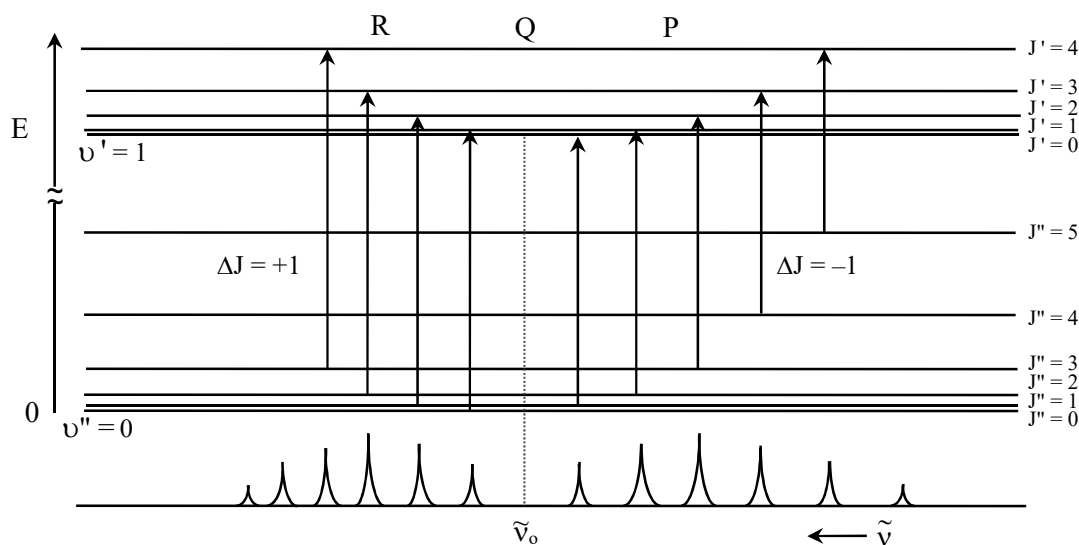


Figure 27.6.3: Rotation-vibration transitions for a diatomic molecule. $\Delta J = 0$ is forbidden for a diatomic with a singlet ground electronic state and no net orbital angular momentum.

Consider a transition from an initial vibration-rotation state given by the quantum numbers ν'' , J'' to a final rotation-vibration state ν' , J' , giving the transition $\nu', J' \leftarrow \nu'', J''$, Figure 27.5.3. The fundamental vibration transition is from the $\nu'' = 0$ to $\nu' = 1$ levels. Most molecules are found in their lowest energy vibration state, $\nu'' = 0$. However, the Boltzmann distribution of molecules among the rotational levels produces a wide range of initial rotational states. Therefore, the fundamental vibration of a molecule consists of a series of closely spaced lines that correspond to the $\nu = 0$ to 1 vibrational transition and wide range of rotational transitions, $1, J' \leftarrow 0, J''$. The selection rule for rotational transitions is $\Delta J = \pm 1$. For example, $1, 1 \leftarrow 0, 0$, $1, 2 \leftarrow 0, 1$, and $1, 3 \leftarrow 0, 2$ have $\Delta J = +1$, and are said to be part of the **R-branch**. Also, $1, 0 \leftarrow 0, 1$, $1, 1 \leftarrow 0, 2$, $1, 2 \leftarrow 0, 3$ have $\Delta J = -1$, and are part of the **P-branch**. The $\Delta J = 0$ transition is forbidden for a

singlet ground state and no net orbital angular momentum and is therefore absent, which would otherwise give the Q branch.

The energy change for the transitions, neglecting anharmonicity and centrifugal distortion, are:

$$\Delta E_{\nu', J' \leftarrow \nu'', J''} = E_{\nu', J'} - E_{\nu'', J''} = h\nu_0 (\nu' - \nu'') + \tilde{B}' hc J'(J'+1) - \tilde{B}'' hc J''(J''+1) \quad 27.6.1$$

If the bond length of the molecule doesn't change much on going to the higher vibrational state then $\tilde{B}' = \tilde{B}'' = \tilde{B}$. For $\Delta\nu = +1$ and R-branch $\Delta J = +1$ transitions, setting $J' = J''+1$ and simplifying Eq. 27.6.1 gives:

$$\Delta E_{\nu'+1, J''+1 \leftarrow \nu'', J''} = h\nu_0 + 2\tilde{B}hc (J''+1) \quad (J'': \text{lower level}) \quad 27.6.2$$

For $\Delta\nu = +1$ and P-branch $\Delta J = -1$ transitions, setting $J' = J''-1$ and simplifying Eq. 27.6.1 gives:

$$\Delta E_{\nu'+1, J''-1 \leftarrow \nu'', J''} = h\nu_0 - 2\tilde{B}hc J'' \quad (J'': \text{lower level}) \quad 27.6.3$$

This simplification gives the spectrum as a series of equally spaced lines with the spacing between adjacent lines $2\tilde{B}hc$, Figure 27.6.4. For example for adjacent P-branch lines:

$$\begin{aligned} \Delta E_{\nu'+1, J''+2 \leftarrow \nu'', J''+1} - \Delta E_{\nu'+1, J''+1 \leftarrow \nu'', J''} &= -2\tilde{B}hc (J''+1+1) + 2\tilde{B}hc (J''+1) \\ &= -2\tilde{B}hc \end{aligned} \quad 27.6.4$$

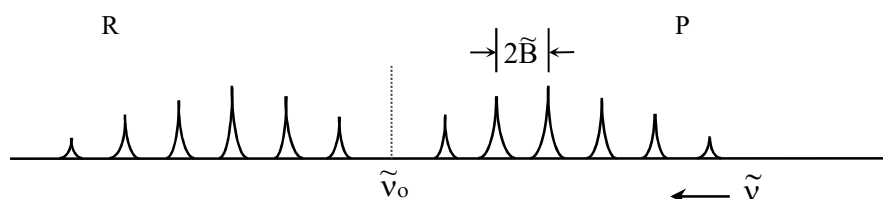


Figure 27.6.4: Rotation-vibration transitions with equal bond length in the upper and lower vibrational state, giving $\tilde{B}_{\nu'} = \tilde{B}_{\nu''}$ and the spacing between transitions is constant.

Often, however, the bond length does change significantly, so that Eq. 27.6.1 must be used. As discussed in Sec. 27.4, the observed \tilde{B} -value is averaged over the motion of the nuclei in the corresponding vibrational state. For anharmonic potentials the averaged bond length increases with vibrational quantum number, because the wave function amplitude increases at the outer turning point. As the bond length increases the \tilde{B} -value decreases, $\tilde{B}' < \tilde{B}''$. The dependence of the rotational constant on the vibration level can be expressed as a Taylor series expansion in $(\nu + 1/2)$. Keeping only the linear term gives:

$$\tilde{B}_{\nu} = \tilde{B}_e - \tilde{\alpha}_e(\nu + 1/2) \quad 27.6.5$$

where \tilde{B}_e is the rotational constant evaluated at the equilibrium internuclear separation and $\tilde{\alpha}_e$ is the vibration-rotation interaction constant in cm^{-1} , Table 27.6.1. Eq. 27.6.1 can be expressed entirely in wave numbers by dividing by hc :

$$\tilde{\nu} = \Delta E_{\nu', J' \leftarrow \nu'', J''} / hc = \tilde{\nu}_0 (\nu' - \nu'') + \tilde{B}' J'(J'+1) - \tilde{B}'' J''(J''+1) \quad (J'': \text{lower level}) \quad 27.6.6$$

where $\tilde{\nu}$ is the wave number of the transition and $\tilde{\nu}_0$ is the fundamental vibration frequency, in cm^{-1} . Substituting Eq. 27.6.4 into Eq. 27.6.5 and taking $\nu' - \nu'' = 1$ gives:

$$\tilde{\nu} = \tilde{\nu}_0 + (\tilde{B}_e - \tilde{\alpha}_e(\nu + \frac{1}{2})) J'(J'+1) - \tilde{B}_0 J''(J''+1) \quad 27.6.7$$

For the R-branch, where $\Delta J = +1$ and $J' = J''+1$, Eq. 27.6.7 simplifies to:

$$\tilde{\nu}_R = \tilde{\nu}_0 + (2\tilde{B}_e - 3\tilde{\alpha}_e) + (2\tilde{B}_0 - 4\tilde{\alpha}_e) J'' - \tilde{\alpha}_e J''^2 \quad (J'': \text{lower level}) \quad 27.6.8$$

For the P-branch, where $\Delta J = -1$ giving $J' = J''-1$, Eq. 25.5.7 simplifies to:

$$\tilde{\nu}_P = \tilde{\nu}_0 - (2\tilde{B}_e - 2\tilde{\alpha}_e) J'' - \tilde{\alpha}_e J''^2 \quad (J'': \text{lower level}) \quad 27.6.9$$

With $\tilde{B}' < \tilde{B}''$, each line moves to lower wave number in proportion to the J''^2 value. In other words, lines further away from $\tilde{\nu}_0$ move more than lines closer to $\tilde{\nu}_0$. The R-branch lines move closer together and the P-branch lines move further apart, Figure 27.6.5. Eqs. 27.6.8 and 27.6.9 can be combined by defining a new variable m , where $m = J''+1$ for the R-branch and $m = -J''$ for the P-branch, Figure 27.6.5:

$$\tilde{\nu}_m = \tilde{\nu}_0 + (2\tilde{B}_e - 2\tilde{\alpha}_e) m - \tilde{\alpha}_e m^2 \quad 27.6.10$$

Using Eq. 27.6.10, transition wave numbers are fit to a second order polynomial in m to extract the spectroscopic constants.

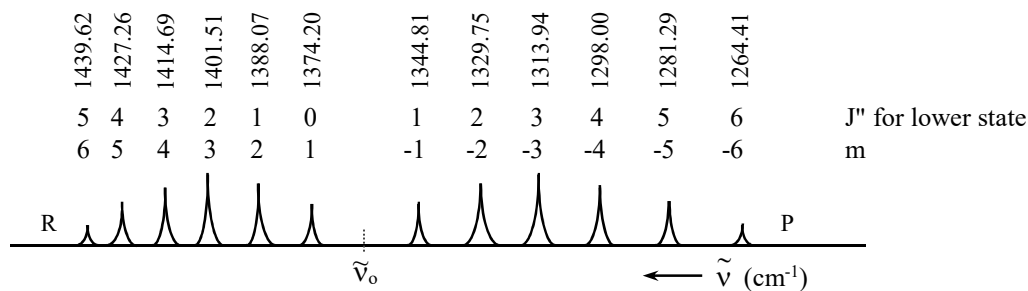


Figure 27.6.5: Vibration-rotation spectrum for ${}^7\text{LiH}$ (schematic). Line indexing for Eq. 27.6.9 with $m = J''+1$ for the R- and $m = -J''$ for the P-branch.

Example 27.6.1: Molecular Structure and Vibration-Rotational spectroscopy

Use the peak positions in Figure 27.6.5 to determine the equilibrium bond length R_e , the fundamental vibration frequency $\tilde{\nu}_0$, the force constant, and the vibration-rotation interaction coefficient for ${}^7\text{LiH}$.

Answer: www The wave numbers from the figure are fit to a quadratic polynomial in m using Eq. 27.6.10 and the “Non-Linear Least Squares” applet on the text Web site or companion CD. The polynomial coefficients are related to the parameters in Eq.27.6.10 as:

$$y = am^2 + bm + c \quad \text{with} \quad a = -\tilde{\alpha}_e \quad b = (2\tilde{B}_e - 2\tilde{\alpha}_e) \quad c = \tilde{\nu}_0 \quad 27.6.11$$

J'←J''	5←6	4←5	3←4	2←3	1←2	0←1	1←0	2←1	3←2	4←3	5←4	6←5
m	-6	-5	-4	-3	-2	-1	1	2	3	4	5	6
$\tilde{\nu}$ (cm ⁻¹)	1264.41	1281.29	1298.00	1313.94	1329.75	1344.81	1374.20	1388.07	1401.51	1414.69	1427.26	1439.62

=====
Results
=====

$$a = -0.2151 \pm 0.00192$$

$$b = 14.59676 \pm 0.006$$

$$c = 1359.7249 \pm 0.037$$

sum of squared residuals = 0.05908

stand. dev. y values = 0.08102

correlation between a & b = 0

correlation between b & c = 0

correlation between a & c = -0.7789

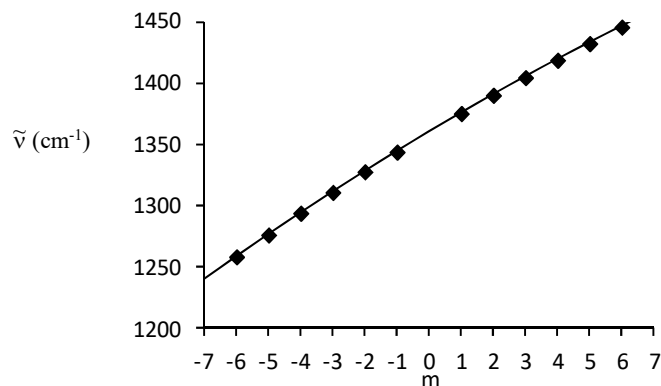


Figure 27.6.6: Quadratic curve fitting to the peak positions for ⁷LiH using $m = J+1$ for the R-branch and $m = -J$ for the P-branch.

The reduced mass for ⁷LiH is:

$$\mu = \frac{m_1 m_2}{m_1 + m_2} = \frac{(7.016004)(1.007825)}{7.016004 + 1.007825} (\text{g mol}^{-1}) \frac{1}{N_A} (1 \text{ kg} / 1000 \text{ g}) = 1.46333136 \times 10^{-27} \text{ kg}$$

Using the fit coefficients: $\tilde{\nu}_0 = 1359.72 \text{ cm}^{-1}$ and $\tilde{\alpha}_e = 0.2151 \text{ cm}^{-1}$

with Eq. 27.6.11: $\tilde{B}_e = (b + 2\tilde{\alpha}_e)/2 = (14.5967 + 2(0.2151))/2 \text{ cm}^{-1} = 7.5135 \pm 0.0036 \text{ cm}^{-1}$

with Eq. 27.4.2: $I = \hbar/(4\pi\tilde{B}_e) = 1.05457266 \times 10^{-34} \text{ J s} / [4\pi(7.5135 \text{ cm}^{-1})(2.997925 \times 10^{10} \text{ cm s}^{-1})]$
 $= (3.72567 \pm 0.0018) \times 10^{-47} \text{ kg m}^2$

with Eq. 27.4.2: $R_e = (I/\mu)^{1/2} = (1.59563 \pm 0.00038) \times 10^{-10} \text{ m} = 1.59563 \pm 0.00038 \text{ \AA}$

with Eq. 27.5.4: $\tilde{\kappa} = 4\pi^2 c^2 \tilde{\nu}_0^2 \mu = 4\pi^2 (2.99792 \times 10^{10} \text{ cm s}^{-1})^2 (1359.72 \text{ cm}^{-1})^2 (1.463331 \times 10^{-27} \text{ kg})$
 $\tilde{\kappa} = 95.99 \text{ N m}^{-1}$

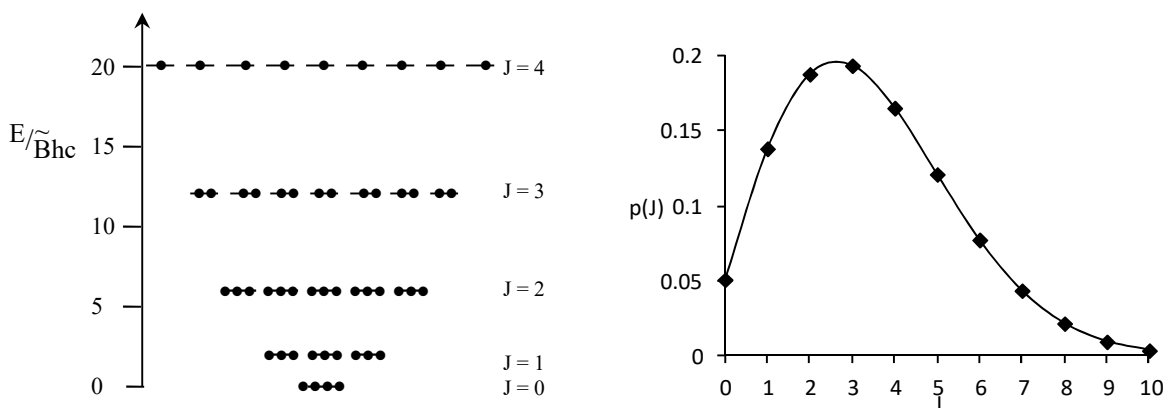
LiH has a comparatively large vibration-rotation interaction constant, which means that the bond length change with vibrational state is significant, which in turn suggests a comparatively anharmonic vibrational potential. For a harmonic potential, the equilibrium bond length is constant with vibrational level.

The intensity of the lines is determined by the Boltzmann distribution of molecules in rotational states J , Figure 27.6.7. The population of each individual state decreases with increasing J . However, the degeneracy of the rotational states, $g_J = 2J + 1$, gives a maximum population in energy levels greater than $J = 0$. As a consequence, the intensity of the rotational fine-structure lines starts at intermediate intensity for $J = 0$ and passes through a maximum for successively higher J states.

Table 27.6.1^(DS): Ground State (GS) Spectroscopic Properties of Diatomic Molecules.²⁻⁷

Molecule	$\tilde{\nu}_e(\text{cm}^{-1})$	$\tilde{\nu}_e\chi_e(\text{cm}^{-1})$	$\tilde{B}_e(\text{cm}^{-1})$	$\tilde{\alpha}_e(\text{cm}^{-1})$	$\tilde{D}_e(\text{cm}^{-1})$	$R_e(\text{\AA})$	$D_0(\text{eV})$	GS
$^1\text{H}^1\text{H}$	4401.21	121.34	60.853	3.062	0.0471	0.7414	4.4776	$^1\Sigma_g^+$
$^7\text{Li}^1\text{H}$	1405.498	23.168	7.51373	0.21639	8.617×10^{-4}	1.5957	2.429	$^1\Sigma_g^+$
$^{12}\text{C}^1\text{H}$	2860.75	64.44	14.460	0.536	14.5×10^{-4}	1.1199	3.46	$^2\Pi$
$^{14}\text{N}^1\text{H}$	3282.7	79.0	16.6679	0.6504	17.1×10^{-4}	1.0362	3.69	$^3\Sigma^-$
$^1\text{H}^{19}\text{F}$	4138.385	89.943	20.9537	0.7934	21.51×10^{-4}	0.91681	5.86	$^1\Sigma_g^+$
$^1\text{H}^{35}\text{Cl}$	2990.925	52.800	10.5933	0.3070	5.32×10^{-4}	1.27455	4.432	$^1\Sigma_g^+$
$^7\text{Li}^7\text{Li}$	351.407	2.583	0.67253	0.00705	9.87×10^{-6}	2.6729	1.06	$^1\Sigma_g^+$
$^{12}\text{C}^{16}\text{O}$	2169.756	13.288	1.93160	0.01751	6.121×10^{-6}	1.1283	11.108	$^1\Sigma_g^+$
$^{14}\text{N}^{14}\text{N}$	2358.6	14.324	1.99824	0.01732	5.8×10^{-6}	1.0977	9.756	$^1\Sigma_g^+$
$^{14}\text{N}^{16}\text{O}$	1904.135	14.088	1.70489	0.01754	0.54×10^{-6}	1.15077	6.497	$^2\Pi$
$^{16}\text{O}^{16}\text{O}$	1580.16	11.9513	1.4456	0.01593	4.839×10^{-6}	1.20752	5.126	$^3\Sigma_g^-$
$^{35}\text{Cl}^{35}\text{Cl}$	559.75	2.6943	0.2442	0.00152	0.186×10^{-6}	1.988	2.476	$^1\Sigma_g^+$

Spectroscopic parameters are a sensitive measure of molecular structure, giving bond lengths, angles, and dissociation energies. However, gross selection rules limit the molecules that can be studied by absorption techniques to those with permanent dipole moments for rotational absorption spectroscopy and to normal modes with a changing dipole moment for vibrational absorption spectroscopy. These restrictions leave out many interesting molecules and normal modes. Assigning the normal modes for polyatomic molecules is difficult if some of the normal modes are not observable because of symmetry. Raman spectroscopy, which is a light scattering technique, fills in the gaps left by absorption spectroscopy and has additional advantages as well.

Figure 27.6.7: Relative population of rotational states for H^{35}Cl at room temperature, with $\tilde{B}_0 = 10.59 \text{ cm}^{-1}$.

27.7 Raman Spectroscopy

The intensity and frequency of light scattered by molecules is an important probe of molecular structure and motion. In a scattering experiment, monochromatic radiation, usually from a laser, is incident on a sample at frequency $\tilde{\nu}_0$, Figure 27.7.1. The scattered light is focused through a lens into a monochromator or interferometer producing a spectrum of the scattered intensity.

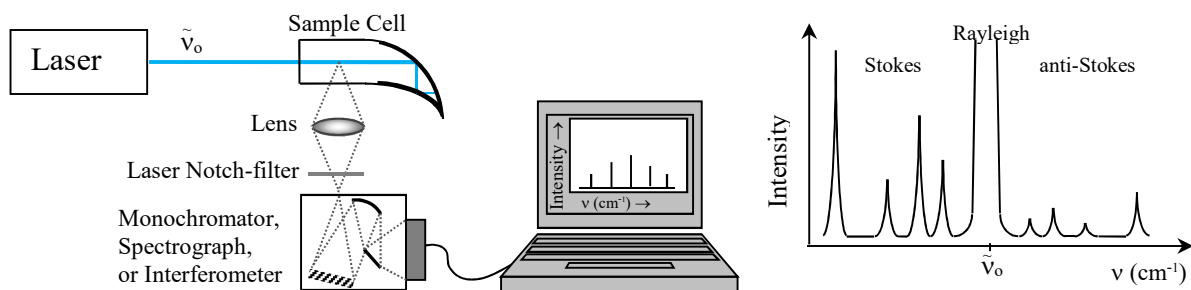


Figure 27.7.1: Raman Spectroscopy. A monochromatic laser is incident on the sample. The light is scattered over a wide range of angles. A spectrum of the scattered light is determined. The sample cell for gases is a Wood's horn (shown). Liquid sample cells include glass cuvettes and capillary tubes. The Rayleigh line is truncated.

The vast majority of the scattered light is at the incident frequency, which is called **elastic** or **Rayleigh scattering**, Figure 27.7.2a. The line width of the Rayleigh scattering is a measure of molecular motion. A small fraction of the scattered intensity is shifted from the incident frequency by interaction with rotations or vibrations of the molecule. Such interactions give rise to **inelastic** or **Raman scattering**, Figure 27.7.2bc. To conserve energy, the wave number difference between the scattered and incident light gives the energy of the molecular transition:

$$\Delta\tilde{\nu} = \tilde{\nu}_0 - \tilde{\nu}_{\text{scattered}} \quad \Delta E = hc|\Delta\tilde{\nu}| \quad 27.7.1$$

If the final rotational or vibrational state is higher in energy than the initial state, the scattered light is lower in energy than the incident light. This light is “redder” than the incident light and is called a **Stokes** transition, Figures 27.7.1 and 27.7.2b. Alternately, if the final rotational or vibrational state is lower in energy than the initial state, the scattered light is higher in energy than the incident light. This light is “bluer” than the incident light and is called an **anti-Stokes** transition, Figure 27.7.2c. The anti-Stokes peak positions mirror the Stokes lines. The energy differences are small compared to the energy of the incident irradiation. For example a helium-neon laser operating in the red at 632.8 nm corresponds to $15,800 \text{ cm}^{-1}$, while rotational transitions are typically less than 10 cm^{-1} and vibrational transitions are typically in the $\sim 30\text{--}4000 \text{ cm}^{-1}$ range. The difference between fluorescence and Raman scattering is that fluorescence requires that the molecule have an excited state with an absorbance band at the incident frequency. For Raman scattering the light is not absorbed. Rather, the molecule interacts with the incident photon for a very short period of time, $\sim 10^{-15} \text{ s}$. Scattering can be thought of as a transient increase of the energy of the molecule into a **virtual state** with the prompt reemission of the photon at or very near the same frequency, in one concerted step. The energy of the virtual state is determined by the energy of the incident photon and does not necessarily correspond to a

molecular excited state. Subject to selection rules, all molecules give Raman spectra using a wide range of incident laser frequencies. Typical lasers for Raman spectroscopy range from near-infrared solid-state diode lasers operating at 1064 nm, green diode-pumped solid-state lasers at 514.5 nm, blue optically-pumped solid-state lasers at 488 nm, or ultraviolet helium-cadmium lasers at 325 nm.

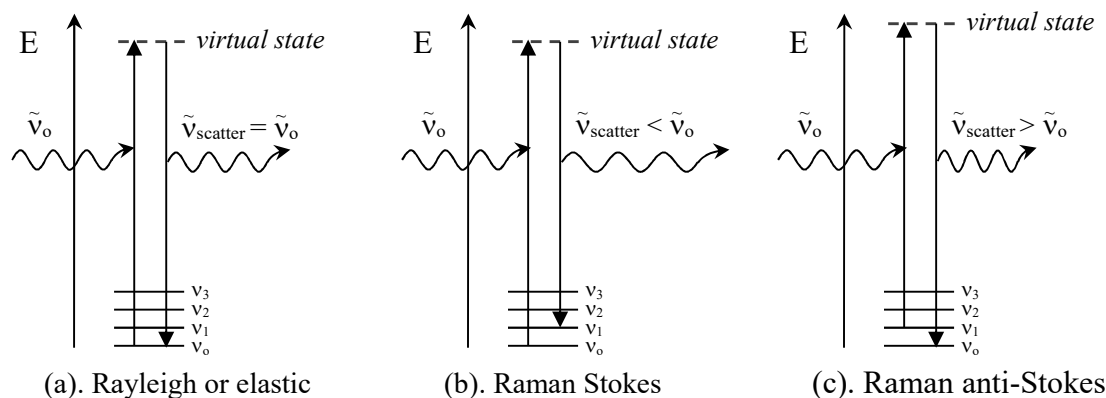


Figure 27.7.2: (a). Rayleigh scattering is at the irradiation frequency, ν_0 . (b). Raman scattering conserves energy with changes in the rotational or vibrational state of the molecule by inelastic scattering of the radiation. Stokes scattering is redder than the incident frequency. (c). Anti-Stokes scattering is bluer than the incident frequency. Vibrational levels are shown for illustration purposes.

The resulting Raman spectra have similar appearance to the corresponding rotational or vibrational absorption spectra, especially if only the Stokes bands are displayed, Figures 27.7.3 and 27.3.4. A major difference is the appearance of the intense, unshifted Rayleigh band at the incident laser wavelength, Figure 27.7.3. A notch-filter is usually placed in front of the monochromator to decrease the intensity of the Rayleigh band, allowing the Raman bands to be more easily displayed. A **notch filter** absorbs in a narrow band of frequencies centered on the incident laser frequency, while allowing redder or bluer light to pass unattenuated. Given that Raman spectra appear to be so similar to microwave or infrared absorption spectra, what is the need for Raman spectroscopy?

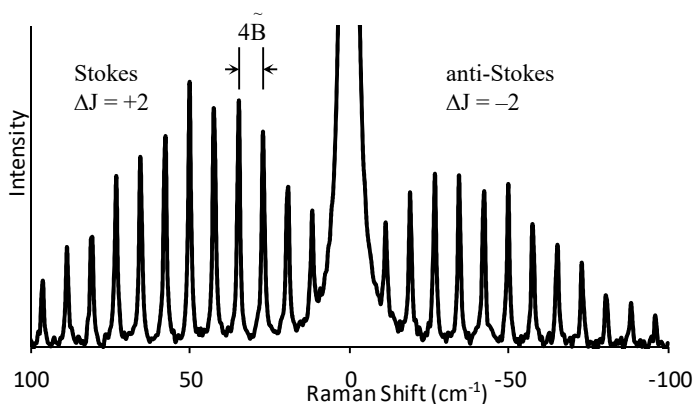


Figure 27.7.3: Rotational Raman spectrum of CO gas.

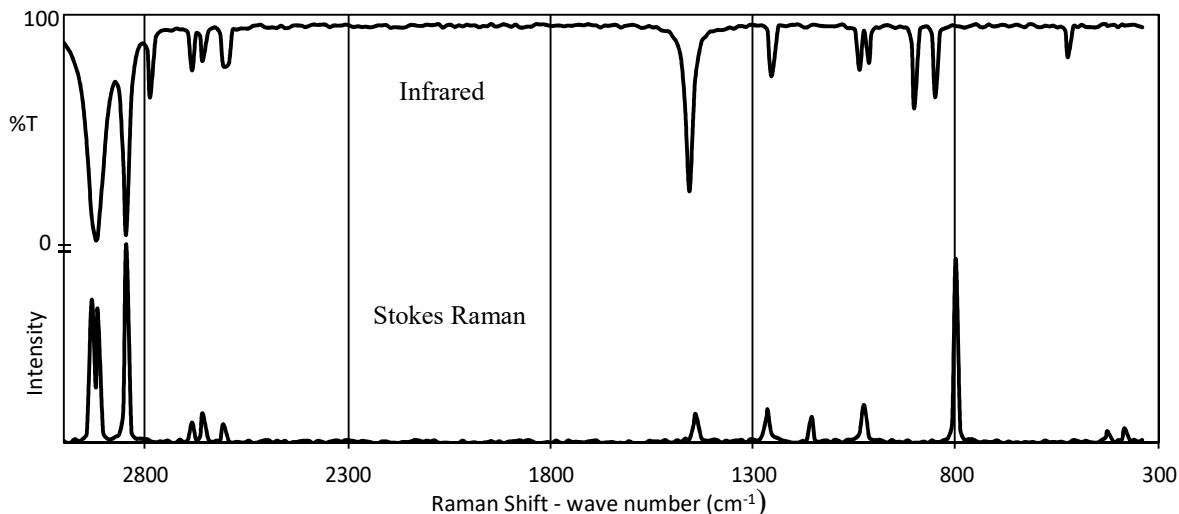


Figure 27.7.4: Vibrational infrared absorption and Raman spectra of liquid cyclohexane. Some transitions occur only in the infrared and some occur only in the Raman. The Rayleigh line is off-scale to the right.

Selection Rules are Different for Light Scattering: In rotational absorption spectroscopy, the intensity of a transition is proportional to the permanent dipole moment. In rotational Raman scattering, the intensity of the transition is proportional to the induced dipole moment. The interaction of the electric field of light with a molecule produces an **induced dipole moment**. The induced dipole moment is proportional to the **polarizability** of the molecule and the strength of the electric field of the incident light, \vec{E} . For a spherical molecule, such as CH_4 , the induced dipole moment $\vec{\mu}$ is given as:

$$\vec{\mu}_{\text{ind}} = \alpha \vec{E} \quad (\text{spherical top}) \quad 27.7.2$$

where α is the polarizability. Molecules with no permanent dipole moment still have an induced dipole upon interaction with light. The polarizability of a molecule is the ease of distortion of the electronic distribution.

Polarizable molecules are “squishier” than non-polarizable molecules. In general, polarizability increases with increasing number of electrons. For example, polarizability increases in the order $\text{HF} < \text{HCl} < \text{HBr}$ or $\text{C}_2\text{H}_2 < \text{C}_3\text{H}_6 < \text{C}_6\text{H}_6$. Polarizability decreases as electrons are more tightly held. For example, polarizability decreases across the isoelectronic series $\text{Cl}^- > \text{Ar} > \text{K}^+$. As the nuclear charge increases across the isoelectronic series, the electrons are more tightly held, and the atomic or ionic volume decreases. The result is that for a given number of electrons, the larger the volume of an ion or molecule the more easily the electron distribution is distorted.

The polarizability of non-spherical molecules depends on the orientation of the molecule with respect to the direction of the electric vector of the incident light. For example, the polarizability of CO_2 is larger along the internuclear axis than perpendicular to the internuclear axis. The induced dipole moment is:

$$\begin{pmatrix} \mu_x \\ \mu_y \\ \mu_z \end{pmatrix}_{\text{ind}} = \begin{pmatrix} \alpha_{xx} & \alpha_{xy} & \alpha_{xz} \\ \alpha_{yx} & \alpha_{yy} & \alpha_{yz} \\ \alpha_{zx} & \alpha_{zy} & \alpha_{zz} \end{pmatrix} \begin{pmatrix} E_x \\ E_y \\ E_z \end{pmatrix} \quad \text{or} \quad \vec{\mu}_{\text{ind}} = \alpha \vec{E} \quad 27.7.3$$

where $\underline{\alpha}$ is the symmetric square matrix of polarizability components. Completing the matrix multiplication gives:

$$\begin{aligned}\mu_{x,\text{ind}} &= \alpha_{xx} E_x + \alpha_{xy} E_y + \alpha_{xz} E_z \\ \mu_{y,\text{ind}} &= \alpha_{yx} E_x + \alpha_{yy} E_y + \alpha_{yz} E_z \\ \mu_{z,\text{ind}} &= \alpha_{zx} E_x + \alpha_{zy} E_y + \alpha_{zz} E_z\end{aligned}\tag{27.7.4}$$

A matrix that expresses the directionality of an atomic or molecular property is called a **tensor**. Polarizability, moments of inertia, and NMR chemical shifts are tensor properties. The directionality of the polarizability is expressed in an analogous fashion to the moment of inertia, Section 27.4, and like the moment of inertia a principal coordinates frame can be found by reorienting the molecule about the axes to give zeros for the off-diagonal components. In the principle coordinates frame, the molecule is visualized as an ellipse, with polarizability components α_{xx} , α_{yy} , and α_{zz} , Figure 27.7.5.

Spherical tops are said to have an **isotropic** polarizability, with $\alpha_{xx} = \alpha_{yy} = \alpha_{zz}$. Non-spherical molecules have an **anisotropic** polarizability, with either $\alpha_{zz} \neq \alpha_{xx} = \alpha_{yy}$ for symmetric tops or $\alpha_{zz} \neq \alpha_{xx} \neq \alpha_{yy}$ for asymmetric tops. In light scattering experiments the electric field of light interacts with the induced dipole moment. For a rotating molecule to present an oscillating induced dipole moment, the molecule must have an anisotropic polarizability. As a result, symmetrical tetrahedral and octahedral molecules do not give either rotational absorption or rotational Raman spectra; CH_4 and SF_6 do not give rotational Raman spectra. However, homonuclear diatomics and symmetric linear molecules, while lacking a permanent dipole, do give Raman spectra. For example, pure rotational Raman spectra are observable for O_2 , N_2 , Cl_2 , CO_2 , and $\text{HC}\equiv\text{CH}$.

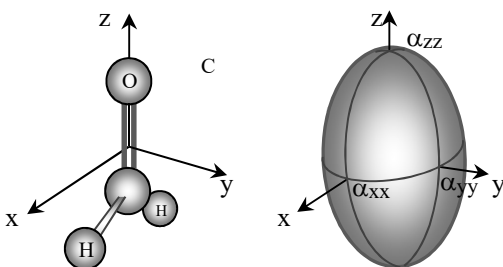


Figure 27.7.5: Molecular polarizability is visualized as an ellipse with dimensions α_{xx} , α_{yy} , and α_{zz} in the principle coordinates frame. The selection rule for rotational Raman is that the molecule must have an anisotropic polarizability.

Rotational Raman: Rotational Raman spectroscopy is analogous to rotational absorption spectroscopy, subject to the selection rule requiring an anisotropic polarizability. A Wood's horn is used as a sample cell for low pressure gases to decrease the intensity of stray light at the incident frequency. This cell has a conical end that is painted black to absorb the transmitted light. Another difference is that the specific selection rule is $\Delta J = \pm 2$ ($\Delta J = 0$ gives Rayleigh scattering). The change in angular momentum quantum number of two results because two photons are involved, the incident and scattered photons. Using Eq. 27.7.1, the Stokes Raman shift for a transition from initial state J'' to final state $J' = J'' + 2$ occurs at:

$$\Delta\tilde{\nu} = \tilde{F}_{J''+2} - \tilde{F}_{J''} = \tilde{B}[(J''+2)(J''+2+1) - J''(J''+1)] = 2\tilde{B}(2J''+3) \quad (J'': \text{lower level}) \quad 27.7.5$$

for $J'' = 0, 1, 2, \dots$. The Stokes shifts are to lower wave number, relative to the incident laser. The anti-Stokes shift for a transition from initial state J'' to final state $J' = J''-2$ occurs at:

$$\Delta\tilde{\nu} = \tilde{F}_{J''-2} - \tilde{F}_{J''} = \tilde{B}[(J''-2)(J''-2+1) - J''(J''+1)] = -2\tilde{B}(2J''-1) \quad (J'': \text{lower level}) \quad 27.7.6$$

for $J'' = 2, 3, 4, \dots$. The negative sign relates that the anti-Stokes shifts are to higher wave number, relative to the incident laser. The spacing between adjacent transitions is $4\tilde{B}$. Our treatment is valid for molecules lacking symmetry, for example heteronuclear diatomics and unsymmetrical linear molecules such as N_2O . We will discuss the case of homonuclear diatomics and symmetrical linear triatomics, such as CO_2 , in the chapter on statistical mechanics. Rotational Raman is complementary to microwave absorption because of the change in selection rule. The selection rules for vibrational absorption and Raman scattering also differ.

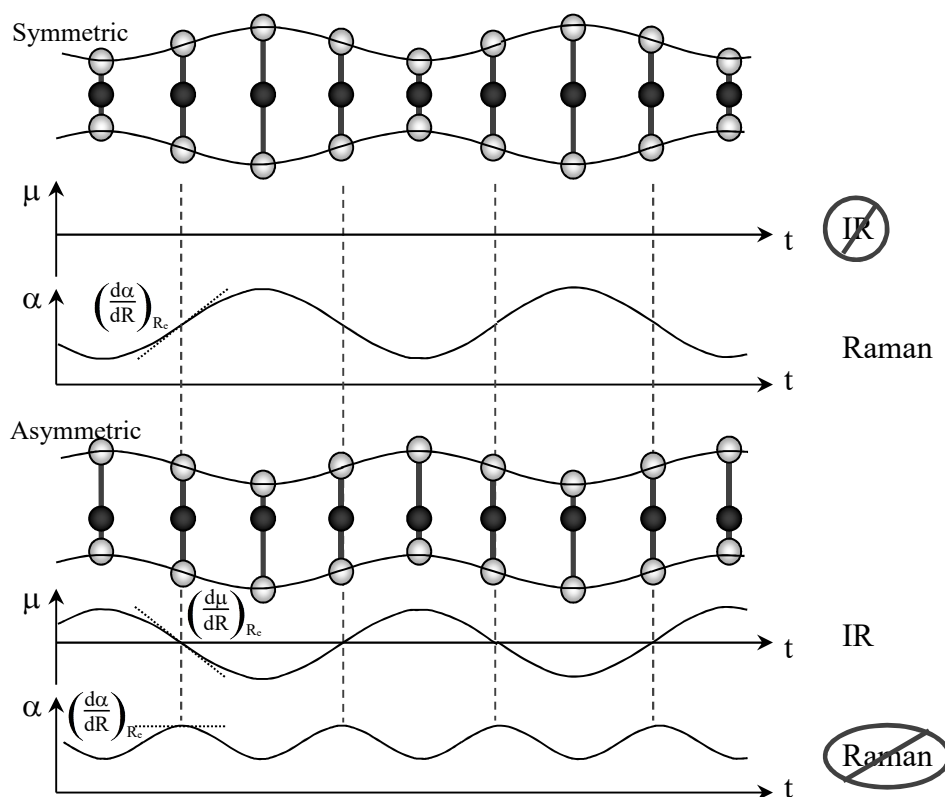


Figure 27.7.6: Symmetric and asymmetric stretch of CO_2 . The equilibrium positions are at the dotted vertical line. The symmetric stretch gives no dipole moment; the symmetric stretch is infrared inactive and Raman active. The derivative of the polarizability for the asymmetric stretch of CO_2 vanishes; the asymmetric stretch is infrared active and Raman inactive.⁸

Vibrational Raman and Absorption Spectroscopy are Complimentary: The selection rule for vibrational Raman spectroscopy is that an element of the polarizability must change during the vibration. For a diatomic molecule, the selection rule is that at least one derivative of the polarizability with respect to the bond length cannot vanish:

$$\left(\frac{d\alpha_{ij}}{dR}\right)_{R_0} \neq 0 \quad \text{with } ij = xx, yy, zz, xy, xz, yz \quad 27.7.7$$

where R is the bond length. For a polyatomic, the derivative is with respect to the normal coordinate of the vibration. The derivative is evaluated at the equilibrium bond length. Homonuclear diatomics are inactive in infrared absorption but are active in Raman scattering. For example, O_2 , N_2 , Cl_2 are infrared inactive and Raman active. Heteronuclear diatomics are both infrared and Raman active.

For polyatomic molecules, the change in dipole moment and polarizability during each normal mode must be determined. We can use the volume of the molecule as an indicator of the polarizability. For example, the symmetric stretch of CO_2 gives no dipole moment. However, the symmetric stretch changes the polarizability, because the normal mode changes the volume of the molecule, Figure 27.7.6. The symmetric stretch of CO_2 is infrared inactive and Raman active. For the asymmetric stretch, the dipole moment changes. However, the volume of the molecule is the same at the positive and negative extremes of the vibration. As a consequence the polarizability has a zero derivative at the equilibrium geometry. The asymmetric stretch and bends of CO_2 are infrared active and Raman inactive.

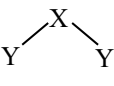
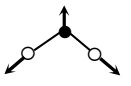
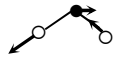
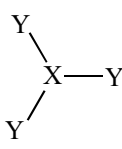
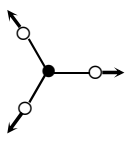
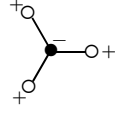
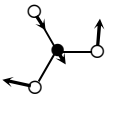
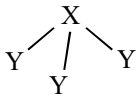
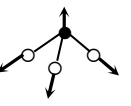
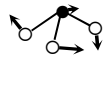
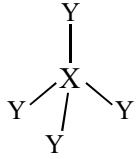
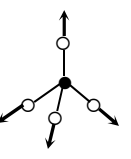
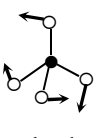
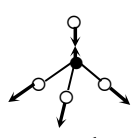
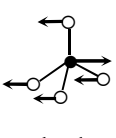
Transitions that are weak or missing in the infrared are often present in the Raman spectra or vice versa. In this sense, vibrational infrared absorption and Raman scattering are complimentary. However, a normal mode can be neither infrared nor Raman active. For a molecule with a center of symmetry, vibrational modes are either infrared active or Raman active, but not both. This restriction is called the **Exclusion rule**. Molecules with a **center of symmetry** have an inversion center. For example, O_2 , N_2 , CO_2 , $HC\equiv CH$, C_6H_6 , $PtCl_4^{2-}$, and SF_6 have an inversion center, are therefore **centrosymmetric**, and the exclusion rule applies. However, N_2O , H_2O , SO_2 , SO_3 , CO_3^{2-} , NH_3 , CH_4 , and $H_2C=CH_2$ do not have a center of symmetry, are not centrosymmetric, and are both infrared and Raman active. The selection rules for the normal modes for several types of small molecules are shown in Table 27.7.1. The point group and symmetry species (e.g. Σ_g^+ , a_1' , a_2'') come from group theory and can be thought of as convenient descriptive names of the normal modes. The application of group theory to rotational and vibrational spectroscopy is covered in the next section.

Raman Transitions of Totally Symmetric Normal Modes are Polarized: Assigning normal modes is aided by collecting Raman spectra with specific polarization, Figure 27.7.7. The Raman spectrum is determined with the direction of polarization of the detected light either parallel, I_{\parallel} , or perpendicular, I_{\perp} , to the incident laser radiation. **Totally symmetric** normal modes maintain the full symmetry of the molecule. For example, the symmetric stretch of CO_2 maintains the equal bond lengths and linear shape of the equilibrium geometry. The symmetric stretch of CO_2 is a totally symmetric vibration. The asymmetric stretch removes the mirror plane and the bending vibrations remove the linear geometry and are therefore not totally symmetric. The depolarization ratio, ρ , is defined as:

$$\rho \equiv \frac{I_{\perp}}{I_{\parallel}} \quad 27.7.8$$

The depolarization ratio is determined by the change in components of the polarizability with the normal mode coordinates, Eq. 27.7.3. The depolarization ratio is $\rho = 3/4$ for vibrations that are not totally symmetric and $\rho \leq 3/4$ for totally symmetric vibrations.

Table 27.7.1: Selection Rules for Representative XY_2 , XY_3 , and XY_4 Molecules or Ions.

Species	Point group	Normal Modes*			
$Y-X-Y$	$D_{\infty h}$ linear	 ν_1 symm stretch Σ_g^+ (R_p)	 ν_2 bend Π_u (IR)	 ν_3 stretch Σ_u^+ (IR)	
	C_{2v} bent	 ν_1 symm stretch a_1 (IR, R_p)	 ν_2 bend a_1 (IR, R_p)	 ν_3 stretch b_2 (IR, R_d)	
	D_{3h} trigonal planar	 ν_1 symm stretch a_1' (R_p)	 ν_2 symm bend a_2'' (IR)	 ν_3 stretch e' (IR, R_d)	 ν_4 bend e' (IR, R_d)
	C_{3v} trigonal pyramidal	 ν_1 symm stretch a_1 (IR, R_p)	 ν_2 symm bend a_1 (IR, R_p)	 ν_3 stretch e (IR, R_p)	 ν_4 bend e (IR, R_d)
	T_d tetrahedral	 ν_1 symm stretch a_1 (R_p)	 ν_2 bend e (R_d)	 ν_3 stretch t_2 (IR, R_d)	 ν_4 bend t_2 (IR, R_d)

* IR is infrared active, R is Raman active, p is polarized, and d is depolarized, e modes are doubly degenerate, t modes are triply degenerate.

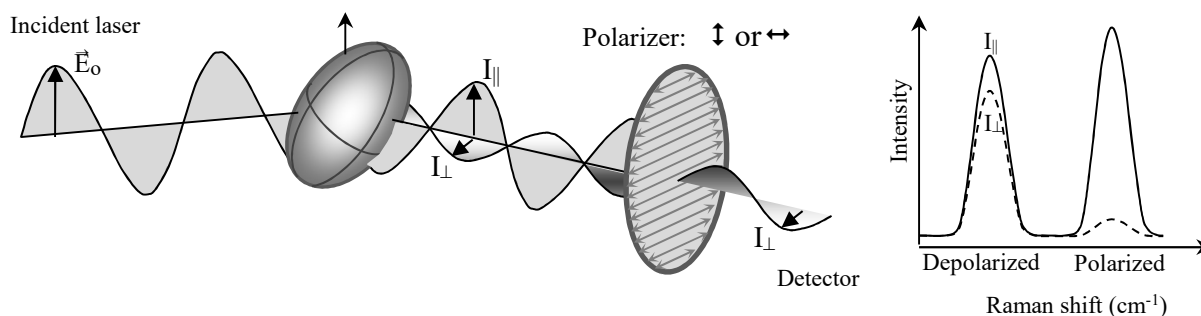


Figure 27.7.7: Depolarization ratios help identify Raman transitions. The spectrum is determined with the plane of polarization parallel and perpendicular to the incident polarization (depolarized I_{\perp} determination illustrated). Strongly polarized bands have $\rho \cong 0$.

Transitions with depolarization ratios $< \frac{3}{4}$ are said to be polarized. The symmetric stretch of CO_2 is polarized, and the asymmetric stretch and bend are depolarized. The depolarization ratio can be near zero for totally symmetric vibrations of molecules with high symmetry, such as CO_2 , SF_6 , and CCl_4 . The normal mode polarization is included in Table 27.7.1.

Forbidden Transitions Can Borrow Intensity from Allowed Combinations and Overtones:

Complications sometimes arise in infrared and Raman spectra. A formally forbidden transition may appear, or the intensity of a weak transition may be larger than expected, or a transition that is expected to be a single line may appear as a doublet. These deviations from expected behavior occur through a **Fermi resonance** of degenerate transitions. For example, in the Raman spectrum of CO_2 , the fundamental symmetric stretch is strong and the fundamental bending vibration is absent, as expected. However, a peak for the first overtone of the bending vibration appears as strongly as the symmetric stretch. In general, overtones are expected to be much less intense than the corresponding fundamentals. The symmetric stretch is at 1388 cm^{-1} in the Raman and the bend is at 667 cm^{-1} in the infrared. The first overtone of the bend at $2(667 \text{ cm}^{-1}) = 1334 \text{ cm}^{-1}$ is nearly degenerate with the symmetric stretch. The first overtone of the bend borrows, or steals, intensity from the Raman allowed symmetric stretch. The interaction results in a small shift of the Raman allowed symmetric stretch to 1389 cm^{-1} and the appearance of the bend first overtone at 1285 cm^{-1} , Figure 27.7.8. The interaction of two nearly degenerate transitions of the same symmetry commonly produces a closely spaced doublet. The first transition takes on some of the character of the second, and the second takes on some of the character of the first; the two states mix. The mixing of degenerate or nearly degenerate states is a general result that occurs in a wide variety of circumstances. For example, if the two wave functions are ψ_1 and ψ_2 , perturbation theory predicts that two new orthogonal states result: $\Psi_+ = a\psi_1 + b\psi_2$ and $\Psi_- = b\psi_1 - a\psi_2$. Anharmonicity is the perturbation that causes a Fermi resonance.

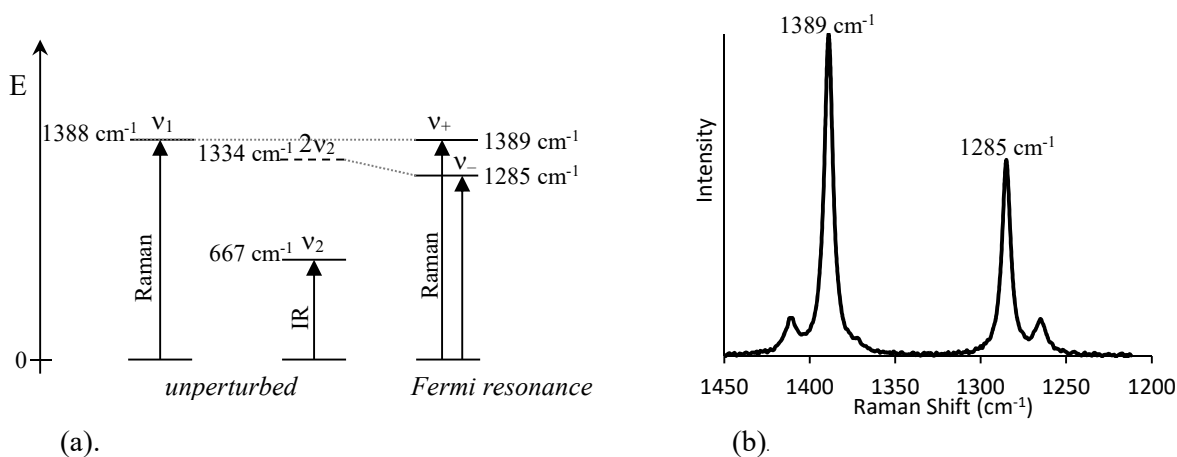


Figure 27.7.8: (a). Fermi Resonance in CO_2 . Nearly degenerate transitions of the same symmetry can borrow intensity to give peaks that are not expected. (b). Raman spectrum of super-critical CO_2 . The smaller side peaks are hot bands.⁹

In Raman spectra of CCl_4 and benzene, closely spaced doublets appear that are Fermi resonances between a fundamental stretch and a combination band. In some ketones, the stretch near 1800 cm^{-1} is a doublet that is caused by a Fermi resonance with an HCH-bend overtone.

Raman Spectroscopy Works Well in Water and is Enhanced On Some Surfaces: One advantage of Raman spectroscopy is that water is an ideal solvent. In infrared absorption, water is problematic because water has high infrared absorption over broad regions of the spectrum. Water is a weak Raman scatterer. Studies of inorganic species, water soluble polymers, and surfactants are facilitated by the ideal qualities of water as a solvent for Raman spectroscopy. Glass, quartz, and plastics have high absorption in the mid-infrared. As a result, cell windows for infrared studies are often formed from water soluble salts, such as NaCl and KBr. However, glass sample cells work well for Raman, since the spectra are taken in the visible or near infrared. Glass cuvettes, NMR tubes, and melting point capillaries are commonly used sample cells. Raman is employed for explosives screening in airports using hand-held spectrometers. Raman spectra can be acquired directly through plastic containers of personal care products, such as shampoo and mouth-wash bottles. The biggest disadvantage of Raman spectroscopy is the poor sensitivity. Approximately only one in 10^9 photons is scattered in Raman processes.

Numerous methods have been devised to enhance Raman scattering. In surface-enhanced Raman spectroscopy, SERS, a roughened metal surface greatly enhances Raman scattering of surface absorbed molecules. Silver and gold nano-particles are also commonly used for SERS. Silver particles support collective surface excitations upon visible light irradiation that enhance the local electric field strength at the surface. Raman spectra of surface absorbed species on roughened or nano-particle silver are attainable with orders of magnitude enhancement over comparable homogeneous solutions. The collective surface excitations, which are called **surface plasmons**, result from collective motion of the electrons near the surface of the metal. The effect is to create electron density waves that propagate along the surface. A useful analogy is to compare the motion of the electrons to the propagation of sound waves. For sound the energy of the wave is propagated by oscillating regions of high and low molecule density. For surface plasmons the energy of the wave is propagated by oscillating regions of high and low electron density at the surface. The effect of the plasmon is to create a strong oscillating electric field near the surface, which is called the **evanescent wave**. This electric field is greater than would have been produced by a single photon. The evanescent wave enhances the induced dipole moment, Eq. 27.7.3. Surface plasmons are discussed, in conjunction with SPR kinetics, in Section 5.4. One caution is that SERS can have a different pattern of transition intensities compared to pure Raman spectra, because molecules can change symmetry upon absorption to the metal surface. We next consider the effect of molecular symmetry on rotational and vibrational spectra.

27.8 The Effects of Molecular Symmetry: Group Theory

Group theory provides a succinct description of the shape of a molecule and the effect the shape has on molecular properties. The goal of the spectroscopic applications of group theory is to predict if a given transition is allowed or forbidden. For IR absorption, if the transition electric dipole moment is non-zero, $\int \Psi_j^* \hat{\mu} \Psi_i d\tau \neq 0$, the transition is allowed, Eqs. 27.1.6-27.1.10. If the transition electric dipole moment vanishes, $\int \Psi_j^* \hat{\mu} \Psi_i d\tau = 0$, the transition is forbidden. Determining the number of forbidden transitions provides useful information and can be the key to determining the shape of a molecule from spectra. Group theory is a mathematically elegant theory. However, a discussion of the mathematical principles is beyond the scope of this text. Rather, we will take a practical approach and explore the relationship of molecular symmetry to spectroscopic properties through examples. We first describe how to characterize the symmetry of a molecule by a point group and the corresponding symmetry of the vibrational normal modes.

Then we use the point group symmetry to determine the normal modes that cause a transition dipole to vanish.

The Symmetry of a Molecule Is Described by a Point Group: The symmetry of a molecule is determined upon rotation, reflection, and inversion. Consider first rotation symmetry. Formaldehyde has a two-fold rotation axis, CHCl_3 and BF_3 have a three-fold rotation axis, and benzene has a six-fold rotation axis, Figure 27.8.1. Symbolically, the **proper rotation axes** are listed as C_n , where n is the order of the rotation; CHCl_3 has a C_3 axis and benzene has a C_6 axis. Symmetrical molecules can have more than one rotation axis. For example, BF_3 and benzene have three unique C_2 -axes, Figure 27.8.1cd. The lower order rotation axes are often implied by the higher-order symmetry. The highest order rotation axis is called the **principle axis** and is assigned as the z -direction by convention.

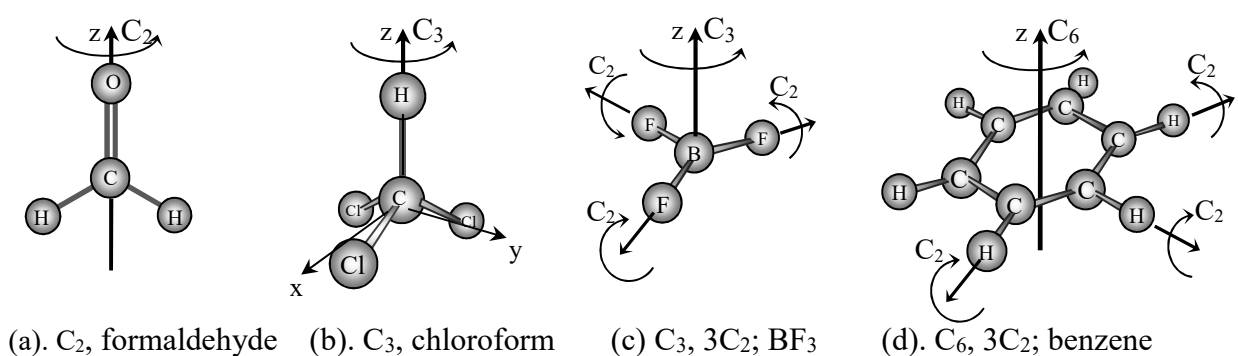


Figure 27.8.1: n -Fold proper rotation axes, C_n .

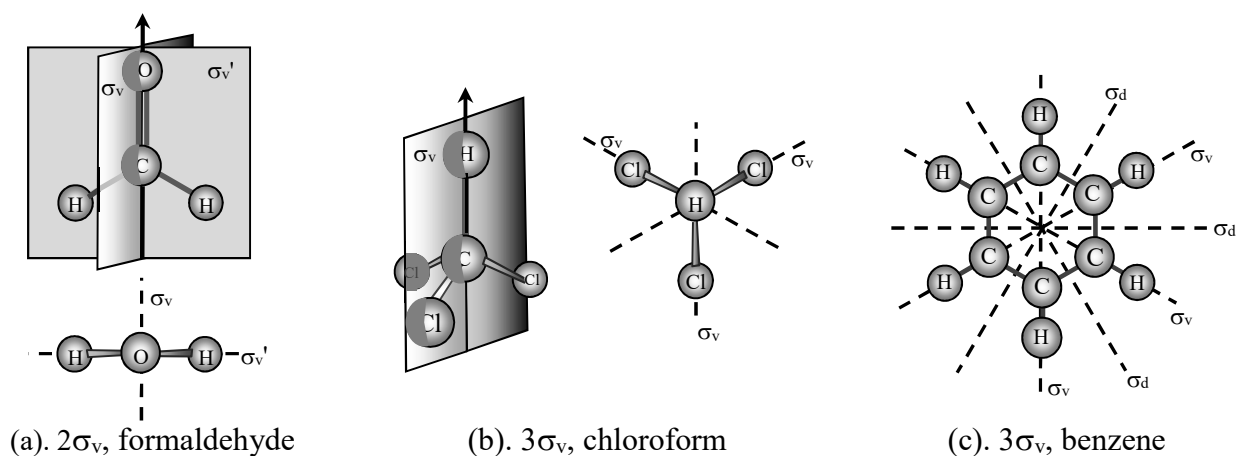


Figure 27.8.2: Vertical reflection planes, σ_v . (a). Formaldehyde perspective illustration (top) and the projection along the C_2 -axis (bottom). (b). Only one of the three σ_v planes is shown in the chloroform perspective illustration, for simplicity (left). All three σ_v -planes are shown in the projection along the C_3 -axis (right) (c). Benzene projection along the C_6 -axis.

Next consider reflection symmetry. For example, reflection across a plane that includes the x - and z - axes, σ_{xz} , inverts the coordinate perpendicular to the symmetry plane: $(x,y,z) \rightarrow (x,-y,z)$. Two types of reflection planes are found in objects. A **vertical reflection plane**, σ_v , includes the

principle axis. For example, formaldehyde has two σ_v -planes, one in the plane of the nuclei and one perpendicular to the plane of the nuclei, Figure 27.8.2a. Chloroform and BF_3 have three σ_v -planes. Benzene has six σ_v -planes, three pass through the nuclei and three between the nuclei, Figure 28.8.2c. In highly symmetrical molecules, like benzene, a distinction is made between two types of σ_v -planes. Dihedral-reflection planes, labeled σ_d , bisect two C_2 -axes that are perpendicular to the principal axis. In general, the σ_v -planes are the set that pass through the maximum number of nuclei and the σ_d -planes are the set that pass through the fewest nuclei.

The second type of reflection plane is a **horizontal reflection plane, σ_h** . A horizontal reflection plane is perpendicular to the principle axis. Benzene and BF_3 have a σ_h -plane, while formaldehyde and chloroform do not, Figure 27.8.3.

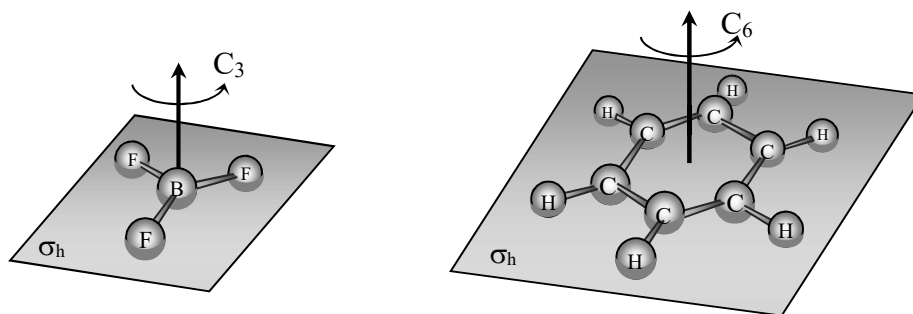


Figure 27.8.3: Horizontal reflection planes, σ_h .

Next consider inversion. We introduced the **inversion** operation in the molecular structure chapter for the characterization of the molecular orbitals of diatomic molecules. The inversion operation, i , inverts all the coordinates across the center of mass: $(x,y,z) \rightarrow (-x,-y,-z)$. Homonuclear diatomic molecules have an inversion center. Benzene has an inversion center, while formaldehyde, chloroform, and BF_3 do not.

One additional type of symmetry operation is required to completely characterize all molecules. An **improper rotation, S_n** , is an n -fold rotation followed by a horizontal reflection. Methane has an S_4 -axis and ethane has an S_6 axis, Figure 27.8.4. An S_2 is equivalent to inversion: $C_2\sigma_h = i$.

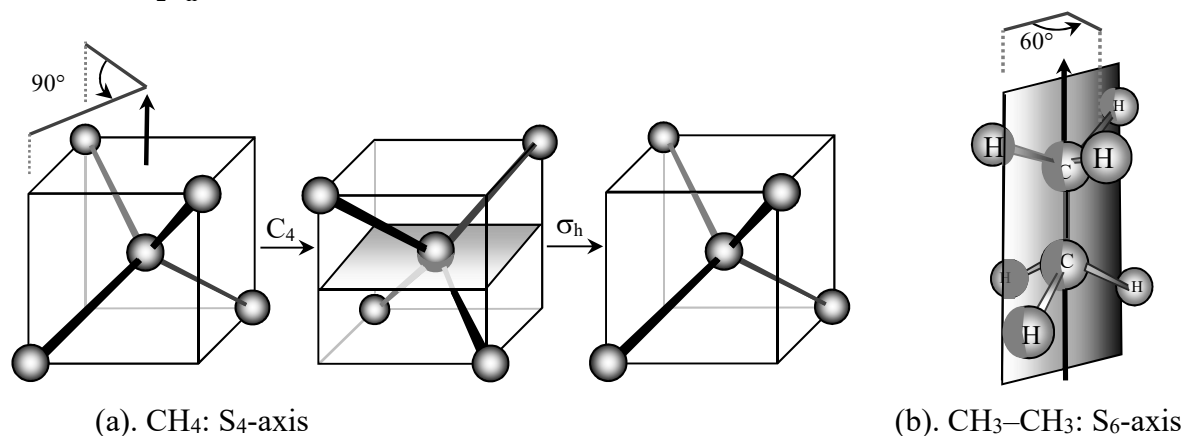


Figure 27.8.4: Improper rotation axes, S_n , combine a rotation by $360^\circ/n$ and a horizontal reflection. Methane has an S_4 -axis and ethane has an S_6 axis.

Methane has C_3 and C_2 -axes in addition to three S_4 -axes, Figure 27.8.5a. The three C_2 -axes are collinear with the S_4 -axes. Because there are multiple C_3 axes, tetrahedral molecules don't have a distinct principle axis. Methane has three σ_d -planes, Figure 27.8.5b.

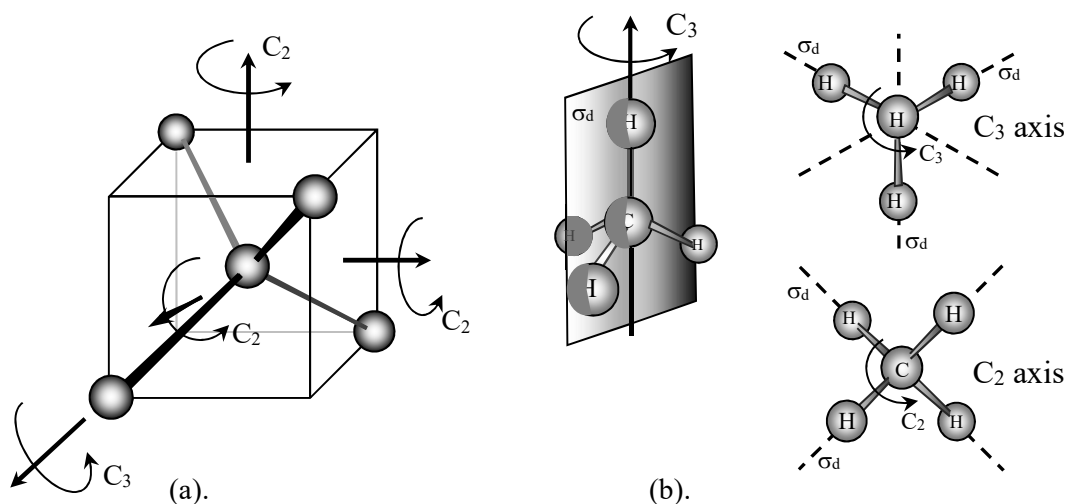


Figure 27.8.5: (a). C_3 and C_2 axes for CH_4 . Only one of the three C_3 -axes is shown. (b). Dihedral reflection planes, σ_d . For the perspective view, only one dihedral reflection plane is shown. For the view down the C_2 -axis, only two of the dihedral planes are shown.

A molecule is assigned to a **point group** on the basis of its symmetry operations. The point group summarizes all the geometric relationships of the molecule. A listing of the symmetry operations that define the various point groups is given in Table 27.8.1. The order of the group, h , is the total number of symmetry operations of the group. For mathematical completeness, the **unity operator**, E , is defined. The effect of the unity operator is to leave everything unchanged. The unity operator takes the place of multiplication by one in simple arithmetic: $1(x) = x$. Every molecule has E as one of its symmetry operations. The sequential application of related symmetry operations gives the unity operator. For example, three successive C_3 rotations leaves the molecule unchanged: $C_3C_3C_3 = E$. Two successive inversions leaves the molecule unchanged, $ii = E$.

Completely unsymmetrical molecules only have the unity operation and are in point group C_1 . If a molecule has only the unity operation and inversion, the point group is C_i . Water has a C_2 -axis and two vertical mirror planes, giving the point group as C_{2v} , Figure 26.6.4. BF_3 has a C_3 -axis and a σ_h -plane giving D_{3h} . Benzene has a C_6 -axis and a σ_h giving the D_{6h} point group. Rotation by any angle about the internuclear axis leaves a linear molecule unchanged, giving a C_∞ -axis. Heteronuclear diatomics and unsymmetrically substituted linear triatomics, such as N_2O , are in point group $C_{\infty v}$. Homonuclear diatomics and Y-X-Y linear triatomics, such as CO_2 , have a σ_h -plane giving $D_{\infty h}$. Methane is in the T_d point group. The complete listings of all the symmetry operations of each point group are given in the first row of the group's **character table**, Table 27.8.2, and Figure 27.8.6.

Table 27.8.1: Point Group Operations with the Order of the Principle axis, n .¹⁰

Point Group	Important Symmetry Operations	Example	h
C_1	E	HCFCIBr	1
C_i	i	$C_2H_2F_2Cl_2$	2
C_s	σ	O=CHCl, CH_2ClBr	2
C_n	C_n	H_2O_2 , B(OH) ₃	n
S_n (note*)	S_n	$S_4N_4F_4$	n
C_{nv}	C_n, σ_v	H_2O , O_3 , NH_3	$2n$
C_{nh}	C_n, σ_h	<i>trans</i> - CH_2F_2	$2n$
D_n	$C_n, \perp C_2$	$Co(en)_3^{3+}$	$2n$
D_{nd}	$C_n, \perp C_2, \sigma_d$	C_3H_2 , C_2H_6	$4n$
D_{nh}	$C_n, \perp C_2, \sigma_h$	C_2H_4 , BF_3 , C_6H_6	$4n$
$C_{\infty v}$	linear molecules with no center of inversion	HCl, N_2O	∞
$D_{\infty h}$	linear molecules with a center of inversion	O_2 , CO_2	∞
T_d	tetrahedral symmetry (C_3, C_2, S_4, σ_d)	CH_4 , CCl_4	24
T_h	tetrahedral symmetry, σ_h	$Cu(NO_2)_6^{4-}$	24
O_h	octahedral symmetry ($C_4, C_3, C_2, S_6, S_4, \sigma_h, \sigma_d$)	SF_6	48
I_h	icosahedral symmetry	C_{60} , $B_{12}H_{12}^{2-}$	120

* For S_n , n must be even, otherwise, $S_n = C_{nh}$

Table 27.8.2^(DS): Character Tables for Common Point Groups C_{2v} , C_{3v} , D_{3h} , T_d .

C_{2v}	E	C_2	σ_v	σ_v'	$h = 4$	
A_1	1	1	1	1	z, z^2, x^2, y^2	
A_2	1	1	-1	-1	xy	R_z
B_1	1	-1	1	-1	y, yz	R_x
B_2	1	-1	-1	1	x, xz	R_y

C_{3v}	E	$2C_3$	$3\sigma_v$	$h = 6$	
A_1	1	1	1	z, z^2, x^2+y^2	
A_2	1	1	-1		R_z
E	2	-1	0	$(x,y), (x^2-y^2, xy), (xz, yz)$	(R_x, R_y)

D_{3h}	E	σ_h	$2C_3$	$2S_3$	$3C_2'$	$3\sigma_v$	$h = 12$	
A_1'	1	1	1	1	1	1	z^2, x^2+y^2	
A_2'	1	1	1	1	-1	-1		R_z
A_1''	1	-1	1	-1	1	-1		
A_2''	1	-1	1	-1	-1	1	z	
E'	2	2	-1	-1	0	0	$(x, y), (xy, x^2-y^2)$	
E''	2	-2	-1	1	0	0	(xz, yz)	(R_x, R_y)

T_d	E	$8C_3$	$3C_2$	$6\sigma_d$	$6S_4$	$h = 24$	
A_1	1	1	1	1	1	$x^2+y^2+z^2$	
A_2	1	1	1	-1	-1		
E	2	-1	2	0	0	$(3z^2-r^2, x^2-y^2)$	
T_1	3	0	-1	-1	1		(R_x, R_y, R_z)
T_2	3	0	-1	1	-1	$(x, y, z), (xy, xz, yz)$	

Vibrations Behave Differently Under Transformations of the Point Group: The next step in determining the selection rules of normal mode vibrations is to determine how each normal mode transforms according to the symmetry operations of the point group. Character tables are the key to this determination. Consider a symmetrical, bent triatomic like H_2O , which is in the C_{2v} point group. The normal modes are the ν_1 -symmetric stretch, ν_2 -bend, and ν_3 -asymmetric stretch, Figure 27.8.7. All the normal mode displacements are in-plane for C_{2v} . The transformation properties of the normal mode displacements determine the corresponding symmetry species that represents the normal mode. The symmetry species are the **irreducible representations** of the group. In the character table for C_{2v} , the rows labeled A_1 , A_2 , B_1 , and B_2 are the irreducible representations of the group.

Each irreducible representation describes a unique set of symmetry properties for an object, Figure 27.8.6. The types of objects include molecular translations, molecular rotations, normal modes, and molecular orbitals. We used these representations in assigning the symmetry properties of the molecular orbitals for bent triatomics; a rotation by 180° corresponds to a C_2 -rotation, Figure 26.6.4. Comparing Table 27.8.2 for C_{2v} and the orbital symmetry properties listed in Figure 26.6.4, note that the symmetric and antisymmetric behavior under C_2 -rotations and σ_v -reflections is taken from the rows of the character table; a character of 1 corresponds to symmetric and a -1 to antisymmetric. Lobes of molecular orbitals are characterized by their phase. The normal modes are drawn with vectors representing the atoms displacements. For normal modes, if the phases of the displacement vectors in expansion or contraction are unchanged by the symmetry transformation, the result is symmetric. If the direction vectors change direction, for example from expansions to contractions, the mode is antisymmetric.

Point Group	Classes of symmetry operations			Order of group (total operations)		
C_{3v}	E	(2) C_3	(3) σ_v	h = 6		
A_1	1	1	1	z (and T_z)	z^2, x^2+y^2	R_z (R_x, R_y)
A_2	1	1	-1	(x,y) (and T_x, T_y)	$(x^2-y^2, xy), (xz, yz)$	
E	2	-1	0			
Irreducible representations of the group-symmetry species for objects	Characters of the irreducible representations			IR activity and molecular translations, T	Raman activity	Molecular Rotations

Figure 27.8.6: Character tables give the transformation properties of the normal modes or molecular orbitals for a molecule with the point group symmetry.¹¹ Operations of the same type are grouped in classes. Functions in parenthesis are degenerate and transform together.

Normal modes are either symmetric or antisymmetric with respect to the transformations of the point group. In Figure 27.8.7, for the ν_1 -symmetric stretch, a rotation about the principle axis or a reflection across the σ_v -plane converts the displacement vector for the hydrogen on the left into the displacement vector for the hydrogen on the right; ν_1 is symmetric with respect to C_2 and σ_v giving a_1 -symmetry. The same symmetric transformations result for the ν_2 -bend, giving the bend also as a_1 . For the ν_3 -symmetric stretch, a rotation about the principle axis or a reflection across

the σ_v -plane inverts the displacement vector for the hydrogen on the left compared the displacement vector for the hydrogen on the right; v_3 is antisymmetric with respect to C_2 and σ_v giving b_2 -symmetry.

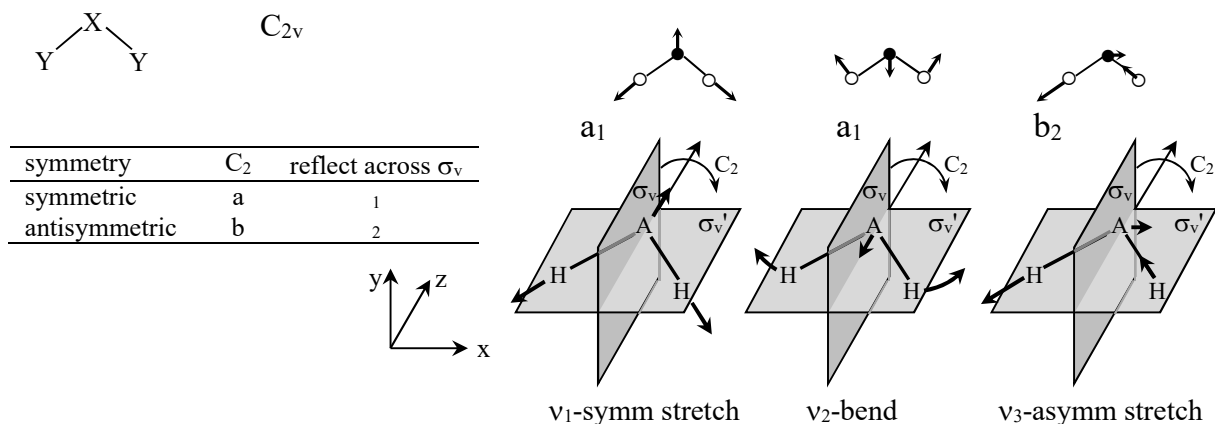


Figure 27.8.7: Symmetry properties of the normal modes of a symmetrical, bent triatomic, point group C_{2v} . The symmetry of the normal mode is given by the irreducible representation. (Out of plane motions correspond to rotations for a bent triatomic.)

The Transition Dipole Has a Corresponding Symmetry: The transition electric dipole moment of a molecule is given by the integrals of the vector components of the electric dipole, Eq. 27.1.7:

$$\mu_{tr,x} \propto -e \int \chi_{v'}(x - x_e) \chi_{v''} dq \quad \mu_{tr,y} \propto -e \int \chi_{v'}(y - y_e) \chi_{v''} dq \quad \mu_{tr,z} \propto -e \int \chi_{v'}(z - z_e) \chi_{v''} dq \quad 27.8.1$$

where dq represents the progress of the normal coordinates of the vibration. To determine if the components of the transition dipole vanish, we need to determine the symmetry properties of the x , y , and z -components of the electric dipole moment operator. As a convenient visual device, the p_x , p_y , and p_z -atomic orbitals have the same functional form as the dipole moment components with respect to the functions x , y , and z , Eq. 25.2.8 and Figure 27.8.8. The atomic orbitals are easier to visualize.

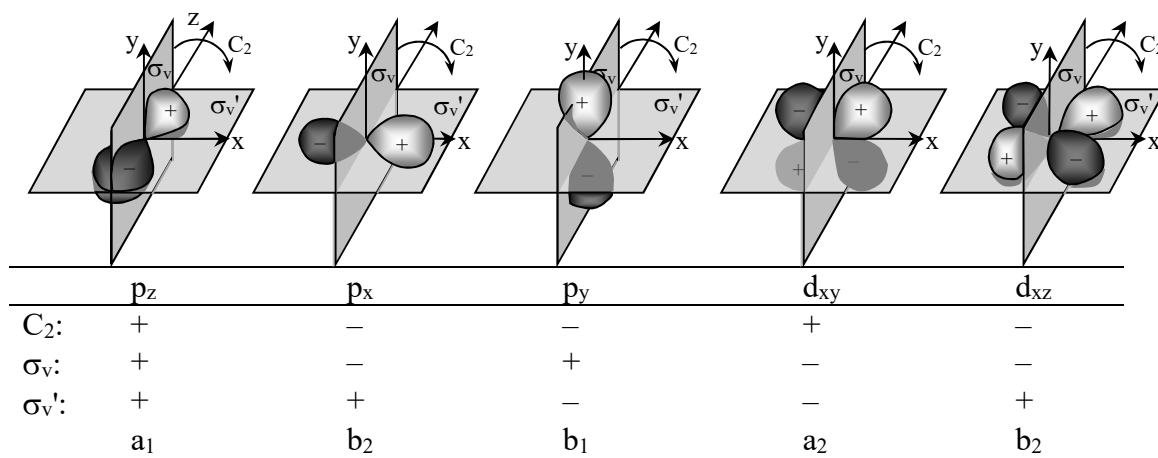


Figure 27.8.8: Transformation of atomic p - and two d -orbitals under point group C_{2v} .

The p_z -orbital retains the same sign under all transformations; the p_z -orbital and the z -component of the dipole moment operator transform according to the totally-symmetric representation of the point group, a_1 . The p_x -orbital changes sign upon rotation about the C_2 -axis and upon reflection across the σ_v -plane, but retains the same sign upon reflection across the σ_v' -plane; accordingly, the p_x -orbital and the x -component of the dipole moment operator transform according to the b_2 -representation. The p_y -orbital changes sign upon rotation about the C_2 -axis and upon reflection across the σ_v' -plane, but retains the same sign upon reflection across the σ_v -plane; the y -component of the dipole moment operator and the p_y -orbital transform according to the b_1 -representation.

Normal Mode Symmetry Determines IR and Raman Activity: For an interaction to occur between light and a vibrational normal mode, the normal mode must present an oscillating dipole moment. The derivative of the electric dipole moment with respect to the motion of the normal mode must be non-zero, Eq. 27.1.11. By the Born-Oppenheimer approximation in this dipole moment derivative, the electronic portion of the integral is separable from the integral over the nuclear coordinates. The electronic integral can be represented as partial charges on each of the i -atoms, e_i . Starting with Eq. 27.1.5, the resulting electric dipole moment operator for vibrations reduces to a function of just the nuclear coordinates and the partial charge on each atom:^{13,14}

$$\mu_x = \sum e_i x_i \quad \mu_y = \sum e_i y_i \quad \mu_z = \sum e_i z_i \quad (\text{nuclear coordinates}) \quad 27.8.2$$

The transition dipole moment components in the x , y , and z -directions interact with the electric field of light in the x , y , and z -directions, respectively. The following selection rule results in infrared absorption:

In absorption, the transition dipole moment vanishes unless the normal mode transforms according to the same representation as the x , y , or z -component of the dipole moment.

Any one of the x , y , or z -components of the dipole moment suffice. In the gas or liquid phases, molecules rapidly tumble allowing each component of the transition dipole to align with the electric vector of the light. For example with XY_2 C_{2v} molecules, the ν_1 -symmetric stretch and the ν_2 -bend have the same a_1 -symmetry as the z -component of the dipole moment. As a consequence the ν_1 -symmetric stretch and ν_2 -bend give allowed transitions in absorption. The ν_3 -asymmetric stretch, which has the same b_2 -symmetry as the x -component of the dipole moment, also gives an allowed transition. All normal modes of C_{2v} -molecules are possibly infrared-active, as summarized in Table 27.7.1. The normal modes are described as possibly active, because while not forbidden by symmetry, the transition dipole moment may give a result of zero for reasons other than symmetry. Now, what about Raman transitions?

The components of the polarizability transform according to the functions, z^2 , x^2 , y^2 , xy , xz , and yz for C_{2v} molecules, Eq. 27.7.3. Once again we can determine the representation of the symmetry of these operators by comparison to the symmetry of the corresponding atomic orbitals. Compared to the polarizability components, the d -orbitals have the appropriate functional form. Figure 27.8.8 shows that under C_{2v} the d_{xy} -orbital, with lobes between the x - and y -axes, retains the same sign upon rotation by 180° about the z -axis; the d_{xy} -orbital and the xy component of the polarizability transform as a_2 . The d_{xz} -orbital, with lobes between the x - and z - axes, transforms as b_2 . The z^2 -, x^2 -, and y^2 -components are always positive and so transform according to the totally symmetric representation, a_1 . The following selection rule results in Raman scattering:

In Raman scattering, the transition moment vanishes unless the normal mode transforms according to the same representation as a component of the polarizability.

For C_{2v} , the polarizability components taken together include all the irreducible representations of the point group; as a consequence all normal modes are possibly Raman active, as listed in Table 27.7.1.

Symmetry Relationships are Summarized in a Character Table: The irreducible representations of a point group are given symbols A, B, E, and T, except for groups with a C_∞ -axis. Often lower case is used for the symmetry of specific objects, while upper case is used for the corresponding irreducible representation listed in the character table. The A-representations are symmetric with respect to rotation of the highest-fold C_n -axis, while the B-representations are asymmetric. E-representations are two-dimensional, which for vibrations corresponds to doubly degenerate normal modes. T-representations are for triply degenerate normal modes. For groups without an inversion center, the ₁, ₂, and ₃-subscripts differentiate the transformation properties within each type of representation. For groups with an inversion center, the subscript is either _g or _u; g for gerade, even, symmetric and u for ungerade, uneven, antisymmetric. Unfortunately, the ₁, ₂, and ₃-subscripts are arbitrary; different authors and molecular structure programs switch these designations. The E-representation is not related to the identity operator, E. The double use of the E-symbol is not consequential. Some authors use F as a symbol in place of T for triply degenerate representations. The transformation properties of the functions that are the basis for the electric dipole moment and polarizability, functions like x, y, z, xy, xz, etc., are listed at the right in the character tables. The transformation properties of whole-molecule, center-of-mass translations along the x-, y-, and z-axes are identical to the functions x, y, and z: $x = T_x$, $y = T_y$, and $z = T_z$. The transformation properties of molecular rotations around the x-, y-, and z-axes are listed as R_x , R_y , and R_z . Operations of the same type are grouped in classes. The identity element is one class and the rotation operators for a given n are separate classes. The vertical-reflections and dihedral-reflections are separate classes, and inversion is a class. The number of irreducible representations is equal to the number of classes. For example the classes of symmetry transformations for D_{3h} are E, σ_h , $2C_3$, $2S_3$, $3C_2'$, and $3\sigma_v$ giving six irreducible representations. All normal modes of D_{3h} molecules transform according to one of these six irreducible representations.

When determining the symmetry upon transformation of degenerate normal modes, the degenerate modes “transform together.” In general, degenerate states with the same symmetry mix and cannot be separated.

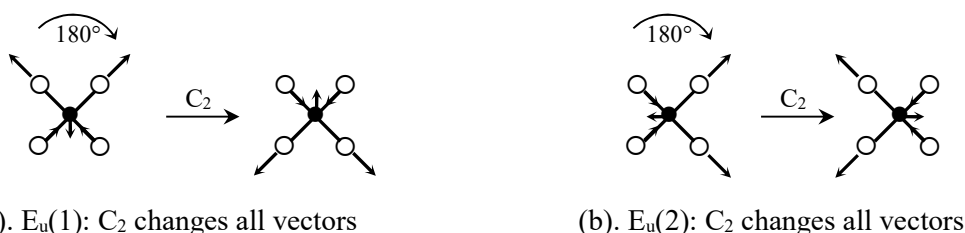


Figure 27.8.9: Degenerate modes transform together. The character of the rotation operation is the combination of the results for both of the degenerate orbitals. For this example asymmetric stretch, the net character is -2 under C_2 -rotation.

For example, consider a square-planar molecule such as XeF₄. The transformation of the doubly-degenerate E_u-normal modes under C₂-rotation is shown in Figure 27.8.9. Transformation of each degenerate mode inverts all atom coordinates, giving -2 for both taken together. Luckily for many small molecules, the assignment of the normal modes corresponding to E- or T-representations can be done simply on the basis of degeneracy and the careful evaluation of the transformation properties can be side-stepped.

The example of the C_{2v}-case is easily done visually. However, molecules with higher symmetry are more difficult and interesting. A general step-by-step procedure to determine the point group transformation properties of normal modes is useful. Ammonia, which is in the C_{3v}-point group, is used as an example.

Ammonia has 3N-6 = 6 normal modes. The number of stretching vibrations is usually equal to the number of bonds. We then expect three stretching vibrations and three bending vibrations for NH₃. The **all-mode vibrational analysis** is:

The characters of the reducible representation of all atom displacements are first determined:

1. The number of atoms that are stationary under transformation by the operations of the classes in the point group is determined. Any convenient transformation within the class can be used, since all operations within the same class are equivalent. The results for NH₃ are listed as *step-1* in Figure 27.8.10. For C₃-rotation only the N-atom is stationary. Two atoms, an N- and H-atom, lie on each σ_v-plane.

2. The sum of the characters for the irreducible representations of the three-translations, Γ_{trans}, is added to the table as *step-2*.

3. The characters of the reducible representation of all atom displacements, Γ_{tot}, are the class-by-class product of the number of stationary atoms and the representation of the translations, Γ_{trans}, as listed as *step-3*.

The characters of the reducible representation of the vibrations are determined:

4-5. The atom displacements include the translation of the center-of-mass and whole-molecule rotations. The corresponding characters must be subtracted from the total, just as we did when deriving the 3N-6 formula for the number of normal modes. The sum of the characters for the irreducible representations of the three-translations, Γ_{trans}, and the three-rotations, Γ_{rot}, are added up from the character table and listed as *steps 4* and *5*. For example, the translations T_x, T_y, and T_z transform according to A₁ + E. The E-irreducible representation is two-dimensional, which represents both T_x and T_y. The characters of A₁ and E add class-by-class to give 3, 0, and 1.

6. The characters for translation and rotation are subtracted from the total giving the reducible representation of the normal modes, Γ_{vib}. The results are listed as *step-6*.

The reducible representation of the vibrations is decomposed into irreducible representations:

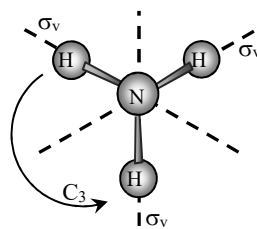
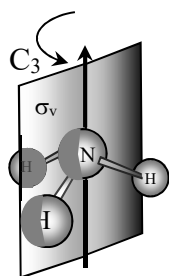
7-9. The number of times that an irreducible representation of the point group appears in the reducible representation of the normal modes is determined by taking the product of Γ_{vib} with the characters of each irreducible representation and then dividing by the order of the group:

$$a_i = \frac{1}{h} \sum_{j=1}^q \chi_j^{vib} \chi_{1,j}^{irr} C_{1,j}^{irr} \quad i = \text{irreducible representation, } j = \text{class} \quad 27.8.2$$

where $\chi_{i,j}^{irr}$ is the character for irreducible representation i and class j from the character table and χ_j^{vib} is the character for the reducible representation of all the vibrations for class j . The sum extends over all classes, q . This sum is analogous to the dot product of vectors. For reference the characters of the irreducible representations are copied into the table as *steps 7-9*. The decomposition for the A_1 irreducible representation is:

$$a_1 = \frac{1}{h} \sum_{j=1}^4 \chi_j^{vib} \chi_{i,j}^{irr} C_{i,j}^{irr} = \frac{1}{6} [\underset{\chi^1}{6} \underset{\chi_{1,1}^{irr}}{(1)} \underset{C_{1,1}^{irr}}{(1)} + \underset{\chi^2}{0} \underset{\chi_{1,2}^{irr}}{(1)} \underset{C_{1,2}^{irr}}{(2)} + \underset{\chi^3}{2} \underset{\chi_{1,3}^{irr}}{(1)} \underset{C_{1,3}^{irr}}{(3)}] = 12/6$$

giving that A_1 appears twice in Γ_{str} . The results for the decomposition are listed in the right-most column of the table. The six normal modes for NH_3 transform according to the irreducible representations: $2A_1 + 2E$.



C_{3v}	E	$2C_3$	$3\sigma_v$	$h = 6$
A_1	1	1	1	z or T_z
A_2	1	1	-1	R_z
E	2	-1	0	(x,y) or (T_x,T_y) (R_x,R_y)

Step	C_{3v}	E	$2C_3$	$3\sigma_v$	Γ	n_i
1	stationary atoms	4	1	2		
2	Γ_{trans}	3	0	1	product w. Γ_{trans}	
3	Γ_{tot}	12	0	2		
4	Γ_{trans}	3	0	1	subtract A_1+E	
5	Γ_{rot}	3	0	-1	subtract A_2+E	
6	Γ_{vib}	6	0	2	$\Gamma_{tot} - \Gamma_{trans} - \Gamma_{rot}$	
7	A_1	1	1	1		$1/h(\Gamma_{vib} \cdot A_1) = 12/6 = 2A_1$
8	A_2	1	1	-1		$1/h(\Gamma_{vib} \cdot A_2) = 0$
9	E	2	-1	0		$1/h(\Gamma_{vib} \cdot E) = 12/6 = 2E$

Figure 27.8.10: Determination of the irreducible representations for the normal modes of XY_3 molecules in the C_{3v} -point group. The normal modes transform as $2A_1 + 2E$, giving six modes with four vibration frequencies.

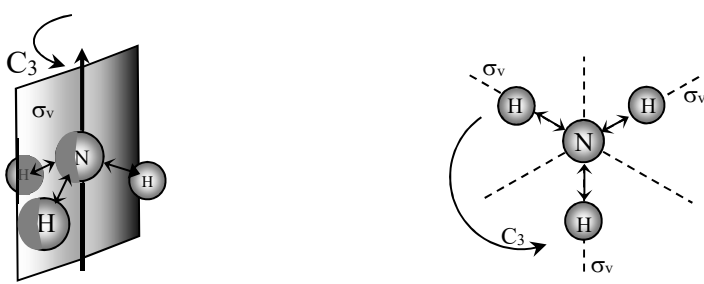
Because the E normal modes are doubly degenerate, the two different A_1 -modes and the two different sets of E-modes give six total normal modes, as expected from the $3N-6$ rule. The next step is to determine the stretching modes. The bending modes are then obtained by difference from the overall total. The irreducible representations of the stretching modes are determined by determining the relative symmetry of the bonds in the molecule:

The characters of the reducible representation of the stretches are determined:

10. The molecule is redrawn with double-headed arrows replacing each bond. In other words the direction of the displacement is not important. The number of arrows that are stationary under transformation by the operations of the classes in the point group is determined. The result is the reducible representation of the stretching vibrations, Γ_{str} . For C_3 -rotation, no arrow is stationary. One arrow lies on each σ_v -plane while the other two arrows are reflected from one side to the other. The results for Γ_{str} for NH_3 are listed as *step-10* in Figure 27.8.11.

The reducible representation of the stretches is decomposed into irreducible representations:

11-13. The decomposition of Γ_{str} is done in the same way as for Γ_{tot} , using Eq. 27.8.2. The result is listed in the right-most column of the table. The stretching modes for NH_3 decompose to $A_1 + E$, giving three stretching modes with two vibration frequencies. From *steps: 7-9* we find that all modes for NH_3 include $2A_1 + 2E$. Subtracting the stretching modes gives the remaining bending modes as also $A_1 + E$. This result verifies the listing in Table 27.7.1.



Step	C_{3v}	E	$2C_3$	$3\sigma_v$	n_i
10	stationary arrows, Γ_{str}	3	0	1	
11	A_1	1	1	1	$1/h(\Gamma_{\text{str}} \cdot A_1) = 6/6 = 1A_1$
12	A_2	1	1	-1	$1/h(\Gamma_{\text{str}} \cdot A_2) = 0$
13	E	2	-1	0	$1/h(\Gamma_{\text{str}} \cdot E) = 6/6 = 1E$

Figure 27.8.11: Determination of the irreducible representations of the stretching vibrations of XY_3 molecules in the C_{3v} -point group. The stretching modes are $A_1 + E$, giving three stretching modes with two vibration frequencies.

27.9 A More Intense Discussion of Transition Probabilities

The interaction of light with matter can be viewed from semi-classical or quantum mechanical perspectives. In this section we expand upon our discussions in Section 27.1. We begin with the semi-classical perspective developed by Einstein and Planck. The goal is to show that the Einstein coefficients for absorption and spontaneous emission are equal, a fact we used in deriving Eq. 27.1.2. To relate the Einstein coefficients, we develop a simple model system. Consider a molecule interacting with the light produced by a blackbody radiator, Figure 27.9.1. Blackbody radiators consist of a cavity with the energy density of the light in thermal equilibrium with the walls of the cavity. Light is created by the oscillation of electrons in the hot cavity walls at temperature T . The blackbody intensity frequency distribution is shown in Figure 23.2.1. The Planck blackbody expression gives the intensity of radiation in an interval of frequency from ν to $\nu + d\nu$ using Eq. 23.2.2 and $\nu = c/\lambda$:

$$I(\nu) d\nu = \frac{2\pi h \nu^3}{c^2} \left(\frac{1}{e^{h\nu/kT} - 1} \right) d\nu \quad (\text{blackbody}) \quad 27.9.1$$

The radiation energy density, $\rho(\nu)$, is related to the intensity through $I(\nu) = \rho(\nu) c/4$, with c the speed of light. The geometric factor of 4 is for an isotropic distribution of light intensity, which is appropriate since the molecule is placed inside the cavity. Using this last relationship, the energy density per unit frequency is:

$$\rho(\nu) = \frac{8\pi h \nu^3}{c^3} \left(\frac{1}{e^{h\nu/kT} - 1} \right) \quad (\text{isotropic blackbody}) \quad 27.9.2$$

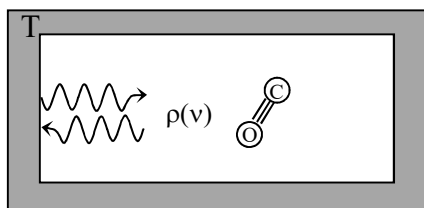


Figure 27.9.1: The molecule is placed inside a blackbody radiator so that thermal equilibrium is established between the walls of the cavity, the radiation energy density inside the cavity, and the molecular transition.

The molecule absorbs and emits light according to Eq. 27.1.2. If the molecular spectroscopic transitions are at equilibrium, the rate of change of the population of each level is zero. Setting Eq. 27.1.2 equal to zero gives the rate of absorption equal to the total rate of depopulation of the excited state:

$$B_{1\leftarrow 0} \rho(\nu) N_0 = B_{1\rightarrow 0} \rho(\nu) N_1 + A_{1\rightarrow 0} N_1 \quad 27.9.3$$

absorption stimulated emission spontaneous emission

At equilibrium the ratio of the populations of the excited and ground states is given by the Boltzmann distribution $N_1/N_0 = e^{-\Delta E/kT}$ with ΔE given by the transition frequency $\Delta E = \epsilon_1 - \epsilon_0 = h\nu$, Eq. 8.9.8. Solving for the equilibrium population ratio from Eq. 27.9.3 and setting the result equal to the Boltzmann population ratio gives:

$$\frac{N_1}{N_0} = \frac{B_{1\leftarrow 0} \rho(\nu)}{B_{1\rightarrow 0} \rho(\nu) + A_{1\rightarrow 0}} = e^{-h\nu/kT} \quad 27.9.4$$

Solving for the radiation energy density from this last equation gives:

$$\rho(\nu) = \frac{A_{1\rightarrow 0}}{B_{1\leftarrow 0} e^{h\nu/kT} - B_{1\rightarrow 0}} \quad 27.9.5$$

At equilibrium the energy density is given by the Planck distribution, Eq. 27.9.2. The two equations are consistent only if $B_{1\leftarrow 0} = B_{1\rightarrow 0}$ giving:

$$A_{1\rightarrow 0} = \frac{8\pi h \nu^3}{c^3} B_{1\leftarrow 0} \quad 27.9.6$$

In other words, the Einstein coefficients for stimulated emission and absorption are equal. Light has the same effect on absorption and on stimulating the excited state to emit light to return to the ground state. As a bonus we also find that the coefficient for spontaneous emission, and hence the fluorescence lifetime, is also determined by the absorption coefficient. Using time-dependent perturbation theory, the Einstein coefficient for absorption is related to the square of the transition dipole moment:

$$B_{1 \leftarrow 0} = \frac{8\pi^3}{3h^2} |\mu_{tr}|^2 \quad 27.9.7$$

The transition dipole moment, Eq. 27.1.7, is readily calculated knowing the wave functions for the two levels coupled in the spectroscopic transition. This last equation is the bridge between quantum mechanical structure and spectroscopy. We now need to determine how to calculate this important molecular property from experimental data.

Oscillator Strength is Proportional to the Integrated Absorption Coefficient: The transition dipole moment is the quantum mechanical measure of the intensity of an absorption transition, Eqs. 27.1.7 and 27.9.7. In this section we determine the quantitative relationship between the transition dipole moment and the experimental transition intensity. The Beer-Lambert Law relates the measured absorption to the molar absorption coefficient, $A = \epsilon \ell [c]$, with ℓ the path length and $[c]$ the concentration of the absorbing species. The absorption coefficient, β , is the intrinsic probability of absorption of a photon, which is related to the molar absorption coefficient by $\beta = 2.303\epsilon$, Eq. 2.4.7. The absorbance A , ϵ , and β vary across the absorption band: $A(\nu)$, $\epsilon(\nu)$, and $\beta(\nu)$, Figure 27.9.2. A transition occurs over a range of wavelengths, because of broadening by motion and rotational and vibrational fine-structure.

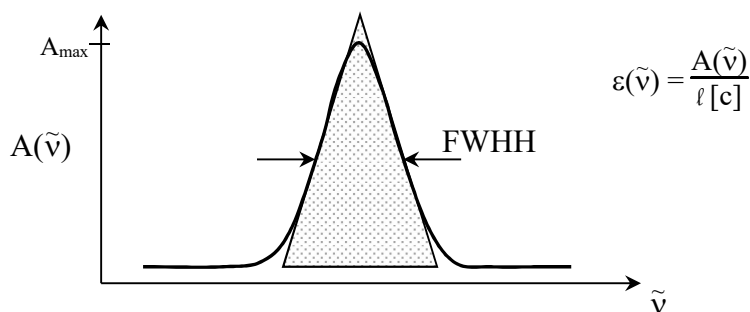


Figure 27.9.2: The integrated absorption coefficient, \mathcal{A} , can be roughly approximated by assuming the transition band is triangular. The concentration of the absorbing species is $[c]$ and the path length is ℓ .

The intensity of a transition is given by the integrated absorption coefficient, \mathcal{A} :

$$\mathcal{A} = \int \beta(\nu) d\nu = \int \beta(\tilde{\nu}) c d\tilde{\nu} \quad 27.9.8$$

The integral is taken across the full-width of the band. If an experimental numerical integral is not available, the integrated absorption coefficient can be roughly approximated by assuming the band is triangular in shape with total area:

$$\mathcal{A} = \text{area} = \frac{1}{2}(\text{base})(\text{height}) = c(\text{FWHH})(2.303 \varepsilon_{\text{max}}) \quad 27.9.9$$

where c is the speed of light and FWHH is the full-width at half-height in cm^{-1} .

We need a good comparison to help decide if an experimental transition has a large or small intensity. The ideal intensity of an electronic transition is modeled by an electron that is bound in a three-dimensional harmonic potential. The harmonic transition frequency, ν_0 , is set equal to the experimental frequency under comparison. The transition dipole moment in the x -direction for a harmonically bound electron is evaluated using harmonic oscillator wave functions with quantum number ν changing from $\nu = 0$ to $\nu = 1$, Table 24.1.1:¹²

$$\mu_{\text{tr},x} = \int_{-\infty}^{\infty} \chi_1^*(-ex)\chi_0 dx = -e(2/\pi)^{1/2} \int_{-\infty}^{\infty} \alpha x e^{-1/2\alpha^2 x^2}(x)e^{-1/2\alpha^2 x^2} dx = e(\hbar/4\pi m_e \nu_0)^{1/2} \quad 27.9.10$$

where e and m_e are the charge and mass of an electron. The y - and z -components are identical to the x -component with $|\mu_{\text{tr}}|^2 = (\mu_{\text{tr},x}^2 + \mu_{\text{tr},y}^2 + \mu_{\text{tr},z}^2)$ in Eq. 27.9.7. The ratio of the experimental intensity to this ideal case of a harmonically bound electron is called the oscillator strength, f :

$$f = \left(\frac{4m_e c \varepsilon_0}{N_A e^2} \right) \mathcal{A} = 6.257 \times 10^{-19} \text{ mol s m}^{-2} \mathcal{A} \quad 27.9.11$$

Allowed electronic transitions have molar absorption coefficients on the order of $\varepsilon \cong 10,000 \text{ L mol}^{-1} \text{ cm}^{-1}$ and corresponding oscillator strengths near 1. Molecular structure programs commonly list spectroscopic intensities as oscillator strengths. The oscillator strength and the transition dipole moment are related by:

$$f = \left(\frac{h\nu m_e}{\pi e^2} \right) B_{1 \leftarrow 0} = \left(\frac{8\pi^2}{3} \right) \left(\frac{m_e \nu}{h e^2} \right) |\mu_{\text{tr}}|^2 = 1.410 \times 10^{42} \nu |\mu_{\text{tr}}|^2 \quad 27.9.12$$

where ν is the experimental transition frequency at the center of the band.

Example 27.9.1: *Integrated Absorption Coefficient, Oscillator Strength, and Transition Dipole*

The maximum absorbance at 255 nm of $1.00 \times 10^{-3} \text{ M}$ benzene in ethanol is 0.16 with a path length of 1.00 cm. The band shows poorly resolved vibrational fine-structure; the full-width at half-height, FWHH, is roughly 4000 cm^{-1} . Calculate the integrated absorption coefficient, oscillator strength, and transition dipole moment.

Answer: The frequency of the transition is $\tilde{\nu} = 1/\lambda = 1/[255 \times 10^{-9} \text{ m}(100 \text{ cm}/1 \text{ m})] = 39,220 \text{ cm}^{-1}$ or $\nu = c\tilde{\nu} = 1.18 \times 10^{17} \text{ s}^{-1}$. From A_{max} , the maximum molar absorption coefficient is:

$$\varepsilon_{\text{max}} = A_{\text{max}}/(\ell[c]) = 0.16/1.00 \text{ cm}/1.00 \times 10^{-3} \text{ mol L}^{-1} = 160 \text{ L mol}^{-1} \text{ cm}^{-1}$$

In SI units, converting the path length to meters and the concentration to mol m^{-3} gives the molar absorption coefficient as:

$$\varepsilon_{\text{max}} = (160 \text{ L mol}^{-1} \text{ cm}^{-1})(100 \text{ cm}/1 \text{ m})(1 \text{ m}^3/1000 \text{ L}) = 16. \text{ m}^2 \text{ mol}^{-1}$$

The units are now that of a cross section per mole. The band width in m^{-1} is: $\text{FWHH} = (4000 \text{ cm}^{-1})(100 \text{ cm}/1 \text{ m}) = 4.0 \times 10^5 \text{ m}^{-1}$. The integrated absorption coefficient assuming a triangular shape is estimated using Eq. 27.9.9:

$$\mathcal{A} = 2.998 \times 10^8 \text{ m s}^{-1} (4.0 \times 10^5 \text{ m}^{-1}) (2.303) (16. \text{ m}^2 \text{ mol}^{-1}) = 4.4 \times 10^{15} \text{ m}^2 \text{ s}^{-1} \text{ mol}^{-1}$$

The oscillator strength gives the intensity as the fraction of the strength of a harmonically bound electron, Eq. 27.9.11:

$$f = 6.257 \times 10^{-19} \text{ mol s m}^{-2} \mathcal{A} = 6.259 \times 10^{-19} \text{ mol s m}^{-2} (4.4 \times 10^{15} \text{ m}^2 \text{ s}^{-1} \text{ mol}^{-1}) = 0.0028$$

The transition dipole moment is then obtained by solving Eq. 27.9.12:

$$|\mu_{\text{tr}}|^2 = \frac{f}{1.410 \times 10^{42} \nu} = \frac{0.0028}{1.410 \times 10^{42} (1.18 \times 10^{17} \text{ s}^{-1})} \quad \text{giving} \quad |\mu_{\text{tr}}| = 1.29 \times 10^{-31} \text{ C m}$$

The conventional units for dipole moments are debyes with $1 \text{ D} = 3.336 \times 10^{-30} \text{ C m}$. The transition dipole moment in debyes is:

$$|\mu_{\text{tr}}| = 1.29 \times 10^{-31} \text{ C m} (1 \text{ D} / 3.336 \times 10^{-30} \text{ C m}) = 0.039 \text{ D}$$

The electronic transition of benzene at 255 nm is a formally forbidden $\pi^* \leftarrow \pi$ transition and therefore quite weak. For example, strongly absorbing dyes have $f \cong 1$ and $|\mu_{\text{tr}}| \cong 1 \text{ D}$.

Harmonic Oscillator Transitions Only Occur Between Adjacent Levels: Finally, we wish to prove that the selection rule for harmonic vibrations is $\Delta v = \pm 1$. The transition dipole moment for a vibrational transition is given by Eqs. 27.1.10 and 24.2.18, with the extension x given by $x = R - R_e$ and $dR = dx$:

$$\int \chi_{v'}(R - R_e) \chi_{v''} dR = N_{v'} N_{v''} \int_{-\infty}^{\infty} H_{v'} e^{-\frac{1}{2}\alpha^2 x^2} x H_{v''} e^{-\frac{1}{2}\alpha^2 x^2} dx \quad 27.9.13$$

The product, $x H_{v''}$, is determined by solving the recursion relationship, Eq. 24.2.20, with $v = v''$:

$$H_{v''+1} = 2\alpha x H_{v''} - 2v'' H_{v''-1} \quad \text{giving} \quad x H_{v''} = (H_{v''+1} + 2v'' H_{v''-1}) / 2\alpha \quad 27.9.14$$

Substitution of this last equation into Eq. 27.9.13 gives two terms for the integral:

$$\frac{N_{v'} N_{v''}}{2\alpha} \left[\int_{-\infty}^{\infty} H_{v'} e^{-\frac{1}{2}\alpha^2 x^2} H_{v''+1} e^{-\frac{1}{2}\alpha^2 x^2} dx + 2v'' \int_{-\infty}^{\infty} H_{v'} e^{-\frac{1}{2}\alpha^2 x^2} H_{v''-1} e^{-\frac{1}{2}\alpha^2 x^2} dx \right] \quad 27.9.15$$

The integrals are given by Eq. 24.2.22; the integrals vanish unless the Hermite polynomials are the same. The first integral vanishes unless $v' = v''+1$ and the second integral vanishes unless $v' = v''-1$. Taken together these results require $\Delta v = v' - v'' = \pm 1$.

27.10 Summary – Looking Ahead

Rotational and vibrational spectroscopy are critical tools in molecular structure determination. The symmetry of a molecule is determined by the appearance or absence of pure rotational transitions and the number of vibration frequencies found in infrared absorption and Raman scattering spectra. Microwave spectroscopy is the most accurate method for the determination of bond lengths and angles. Vibrational spectroscopy provides information on bond strengths through force constants and bond dissociation energies. Of transition intensity measures, Einstein coefficients are useful because of the direct relationship to the kinetic equations for the populations of the coupled levels. Transition dipole moments are the direct link to quantum

molecular structure. Oscillator strengths are relative measures of the strengths of transitions in comparison to an ideal case of a harmonically bound electron. Oscillator strengths make it easy to determine if transition intensities are “large” or “small.” Rotational spectra require a permanent dipole moment in absorption or an anisotropic polarizability in Raman scattering. If pure rotational transitions are not allowed by selection rules, the same information is available from rotational fine-structure in infrared or Raman vibrational transitions. Vibrational spectroscopy is often adequately treated in the harmonic approximation. The effects of anharmonicity include the appearance of overtone, combination, and difference bands. Fermi resonances confound the assignment of the peaks in vibrational spectra. However, Fermi resonances are an instructive example of the general phenomena of the mixing of nearly degenerate states. The infrared and Raman activity of the normal modes of a molecule are predicted using group theory. In absorption, the symmetry species of a normal mode, as given by the irreducible representation, must match a component of the electric dipole operator. The components of the electric dipole operator are proportional to functions x , y , and z . In Raman scattering, the irreducible representation of a normal mode must match a component of the polarizability, which are proportional to x^2 , y^2 , z^2 , xy , xz , and yz .

We next discuss electronic spectroscopy, which usually occurs in the UV-visible region of the electromagnetic spectrum. You probably first encountered spectroscopy through the use of the Beer-Lambert Law to determine molecular concentration, based on electronic transitions in the UV-visible. Beyond concentration measurements, electronic spectroscopy is a rich source of information on the excited states of molecules. At high resolution, rotational and vibrational fine-structure occurs along with electronic transitions. For molecules with forbidden transitions in infrared or Raman spectra, the equivalent information is available using electronic emission transitions in UV-visible spectroscopy.

Chapter Summary

1. Band positions correspond to transitions between allowed quantum states of the system:

$$\Delta E = h\nu = hc/\lambda = hc\tilde{\nu} \qquad \tilde{\nu} = \Delta E/hc \qquad \nu = \tilde{\nu}c$$

2. The net change in population of two coupled states is:

$$\frac{dN_1}{dt} = \nu_{\text{absorb}} - \nu_{\text{stimulated emission}} - \nu_{\text{spontaneous emission}} = B_{1\leftarrow 0} \rho(\nu) N_0 - B_{1\rightarrow 0} \rho(\nu) N_1 - A_{1\rightarrow 0} N_1$$

The Einstein coefficients are $B_{1\leftarrow 0}$ for absorption, $B_{1\rightarrow 0}$ for stimulated emission, and $A_{1\rightarrow 0}$ for spontaneous emission, with $B_{1\leftarrow 0} = B_{1\rightarrow 0}$. The radiation energy density $\rho(\nu)$ is the radiation energy per unit frequency per unit volume, with units J s m^{-3} .

3. The Einstein spontaneous emission coefficient is the inverse of the spontaneous emission lifetime, $A_{1\rightarrow 0} = 1/\tau_{\text{sp}}$.
4. Absorption and spontaneous emission are always in competition. If the rate of spontaneous emission is small the net rate of absorption is proportional to the population difference:

$$\text{net rate} = \frac{dN_1}{dt} \cong B_{1\leftarrow 0} \rho(\nu) [N_0 - N_1]$$

5. The equilibrium Boltzmann population difference is: $N_0 - N_1 \propto 1 - e^{-\Delta E/kT}$ where $\Delta E = \epsilon_1 - \epsilon_0$, k is Boltzmann's constant, T is absolute temperature, and $kT = 207.2 \text{ cm}^{-1}$.

6. The permanent dipole moment of a molecule is the expectation value of the electric dipole moment operator over the electronic wave function of the molecule, Ψ_{el} :

$$\langle \hat{\vec{\mu}} \rangle = \int \Psi_{el}^* (\hat{\vec{\mu}}_{el} + \hat{\vec{\mu}}_{nuclei}) \Psi_{el} d\tau$$

7. The electric dipole moment operator is: $\hat{\vec{\mu}} = \hat{\vec{\mu}}_{el} + \hat{\vec{\mu}}_{nuclei} = - \sum_{i=1}^n e \hat{\vec{r}}_i + \sum_{j=1}^m q_j \hat{\vec{r}}_j$

summed over the coordinates of the n-electrons, $\hat{\vec{r}}_i$, and the m-nuclei, $\hat{\vec{r}}_j$, of charge $q_j = Z_j e$.

8. The intensity of a transition $\Psi_j \leftarrow \Psi_i$ is proportional to the square of the transition dipole moment. The transition dipole moment, $\vec{\mu}_{tr}$, is:

$$\vec{\mu}_{tr} = \langle \vec{\mu} \rangle = \int \Psi_j^* \hat{\vec{\mu}} \Psi_i d\tau \quad \text{giving} \quad B_{1 \leftarrow 0} = \frac{8\pi^3}{3h^2} |\mu_{tr}|^2$$

with each Ψ_i as the product of the electronic, vibrational, and rotational wave functions.

9. Assuming harmonic oscillator vibrational wave functions $\Psi_{vib,i} = \chi_v(R)$, with spherical-harmonic rotational wave functions $\Psi_{rot,i} = Y_{J,m_j}(\theta, \phi)$ and electronic wave functions, $\Psi_{el,i}$:

$$\vec{\mu}_{tr} = \langle \vec{\mu} \rangle = \int [\Psi_{el,j} \chi_{v'}(R) Y_{J',m_{j'}}(\theta, \phi)]^* \hat{\vec{\mu}} \Psi_{el,i} \chi_{v''}(R) Y_{J'',m_{j''}}(\theta, \phi) d\tau$$

where the initial quantum numbers for vibration and rotation are v'' and J'' and the final quantum numbers are v' and J' .

10. Transitions with non-zero transition dipole moments are allowed and with vanishing transition dipole moments are forbidden.
11. For rotational absorption spectroscopy, the gross selection rule requires a permanent electric dipole moment. The specific selection rule conserves angular momentum, $\Delta J = \pm 1$.
12. For vibrational absorption of a diatomic molecule, the transition dipole moment, neglecting third-order terms, is the integral over the internuclear separation, R:

$$\vec{\mu}_{tr} = \left. \frac{d\vec{\mu}}{dR} \right|_{R_e} \int \chi_{v'}(R - R_e) \chi_{v''} dR \quad \text{requiring} \quad \left. \frac{d\vec{\mu}}{dR} \right|_{R_e} \neq 0$$

For a polyatomic the integral is over the progression of the normal mode. The gross selection rule is that the dipole moment of the molecule must change during the vibration. For a harmonic oscillator, the integral vanishes unless $\Delta v = \pm 1$, requiring adjacent levels.

13. For electronic spectroscopy, the transition dipole moment requires that the dipole moment of the molecule must change in the electronic transition between the initial and the final state.
14. Lifetime broadening is always present, $\delta E \delta t \geq \hbar/2$, with δt the intrinsic excited state lifetime.
15. The root-mean-squared speed in the direction of the light propagation and the full-width at half-maximum of a transition caused by the Doppler effect, Δv_D , are:

$$\bar{v}_{x,rms} = \sqrt{\frac{kT}{m}} \quad \Delta v_D = 2 \left(\frac{v_o}{c} \right) \sqrt{\frac{2kT \ln(2)}{m}}$$

where v_o is the wavelength of the stationary source, c is the speed of light, T is the absolute temperature, and m is the molecular mass in kg molecule⁻¹.

16. Assuming a gas-phase two state system, the average time between collisions is inversely proportional to the pressure, P , giving the transition width caused by collisions as $\Delta v_C \cong b P$, where b is the pressure-broadening coefficient, $b \cong 10 \text{ MHz torr}^{-1} \cong 0.25 \text{ cm}^{-1} \text{ bar}^{-1}$.
17. The Fourier decomposition of periodic function $f(t)$ with period L is:

$$f(t) = \sum_{n=0}^{\infty} A_n \cos(2\pi n v_0 t) + \sum_{n=0}^{\infty} B_n \sin(2\pi n v_0 t) \quad v_0 = 1/L$$

18. The Fourier coefficients are calculated as integrals over one period of the function:

$$A_n = 2 \int_0^L f(t) \cos(2\pi n v_0 t) dt \quad B_n = 2 \int_0^L f(t) \sin(2\pi n v_0 t) dt$$

19. The Fourier coefficients over a continuous range of frequencies are:

$$A(v) = 2 \int_0^{\infty} f(t) \cos(2\pi v t) dt \quad B(v) = 2 \int_0^{\infty} f(t) \sin(2\pi v t) dt$$

20. The Fourier expansion is written compactly as $f(t) = \int_{-\infty}^{\infty} g(v) e^{-i2\pi v t} dv$ with Fourier decomposition $g(v) = 2 \int_0^{\infty} f(t) e^{i2\pi v t} dt$. The absorptive response is $Re[g(v)]$ and dispersive response is $Im[g(v)]$.

21. The FT of a rectangular pulse of length t_p gives the full-width of the frequency response to the first zero as the inverse of the pulse width: $1/t_p$:

$$A(v) = 2 \frac{\sin(2\pi v t_p)}{2\pi v} \quad B(v) = 2 \frac{1 - \cos(2\pi v t_p)}{2\pi v}$$

22. The FT of an exponentially damped cosine gives a Lorentzian line shape centered on v_0 , with full-width at half-maximum FWHM = $1/\pi T_2$:

$$f(t) = e^{-t/T_2} \cos(2\pi v_0 t) \quad A(v) = Re[g(v)] = \frac{1}{\pi} \left(\frac{T_2}{1 + 4\pi^2 T_2^2 (v - v_0)^2} \right)$$

23. The equilibrium bond length R_e is at the minimum of the vibrational potential energy curve. The equilibrium bond length R_0 is vibrationally averaged over the $v = 0$ vibrational state: $R_0 > R_e$, but the difference is small.

24. The energies of the rotational states of a diatomic molecule in the rigid-rotor approximation in joules and cm^{-1} , respectively, are:

$$E_J = \tilde{B} h c J(J+1) \quad \tilde{F}_J = \frac{E_J}{h c} = \tilde{B} J(J+1) \quad m_J = 0, \pm 1, \dots, \pm J$$

where \tilde{B} is the rotational constant in terms of the equilibrium bond length: $\tilde{B}_0(R_0)$ or $\tilde{B}_e(R_e)$. I is the corresponding moment of inertia, and μ is the reduced mass in kg:

$$\tilde{B} = \frac{h}{4\pi I c} \quad I = \sum_{i=1}^n m_i r_i^2 = \mu R_0^2 \quad \text{or} \quad I = \sum_{i=1}^n m_i r_i^2 = \mu R_e^2 \quad \mu = \frac{m_1 m_2}{m_1 + m_2}$$

25. The rotational absorption transition, $J' \leftarrow J''$ with $\Delta J = \pm 1$, in joules and wave numbers, is:

$$\Delta E = E_{J''+1} - E_{J''} = 2\tilde{B} h c (J''+1) \quad \Delta \tilde{F} = \tilde{F}_{J''+1} - \tilde{F}_{J''} = 2\tilde{B} (J''+1) \quad (J'': \text{lower level})$$

$$\text{or} \quad \Delta E = E_{J'} - E_{J'-1} = 2\tilde{B} h c J' \quad \Delta \tilde{F} = \tilde{F}_{J'} - \tilde{F}_{J'-1} = 2\tilde{B} J' \quad (J': \text{upper level})$$

26. For isotopomers, the reduced masses determine the difference in rotational constants:

$$\frac{\tilde{B}_2}{\tilde{B}_1} = \frac{\frac{h}{4\pi \mu_2 R_0^2 c}}{\frac{h}{4\pi \mu_1 R_0^2 c}} = \frac{\mu_1}{\mu_2}$$

27. For a rigid rotor, adjacent peaks in the absorption spectrum are separated by $2\tilde{B}$. Real molecules experience a small centrifugal distortion:

$$\tilde{F}_J = \tilde{B} J(J+1) - \tilde{D}_e [J(J+1)]^2 \quad \text{with model prediction} \quad \tilde{D}_e \cong 4\tilde{B}^3/\tilde{\nu}_0^2$$

where \tilde{D}_e is the centrifugal distortion constant and $\tilde{\nu}_0$ is the fundamental vibration frequency.

28. The moment of inertia of a linear triatomic with atom masses m_1 , m_2 and m_3 , and bond lengths R_{12} and R_{23} , is:

$$\textcircled{m_1} \xrightarrow{R_{12}} \textcircled{m_2} \xrightarrow{R_{23}} \textcircled{m_3} \quad I = \left(\frac{m_1 m_3}{m} \right) (R_{12} + R_{23})^2 + \left(\frac{m_2}{m} \right) (m_1 R_{12}^2 + m_3 R_{23}^2)$$

29. A moment of inertia for a polyatomic is a symmetric matrix (tensor) with components:

$$I_{xx} = \sum m_i (y_i^2 + z_i^2) \quad I_{yy} = \sum m_i (x_i^2 + z_i^2) \quad I_{zz} = \sum m_i (x_i^2 + y_i^2)$$

$$I_{xy} = \sum m_i x_i y_i \quad I_{xz} = \sum m_i x_i z_i \quad I_{yz} = \sum m_i y_i z_i$$

The origin is the center of mass.

30. In the principal coordinates frame of reference, the moment of inertia of the molecule is a diagonal matrix with components I_{xx} , I_{yy} , and I_{zz} .

31. Spherical tops have $I_{xx} = I_{yy} = I_{zz}$, symmetric tops have $I_{yy} = I_{xx} = I_{\perp}$ and $I_{zz} = I_{\parallel}$, and asymmetric tops have $I_{xx} \neq I_{yy} \neq I_{zz}$.

32. Symmetric tops have two rotational constants: \tilde{A} for rotation around the z-axis and \tilde{B} for rotation perpendicular to the z-axis (\tilde{B} corresponding to diatomics):

$$\tilde{B} = \frac{\hbar}{4\pi I_{\perp} c} \quad \tilde{A} = \frac{\hbar}{4\pi I_{\parallel} c}$$

33. Asymmetric tops have three rotational constants: $\tilde{A} = \frac{\hbar}{4\pi I_{zz} c}$, $\tilde{B} = \frac{\hbar}{4\pi I_{xx} c}$, $\tilde{C} = \frac{\hbar}{4\pi I_{yy} c}$

34. For spherical tops, $I_{xx} = I_{yy} = I_{zz} = I$ and the rotational transitions are analogous to those for a diatomic molecule. Spherical tops are invisible in rotational spectroscopy, but transitions are excited by collisions.

35. The energy levels for a symmetric top are: $\tilde{F}_{JK} = \tilde{B}J(J+1) + (\tilde{A} - \tilde{B})K^2$ with $J_z = K \hbar$, and $K = 0, \pm 1, \pm 2, \dots, \pm J$. Quantum number K gives the projection of the angular momentum on the molecule-fixed z-axis and describes the type of rotation.

36. Rotational transitions for a symmetric top require $\Delta K = 0$ and $\Delta J = \pm 1$. For a rigid rotor the spectrum is a series of lines separated by $2\tilde{B}$, just like a diatomic:

$$\tilde{\nu}_J = \tilde{F}_{J,K} - \tilde{F}_{J-1,K} = 2\tilde{B}J' \quad (J': \text{upper level})$$

37. Vibrational term values, \tilde{G}_v , are the energy levels in cm^{-1} ; allowed transitions are $\Delta v = \pm 1$:

$$\tilde{G}_v = E/hc = \tilde{\nu}_0 (v + \frac{1}{2}) \quad \Delta\tilde{G} = \tilde{G}_{v+1} - \tilde{G}_v = \tilde{\nu}_0$$

where $\tilde{\nu}_0$ is the observed fundamental vibration frequency. Transitions beginning in different initial v states occur at the same frequency, for a harmonic oscillator.

38. With an anharmonic vibrational potential, the energy is expressed as a power series:

$$E_v = h\nu_e (v + \frac{1}{2}) - h\chi_e \nu_e (v + \frac{1}{2})^2 + h\mathcal{Y}_e \nu_e (v + \frac{1}{2})^3 + \dots$$

where ν_e is the fundamental vibration frequency for small displacements about the equilibrium bond length, χ_e is the **anharmonicity**, and \mathcal{Y}_e is the **second anharmonicity** constant.

39. The value of the derived force constant $\tilde{\kappa}$ varies slightly depending on the vibration frequency used in:

$$\tilde{\nu} = \frac{1}{2\pi c} \sqrt{\tilde{\kappa} \mu} \quad \text{with } \tilde{\nu} = \tilde{\nu}_0 \text{ or } \tilde{\nu}_e: \quad \tilde{\nu}_0 = \tilde{\nu}_e - 2\chi_e \tilde{\nu}_e$$

If $\tilde{\kappa}$ is determined from $\tilde{\nu}_e$, the value corresponds to the second derivative of the vibrational potential curve at the equilibrium internuclear separation, $\tilde{\kappa} = (d^2V/dR^2)_{R_e}$.

40. The Morse Potential is: $V = D_e [1 - e^{-a(R-R_e)}]^2$ with D_e the dissociation energy and $a = \omega_e(\mu/2D_e)^{1/2}$, which determines the steepness of the potential.

41. For a Morse potential the second and subsequent anharmonicity constants are zero:

$$E_v = h\nu_e(v + 1/2) - h\chi_e\nu_e(v + 1/2)^2 \quad \tilde{G}_v = \tilde{\nu}_e(v + 1/2) - \chi_e\tilde{\nu}_e(v + 1)^2$$

giving absorption transitions between adjacent levels $v+1 \leftarrow v$ as:

$$\Delta E_v = h\nu_e - h\chi_e\nu_e 2(v+1) \quad \Delta\tilde{G}_v = \tilde{\nu}_e - \chi_e\tilde{\nu}_e 2(v+1) \quad (v: \text{lower level})$$

42. With anharmonicity the different forms of the bond dissociation energies are related by:

$$D_e = D_0 + 1/2 h\nu_e - 1/4 \chi_e h\nu_e \quad \tilde{D}_e = \tilde{D}_0 + 1/2 \tilde{\nu}_e - 1/4 \tilde{\nu}_e \chi_e$$

43. The bond dissociation energy is given by the anharmonicity. Assuming a Morse potential:

$$\tilde{D}_e = \frac{\tilde{\nu}_e}{4\chi_e} - \frac{\chi_e\tilde{\nu}_e}{4} \equiv \frac{\tilde{\nu}_e}{4\chi_e} \quad \text{and in turn: } \chi_e = \frac{a^2\hbar}{2\mu\nu_e} = \frac{a^2\hbar}{2\mu\omega_e}$$

44. A Birge-Sponer extrapolation with $\Delta\tilde{\nu}_v = \tilde{\nu}_0 - 2\chi_e\tilde{\nu}_e v$ gives the anharmonicity from the slope, where v is the overtone and $\Delta\tilde{\nu}_v$ is the spacing between adjacent transitions. From just the first overtone, the anharmonicity is approximately $\chi_e\tilde{\nu}_e = (\tilde{\nu}_0 - \Delta\tilde{\nu}_1)/2$.

45. Anharmonicity causes vibrational modes to interact giving sum and difference bands, which are usually much less intense than dipole allowed fundamentals.

46. The vibration-rotation transition $v', J' \leftarrow v'', J''$ is at:

$$\Delta E = h\nu_0(v' - v'') + \tilde{B}'hc J'(J'+1) - \tilde{B}''hc J''(J''+1) \quad \tilde{\nu} = \tilde{\nu}_0(v' - v'') + \tilde{B}'J'(J'+1) - \tilde{B}''J''(J''+1)$$

47. In the rigid-rotor approximation, the bond length is constant in the two vibrational levels giving $\tilde{B}' = \tilde{B}'' = \tilde{B}$. For $\Delta v = +1$ and R-branch $\Delta J = +1$ transitions: $\Delta E = h\nu_0 + 2\tilde{B}hc(J''+1)$.

For $\Delta v = +1$ and P-branch $\Delta J = -1$ transitions $\Delta E = h\nu_0 - 2\tilde{B}hc J''$. The spectrum is a series of equally spaced lines with the spacing $2\tilde{B}$.

48. The rotational constant for the vibrational level with quantum number v is, to first-order:

$$\tilde{B}_v = \tilde{B}_e - \tilde{\alpha}_e(v + 1/2)$$

where \tilde{B}_e is the rotational constant at R_e and $\tilde{\alpha}_e$ is the vibration-rotation interaction constant.

49. For the R-branch, $\Delta J = +1$ and $m = J''+1$, and for the P-branch, $\Delta J = -1$ and $m = -J''$, with J'' for the lower level, gives the vibration-rotation transitions as:

$$\tilde{\nu}_m = \tilde{\nu}_0 + (2\tilde{B}_e - 2\tilde{\alpha}_e)m - \tilde{\alpha}_e m^2$$

50. Raman scattering gives the energy of a rotational or vibrational transition as:

$$\Delta\tilde{\nu} = \tilde{\nu}_0 - \tilde{\nu}_{\text{scattered}} \quad \Delta E = hc|\Delta\tilde{\nu}|$$

where $\tilde{\nu}_0$ is the wave number of the incident laser. A Stokes transition (redder) results if the final rotational or vibrational state is higher in energy than the initial state. An anti-Stokes transition (bluer) results if the final rotational or vibrational state is lower in energy than the initial state.

51. The polarizability of a molecule depends on the orientation of the molecule with respect to the direction of the electric vector of the incident light. The induced dipole moment is:

$$\vec{\mu}_{\text{ind}} = \underline{\underline{\alpha}} \vec{E} \quad \begin{pmatrix} \mu_x \\ \mu_y \\ \mu_z \end{pmatrix}_{\text{ind}} = \begin{pmatrix} \alpha_{xx} & \alpha_{xy} & \alpha_{xz} \\ \alpha_{yx} & \alpha_{yy} & \alpha_{yz} \\ \alpha_{zx} & \alpha_{zy} & \alpha_{zz} \end{pmatrix} \begin{pmatrix} E_x \\ E_y \\ E_z \end{pmatrix} \quad \begin{aligned} \mu_{x,\text{ind}} &= \alpha_{xx} E_x + \alpha_{xy} E_y + \alpha_{xz} E_z \\ \mu_{y,\text{ind}} &= \alpha_{yx} E_x + \alpha_{yy} E_y + \alpha_{yz} E_z \\ \mu_{z,\text{ind}} &= \alpha_{zx} E_x + \alpha_{zy} E_y + \alpha_{zz} E_z \end{aligned}$$

where α is the symmetric square matrix of polarizability components (a tensor).

52. Polarizability increases with the number of electrons and molecular volume.
53. Raman selection rules require an anisotropic polarizability for pure rotational transitions and a changing polarizability for vibrational transitions. For non-symmetric linear molecules, rotational Raman transitions have spacing $4\tilde{B}$.
54. The Exclusion Rule is that for a molecule with a center of symmetry, vibrational modes are either infrared active or Raman active, but not both.
55. Raman transitions of totally symmetric normal modes are polarized: $\rho \leq 3/4$, otherwise the depolarization ratio is $\rho = 3/4$.
56. A Fermi resonance results from a perturbation that couples degenerate or nearly degenerate transitions of the same symmetry, allowing weak or forbidden transitions to borrow intensity from allowed transitions. Coupled transitions can be fundamental, overtone, or combination.
57. Rotation axes, C_n , are n-fold axes with rotation angle $360/n$. The highest order rotation axis is the principle axis and is assigned the z-direction by convention. Vertical reflection planes, σ_v , include the principle axis. Dihedral-reflection planes, σ_d , are vertical-planes that bisect two C_2 -axes that are perpendicular to the principal axis and are chosen to pass through the fewest nuclei. A horizontal reflection plane, σ_h , is perpendicular to the principle axis. Inversion, i , inverts coordinates across the center of mass. Improper rotation, S_n , is an n-fold rotation followed by horizontal reflection. The molecular point group is determined by the symmetry elements that describe the shape of the molecule.
58. The character table for a point group lists all the symmetry operations for the group and the transformation properties of the irreducible representations. The irreducible representations are the symmetry species for the molecule. Valid molecular orbitals and normal modes transform as one of the irreducible representations of the point group.
59. In absorption, the transition dipole moment vanishes unless the normal mode transforms according to the same irreducible representation as a component of the electric dipole operator. In Raman scattering, the transition dipole moment vanishes unless the normal mode transforms according to the same irreducible representation as a component of the polarizability.
60. The number of times, n_i , that irreducible representation- i appears in a reducible representation is determined by the decomposition:

$$a_i = \frac{1}{h} \sum_{j=1}^q \chi_j^{vib} \chi_{i,j}^{irr} C_{i,j}^{irr} \quad i = \text{irreducible representation, } j = \text{class}$$

where $\chi_{i,j}^{irr}$ is the character for irreducible representation i and class j from the character table and χ_j^{vib} is the character for the reducible representation of all the vibrations for class j .

61. The characters of the reducible representation of all atom displacements, Γ_{tot} , are the class-by-class product of the number of stationary atoms and the representation of the translations, Γ_{trans} . The characters for translation and rotation are subtracted from the total giving the reducible representation of the normal modes, $\Gamma_{vib} = \Gamma_{tot} - \Gamma_{trans} - \Gamma_{rot}$.
62. The molecule is drawn with double-headed arrows replacing each bond. The characters of the reducible representation of the stretching modes are the number of stationary arrows.
63. The energy density per unit frequency of a black-body is: $\rho(\nu) = \frac{8\pi h \nu^3}{c^3} \left(\frac{1}{e^{h\nu/kT} - 1} \right)$

64. The coefficient for spontaneous emission, the luminescence lifetime $A_{1 \rightarrow 0} = 1/\tau_{\text{sp}}$, the Einstein absorption coefficient, and the transition dipole moment are related by:

$$A_{1 \rightarrow 0} = \frac{8\pi h \nu^3}{c^3} B_{1 \leftarrow 0} \qquad B_{1 \leftarrow 0} = \frac{8\pi^3}{3h^2} |\mu_{\text{tr}}|^2$$

65. Oscillator strength is the transition intensity as a fraction of the idealized intensity of a harmonically bound electron with the same transition frequency, ν :

$$f = \left(\frac{4m_e c \epsilon_0}{N_A e^2} \right) \mathcal{A} = 6.257 \times 10^{-19} \text{ mol s m}^{-2} \mathcal{A} = \left(\frac{h \nu m_e}{\pi e^2} \right) B_{1 \leftarrow 0} = \left(\frac{8\pi^2}{3} \right) \left(\frac{m_e \nu}{h e^2} \right) |\mu_{\text{tr}}|^2 = 1.410 \times 10^{42} \nu |\mu_{\text{tr}}|^2$$

An oscillator strength near one is an intense transition.

Literature Cited

1. D. K. Bohme, E. Herbst, N. Kaifu, S. Saito, *Chemistry and Spectroscopy of Interstellar Molecules*, University of Tokyo Press, 1992, p. 64.
2. M. Karplus, R. N. Porter, *Atoms and Molecules*, W. A. Benjamin, Menlo Park, CA, 1970. Table 7.3.
3. G. Herzberg, *Spectra of Diatomic Molecules*, Van Nostrand, Princeton, NJ, 1950.
4. K. K. Irikura, "Experimental Vibrational Zero-Point Energies: Diatomic Molecules," *J. Phys. Chem. Ref. Data*, **2007**, 36(2), 389-397.
5. B. deB. Darwent, "Bond Dissociation Energies in Simple Molecules," *Nat. Stand. Ref. Data Ser.*, NSRDS-NBS 31, Washington, DC, 1970.
6. W. C. Stwalley, W. T. Zemke, "Spectroscopy and Structure of the Lithium Hydride Diatomic Molecules and Ions," *J. Phys. Chem. Ref. Data*, **1993**, 22(1), 87-112.
(<http://www.nist.gov/data/PDFfiles/jpcrd448.pdf>)
7. K.P. Huber and G. Herzberg, *Molecular Spectra and Molecular Structure, v. 4, Constants of diatomic molecules*, Van Nostrand, Toronto, Canada, 1945.
8. K. S. Pitzer, *Quantum Chemistry*, Prentice-Hall, Englewood Cliffs, NJ, 1953, pp. 232-239.
9. C. F. Windisch Jr., V.-A. Glezakou, P. F. Martin, B. P. McGraild, H. T. Schaeffe, "Raman spectrum of supercritical C¹⁸O₂ and re-evaluation of the Fermi resonance," *Phys. Chem. Chem. Phys.*, **2012**, 14, 2560-2566.
10. D. C. Harris, M. D. Bertolucci, *Symmetry and Spectroscopy: An Introduction to Vibrational and Electronic Spectroscopy*, Oxford, New York, NY, 1978, Table 1-5.
11. J. R. Ferraro, K. Nakamoto, C. W. Brown, *Introductory Raman Spectroscopy, 2nd Ed.*, Academic Press-Elsevier, San Diego, CA, 2003, p. 46.
12. K. S. Pitzer, *Quantum Chemistry*, Prentice-Hall, Englewood Cliffs, NJ, 1953, pp. 265-266.
13. J. S. Winn, *Physical Chemistry*, Harper Collins, New York, NY, 1995. Section 19.3.
14. J. D. Graybeal, *Molecular Spectroscopy*, McGraw Hill, New York, NY, 1988. Section 16.9.

Further Reading

Spectroscopy

- P. F. Bernath, *Spectra of Atoms and Molecules, 2nd Ed.*, Oxford, New York, NY, 2005.
M. Karplus, R. N. Porter, *Atoms and Molecules*, W. A. Benjamin, Menlo Park, CA, 1970.

J. I. Steinfeld, *Molecules and Radiation: An Introduction to Modern Molecular Spectroscopy*, MIT Press, Cambridge, MA, 1985.

G. Herzberg, *Spectra of Diatomic Molecules*, Van Nostrand, Princeton, NJ, 1950.

G. Herzberg, *Molecular Spectra and Molecular Structure, II. Infrared and Raman Spectra of Polyatomic Molecules*, Van Nostrand, Princeton, NJ, 1945.

E. B. Wilson, Jr., J. C. Decius, P. C. Cross, *Molecular Vibrations: The Theory of Infrared and Raman Vibrational Spectra*, McGraw-Hill, New York, NY, 1955.

Group Theory

D. C. Harris, M. D. Bertolucci, *Symmetry and Spectroscopy: An Introduction to Vibrational and Electronic Spectroscopy*, Oxford, New York, NY, 1978.

S. F. A. Kettle, *Symmetry and Structure*, Wiley, Chichester, GB, 1985.

Problems: Rotational and Vibrational Spectroscopy

1. Calculate the ratio, N_1/N_0 , of molecules in the $v = 1$ and $v = 0$ vibrational states for carbon monoxide, CO, at 25.0 °C. Assume a harmonic oscillator with $\tilde{\nu}_e = 2169.8 \text{ cm}^{-1}$ [Hint: at 25.0 °C, $kT = 207.2 \text{ cm}^{-1}$]

2. Calculate the ratio, N_1/N_0 , of molecules in the $J = 1$ and $J = 0$ rotational levels for carbon monoxide, CO, at 25.0 °C. Assume a rigid rotor with $\tilde{B}_e = 1.932 \text{ cm}^{-1}$ [Hint: at 25.0 °C, $kT = 207.2 \text{ cm}^{-1}$]

3. How does the Doppler width of a transition depend on temperature and the mass of the molecule?

4. Calculate the Doppler line width of the $83305. \text{ cm}^{-1}$ electronic transition of HF at 500.0 K. This temperature is on the order of the temperature in the ionosphere.

5. (a). Draw the Fourier transformed spectrum of the function $f(t)$ in Figure 27.3.2 as a histogram, in the same style as the Fourier transforms shown in Figure 27.3.1b for the three Fourier coefficients. (b). The period of the function, L , is $1.00 \times 10^{-3} \text{ s}$. Calculate the lowest frequency Fourier component.

6. Many experiments give a time response that decays exponentially in time: $f(t) = e^{-t/\tau}$, where τ is the time constant for the decay. (a). Show that the Fourier transform, using Eq. 27.3.9, is:

$$g(\nu) = \frac{2\tau}{1 + i2\pi\tau\nu}$$

(b). The square of the magnitude of a complex function is given using Eq. 23.9.9. Show that:

$$g(\nu)^* g(\nu) = \frac{4\tau^2}{1 + 4\pi^2\tau^2\nu^2}$$

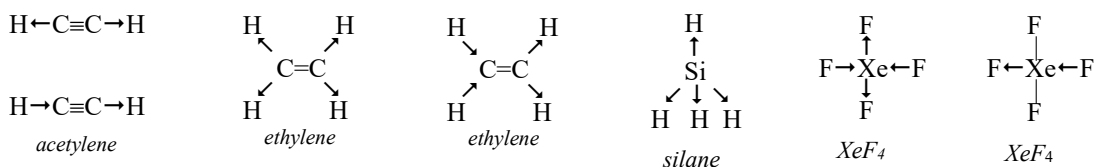
(c). The result of experiments is often given as a magnitude spectrum, $A^2(\nu) = g(\nu)^* g(\nu)$. Do a quick plot of the magnitude spectrum assuming $\tau = 1 \text{ s}$.

7. Which of the following molecules give pure-rotational absorption spectra? N_2 , O_2 , NO , CH , CO , CO_2 , N_2O , SO_2 , C_2H_4 , CH_4 , and $\text{H}_2\text{C}=\text{O}$ (formaldehyde).

8. Which of the following molecules give vibrational absorption spectra? N_2 , O_2 , NO , CH , CO , CO_2 , N_2O , and SO_2 .

9. Which of the following molecules give vibrational Raman spectra? N_2 , O_2 , NO , CH , CO , CO_2 , N_2O , and SO_2 .

10. Which of the following normal modes are infrared active and which are Raman active? The arrows indicate the movement of the exterior atoms. In the asymmetric stretches, the central atoms also move to maintain a fixed center of mass, but that movement is not shown. [Formal group theory is not required for this problem.]



11. The lowest energy transitions in the rotational spectrum of HF are 41.105 and 82.211 cm^{-1} . Calculate the equilibrium bond length of HF , R_0 .

12. Two adjacent lines in the rotational absorption spectrum of $^{14}\text{N}^1\text{H}$ are at 98.036 and 130.714 cm^{-1} . Calculate the equilibrium bond length of NH , R_0 , and the rotational quantum numbers of the lower states of the two transitions.

13. Calculate the moment of inertia of water about the z-axis, which is the figure axis. The rotational constant about the z-axis is $\tilde{A} = 14.512 \text{ cm}^{-1}$. Assume the bond angle is 104.48° .¹ Calculate the O–H bond length.

14. Use Eqs. 27.4.11 to calculate the three moments of inertia of H_2O . Use units of g mol^{-1} for the masses and \AA for the distances. The coordinates of water, aligned with the O-atom at the origin and one O–H bond extending along the x-axis, are:

Atom	x	y	z
O	0	0	0
H	0.9728	0	0
H	-0.2623	-0.9369	0

The coordinates of the center of mass are:

$$x_{\text{cm}} = 1/m \sum m_i x_i \qquad y_{\text{cm}} = 1/m \sum m_i y_i \qquad z_{\text{cm}} = 1/m \sum m_i z_i$$

where m_i is the isotope specific mass of atom- i , with coordinates x_i , y_i , z_i , and total molecular mass $m = \sum m_i$. First, build a spreadsheet to calculate the moment of inertia matrix with the input orientation.² Second, the eigenvalues of this matrix are the three moments of inertia. To calculate the eigenvalues use MatLab, Maple, Mathematica, or the “Eigen” matrix diagonalization applet that is on the textbook Web site or on the companion CD. [Hint: The example spreadsheet shown below uses the same geometry for water as given above, but the orientation is chosen as already aligned with the principal axes. For this aligned example, the off-diagonal elements of the moment of inertia matrix should be zero, within round-off error. You should use these values to

test your spreadsheet. Your final eigenvalues, starting from the orientation listed above, should give the same results; the final moments of inertia should not depend on the input orientation. The spreadsheet was designed to make the addition of atoms easy for larger molecules.]

A1	B	C	D	E	F	G	H	I
2								
3		original data:						
4	atom	mass	x	y	z	mx	my	mz
5	O	15.9949	0	-0.0657	0	0	-1.050865	0
6	H	1.0078	0	0.5222	0.775	0	0.5262732	0.781045
7	H	1.0078	0	0.5222	-0.7752	0	0.5262732	-0.78125
8	sums	18.0105				0	0.0016814	-0.0002
9	com		0	9.33561E-05	-1.11912E-05			
10								
11			$m(x-x_{cm})(y-y_{cm})$	$m(x-x_{cm})(z-z_{cm})$	$m(y-y_{cm})(z-z_{cm})$	$m(x-x_{cm})^2$	$m(y-y_{cm})^2$	$m(z-z_{cm})^2$
12	O	15.9949	0	0	-1.17772E-05	0	0.0692382	2E-09
13	H	1.0078	0	0	0.407794672	0	0.2747216	0.605327
14	H	1.0078	0	0	-0.407888131	0	0.2747216	0.605605
15	sums		0	0	-0.000105236	0	0.6186814	1.210932
16		Results:						
17	I =	x	y	z				
18	x	1.82961						
19	y	0	1.210932206					
20	z	0	0.000105236	0.618681357				

The input atomic coordinates are placed in cells D5:F7. The calculated center of mass coordinates, “com”, are listed in cells D9:F9, which are then used to form the sums for Eqs. 27.4.11. The resulting moment of inertia matrix is listed in cells C18:E20. The moment of inertia matrix is symmetric, so that only the lower triangular matrix need be listed. In the general case, the moment of inertia matrix will not be a diagonal matrix. The final moment of inertia elements are then input into the “eigen” applet to determine the eigenvalues.

15. Calculate the bond force constant, κ , for H^{35}Cl . The fundamental vibration frequency is $\tilde{\nu}_e = 2990.9 \text{ cm}^{-1}$.

16. Does CH or CO have the greater bond strength? Base your answer on the fundamental vibration frequency for ^{12}CH , which is $\tilde{\nu}_e = 2860.75 \text{ cm}^{-1}$, and for $^{12}\text{C}^{16}\text{O}$, which is 2169.76 cm^{-1} , Table 27.6.1.

17. The force constant is defined as the second derivative of the vibrational potential function, Eq. 8.11.2. For a non-harmonic potential, such as the Morse potential in Eq. 27.5.8, we must add the stipulation that the second derivative is evaluated at the equilibrium internuclear distance:

$$\left(\frac{d^2V}{dR^2}\right)_{R=R_e} \equiv \kappa$$

Derive the relationship that determines the Morse a -parameter, Eq. 27.5.8, using the following steps: (a). Show that the second derivative of the Morse potential function, Eq. 27.5.7, is:

$$\frac{d^2V}{dR^2} = -2a^2D_e e^{-a(R-R_e)} + 4a^2D_e e^{-2a(R-R_e)}$$

(b). Evaluate the second derivative at the equilibrium internuclear distance, $R = R_e$, and use the definition of the force constant to give:

$$a = \left(\frac{\tilde{k}}{2 D_e} \right)^{1/2}$$

(c). Use the relationship between the fundamental vibration frequency and the force constant, $\omega_e = 2\pi\nu_e = \sqrt{\tilde{k}/\mu}$, to give Eq. 27.5.8.

18. The bond strength parameters for NF are important in validating bond order-bond strength correlations as displayed in Figure 26.4.12. However, the literature bond dissociation energy for NF varies widely depending on the experimental method used. The bond energy from thermochemical measurements is $297 \pm 42 \text{ kJ mol}^{-1}$ or $3.08 \pm 0.44 \text{ eV}$.³ Determine $\tilde{\nu}_e$, the force constant, zero point energy, and bond dissociation energies \tilde{D}_e and \tilde{D}_o , for ^{14}NF based on the fundamental vibration frequency $\tilde{\nu}_o = 1123.4 \text{ cm}^{-1}$ and anharmonicity $\chi_e \tilde{\nu}_e = 9.0 \text{ cm}^{-1}$. Report the bond dissociation energies in cm^{-1} , eV, and kJ mol^{-1} . Compare the spectroscopic bond dissociation energy, as D_o , with the thermochemical value. What effect does using the spectroscopic value have on the bond order-bond strength correlation in Figure 26.4.12?

19. Bond order-bond strength correlations as displayed in Figure 26.4.12 play an important role in understanding the chemical bond. Figure 26.4.12 is based on second period elements. Do the same quantitative correlations hold for third period elements? Consider NCl as an example. Determine $\tilde{\nu}_e$, the force constant, zero point energy, and bond dissociation energies \tilde{D}_e and \tilde{D}_o , for $^{14}\text{N}^{35}\text{Cl}$ based on the fundamental vibration frequency $\tilde{\nu}_o = 817.358 \text{ cm}^{-1}$ and anharmonicity $\chi_e \tilde{\nu}_e = 5.300 \text{ cm}^{-1}$. Report the bond dissociation energies in cm^{-1} , eV, and kJ mol^{-1} . How well do the force constant and bond dissociation energy of NCl agree with the bond order-bond strength correlation in Figure 26.4.12?

20. Determine $\tilde{\nu}_e$, the force constant, anharmonicity, zero point energy, and the bond dissociation energies \tilde{D}_e and \tilde{D}_o , for H_2 . The fundamental and overtones for H_2 are listed below.

ν	1	2	3	4	5	6	7	8
$\tilde{\nu}_{\nu \leftarrow 0} (\text{cm}^{-1})$	4161.14	8087.11	11782.35	15250.36	18491.92	21505.65	24287.83	26830.97

21. The fundamental and first two overtones in the vibrational spectrum of the OH radical are 3569.8 , 6974.6 , and 10217.8 cm^{-1} , respectively. Determine $\tilde{\nu}_e$, the force constant, anharmonicity, zero point energy, and the bond dissociation energies, \tilde{D}_e and \tilde{D}_o .

22. Calculate the Morse a -parameter for the diatomic molecule Na_2 . The fundamental vibration frequency is $\tilde{\nu}_e = 159.13 \text{ cm}^{-1}$ and the dissociation energy from the bottom of the potential energy well is $\tilde{D}_e = 5886.54 \text{ cm}^{-1}$. The most useful final units for a are \AA^{-1} . [Hint: the units of $(\mu/(2D_e))^{1/2}$ are (s m^{-1}) , so you will need to convert to \AA^{-1} using $1 \text{ \AA} = 1 \times 10^{-10} \text{ m}$. Typical values of a are in the range of $\sim 0.5\text{-}3 \text{ \AA}^{-1}$.]

23. Calculate the Morse a -parameter for H^{35}Cl in \AA^{-1} . The fundamental vibration frequency is $\tilde{\nu}_e = 2990.925 \text{ cm}^{-1}$ and the dissociation energy from the bottom of the potential energy well is $\tilde{D}_e = 37270. \text{ cm}^{-1}$. [Hint: The conversion $1 \text{ cm}^{-1} = 11.96266 \text{ J mol}^{-1}$ is handy. The units of $(\mu/(2D_e))^{1/2}$ are (s m^{-1}) , so you will need to convert to \AA^{-1} using $1 \text{ \AA} = 1 \times 10^{-10} \text{ m}$. Typical values of a are in the range of $\sim 0.5\text{-}3 \text{ \AA}^{-1}$.]

24. Plot the vibrational potential energy function for Na₂. Assume a Morse potential function. The dissociation energy from the bottom of the potential energy well is $\tilde{D}_e = 5886.54 \text{ cm}^{-1}$, the Morse a -parameter is $a = 0.8563 \text{ \AA}^{-1}$, and the equilibrium bond length is $R_e = 3.079 \text{ \AA}$. [See Problem 22 for the calculation of a .]

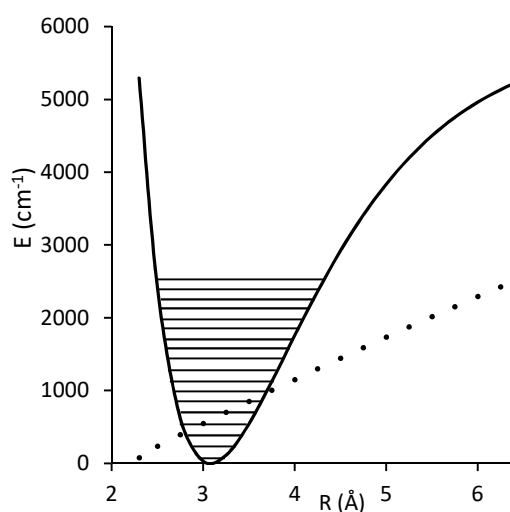
25. Plot the Morse and harmonic vibrational potential energy functions for H³⁵Cl. Assume the fundamental vibration frequency $\tilde{\nu}_e = 2990.9 \text{ cm}^{-1}$, dissociation energy from the bottom of the potential energy well is $\tilde{D}_e = 37270 \text{ cm}^{-1}$, the Morse a -parameter is $a = 1.867 \text{ \AA}^{-1}$, and the equilibrium bond length is $R_e = 1.275 \text{ \AA}$. [See Problem 23 for the calculation of a .]

26. Plot the Morse potential energy function for ⁷LiH. See Table 27.6.1 for the spectroscopic constants. Superimpose on the potential energy surface the 15 lowest vibrational energy levels, including the effects of anharmonicity. [Hints: See Problem 22 for hints on calculating the Morse a -parameter. A few rows of an example spreadsheet for Na₂ are given below. The calculation of the Morse potential, rows B and C, is independent of the calculation of the vibrational energy levels, rows D and E. However, you can use the R values as a dummy variable to superimpose the vibrational energy levels on top of the potential energy curve. In other words, use columns B, C, and E to construct your scatter plot. Join the potential energy data points with a curve, but leave the vibrational levels as dots. The horizontal position of the vibrational level data points will be meaningless, but the vertical position gives the vibrational energies. You can draw in the horizontal lines representing the vibrational levels by hand.]

For Na₂:

A1	B	C	D	E
2	reduced mass	μ	11.495	g mol^{-1}
3	vibration freq.	ν_e	159.125	cm^{-1}
4	anharmonicity	$\nu_e \chi_e$	0.725	cm^{-1}
5	bond length	R_e	3.079	\AA
6	dissociation E	D_o	0.720	eV
7	dissociation E	D_e	5887	cm^{-1}
8	Morse a	a	0.856	\AA^{-1}
9				
10	$R (\text{\AA})$	$V(R) \text{ cm}^{-1}$	ν	$G(\nu) \text{ cm}^{-1}$
11	2.3	5293.9	0	79.4
12	2.5	2423.6	1	237.1
13	2.75	622.8	2	393.3
14	3	28.7	3	548.0
15	3.25	109.4	4	701.4
16	3.5	539.6	5	853.2
17	3.75	1124.8	6	1003.7
18	4	1752.3	7	1152.6
19	4.25	2360.0	8	1300.1
20	4.5	2916.4	9	1446.2

Na₂



27. The overtone wave numbers are given directly by Eq. 27.5.8 for the transition $\nu' \leftarrow 0$:

$$\begin{aligned}
 \tilde{\nu}_{\nu' \leftarrow 0} &= \tilde{G}_{\nu'} - \tilde{G}_0 = \tilde{\nu}_e(\nu' + \frac{1}{2}) - \chi_e \tilde{\nu}_e(\nu' + \frac{1}{2})^2 - \tilde{\nu}_e(0 + \frac{1}{2}) + \chi_e \tilde{\nu}_e(0 + \frac{1}{2})^2 \\
 &= \tilde{\nu}_e \nu' - \chi_e \tilde{\nu}_e(\nu'^2 + \nu' + \frac{1}{4}) + \frac{1}{4} \chi_e \tilde{\nu}_e \\
 &= -\chi_e \tilde{\nu}_e \nu'^2 + (\tilde{\nu}_e - \chi_e \tilde{\nu}_e) \nu' \quad (\text{Morse, } \nu': \text{upper})
 \end{aligned}$$

Rather than plotting adjacent differences in a Birge-Sponer plot, this last equation can be used in least squares curve fitting. The result is essentially equivalent, but the process and the associated

uncertainties are more direct. Use the data in Example 27.5.1 and a quadratic fit to determine $\tilde{\nu}_e$ and $\chi_e\tilde{\nu}_e$ for H^{35}Cl . Compare to the results in the example.

28. Often only the fundamental and first overtone vibration frequencies are observable in infrared spectra. The experimental values for the fundamental and the first overtone are sufficient to obtain a rough estimate of the anharmonicity and the bond dissociation energy. We can use H^{35}Cl as a good test case. Determine $\tilde{\nu}_e$, the force constant, anharmonicity, zero point energy, and the bond dissociation energies \tilde{D}_e and \tilde{D}_0 , for H^{35}Cl . The fundamental and first overtone for H^{35}Cl are 2885.98 and 5667.98 cm^{-1} .

29. A schematic rotational-vibrational absorption spectrum of a diatomic molecule is shown below. The bond length is assumed to be the same in the two vibrational states. Sketch the resulting spectrum if, in the absence of any other changes, (a) the bond length of both vibrational states is increased, (b) the bond force constant is increased, (c) the temperature is increased, and (d) the bond length of just the upper vibrational state is increased.



30. Write a spreadsheet to simulate the rotational-vibrational infrared spectrum of ^{12}CH for the $1 \leftarrow 0$ fundamental vibrational transition at 25°C . Use the spectroscopic constants in Table 27.6.1. Include six R-branch and six P-branch transitions. The relative intensity of the transitions is proportional to the Boltzmann weighting factors of the initial rotational levels for the $\nu = 0$ vibrational state: $p(J'') \propto (2J'' + 1) e^{-B'' J''(J''+1)/kT}$. To emphasize the differences caused by $\tilde{B}' < \tilde{B}''$, compare the appearance for α_e equal to zero, the literature value, and three times the literature value. [Hints: Display your results as an unconnected scatter plot of relative intensity, $p(J'')$, versus the transition wave number. You won't get a "stick" spectrum as in the previous problem, but you can draw lines by hand from each data point to the horizontal axis to sketch the spectrum. Remember that $kT = 207.2 \text{ cm}^{-1}$ at 25°C .]

31. The experimental fundamental vibration frequencies in infrared absorption for N_2O are 2224 cm^{-1} , 1285 cm^{-1} , and 588 cm^{-1} . Assuming N_2O is linear, determine if the bonding configuration is NNO or NON.

32. The experimental fundamental vibration frequencies in infrared absorption for BCl_3 are 985 cm^{-1} , 462 cm^{-1} , and 243 cm^{-1} . The experimental Raman frequencies are 985 cm^{-1} , 471 cm^{-1} , and 243 cm^{-1} . With reference to Table 27.7.1, determine if BCl_3 is planar or trigonal pyramidal. Assign the observed frequencies to the distinct frequencies, $\nu_1 - \nu_4$.^{4,5}

33. The carbonyl stretch for ketones is active in both IR and Raman spectroscopy. Assume a carbonyl stretch occurs at $1800. \text{ cm}^{-1}$. Calculate the wave lengths of the Stokes and anti-Stokes transitions in the Raman spectrum assuming laser excitation using a helium-neon laser at 632.8 nm .

34. Name three advantages of Raman spectroscopy over infrared absorption. Name a disadvantage.

35. Identifying the point group of a molecule is done using Table 27.8.1 or using a flow chart such as Figure P27.1.

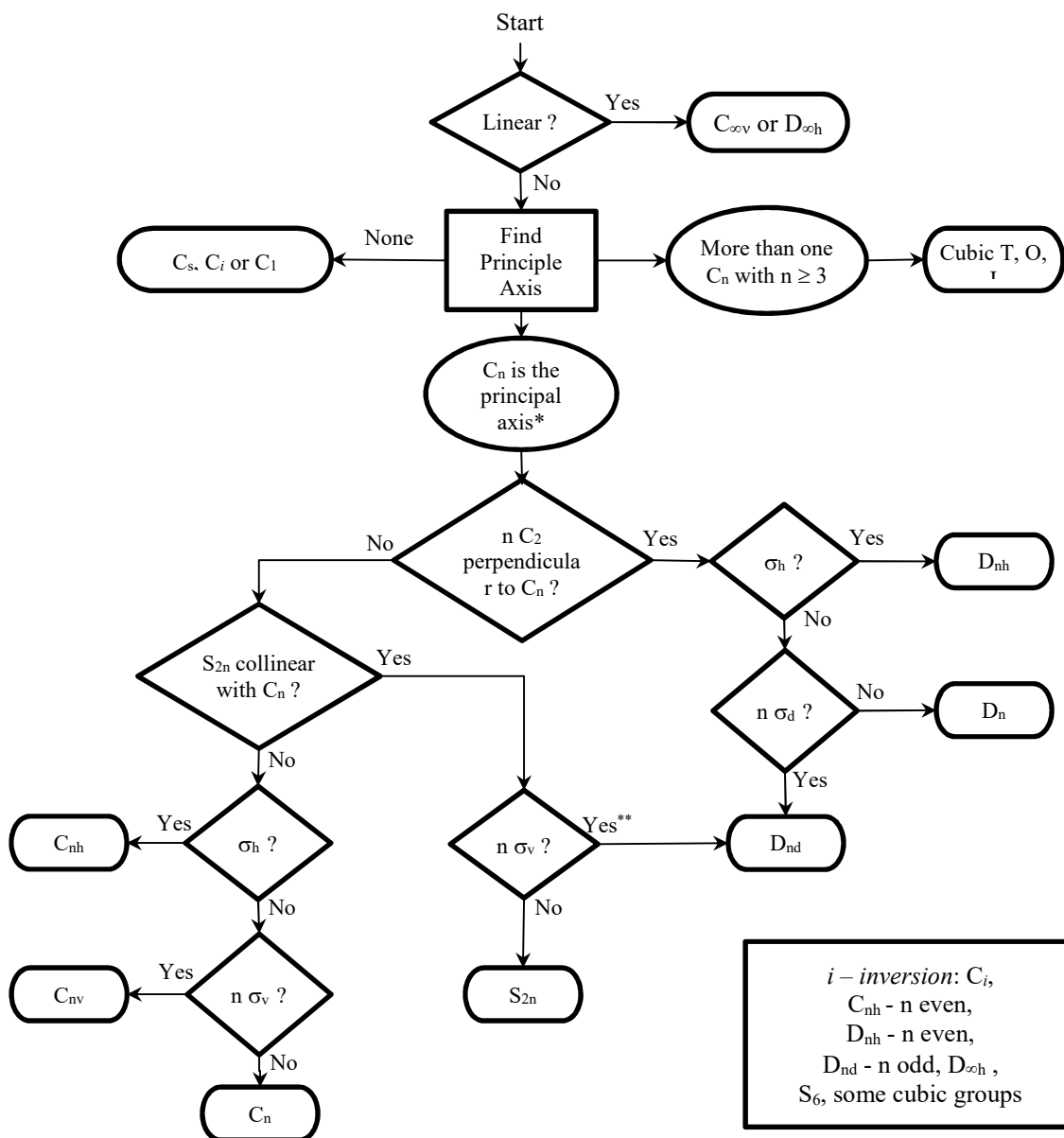


Figure P27. 1: Flow chart to identify the point group of a molecule. * If there are three mutually perpendicular axes, choose the principal axis perpendicular to the axis that passes through the most atoms or the heaviest atoms. ** There are n perpendicular C_2 axes, but they may not be obvious.⁶

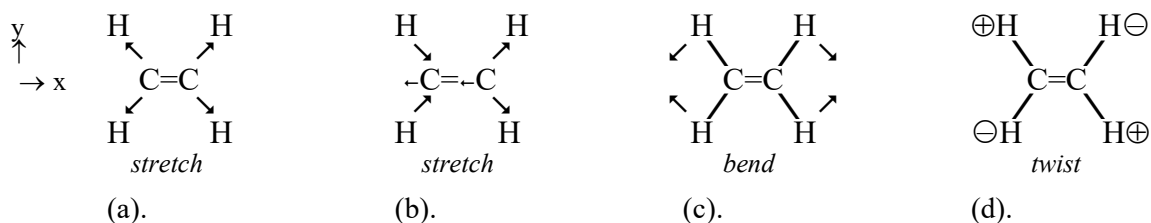
Determine the point group for the following species: (a) SO_2 ; (b) CO_3^{2-} ; (c) C_2H_4 , ethylene; (d) *trans*-1,2- $\text{C}_2\text{H}_2\text{Cl}_2$, *trans*-1,2-dichloroethylene; (e) *cis*-1,2- $\text{C}_2\text{H}_2\text{Cl}_2$, *cis*-1,2-dichloroethylene; (f) ClF_3 (T-shaped); (g) NH_3 ; and (h) C_2H_6 , staggered ethane.

36. Determine the point group for the following species: (a) PtCl_4^{2-} (square planar); (b) PF_5 (trigonal bipyramidal).

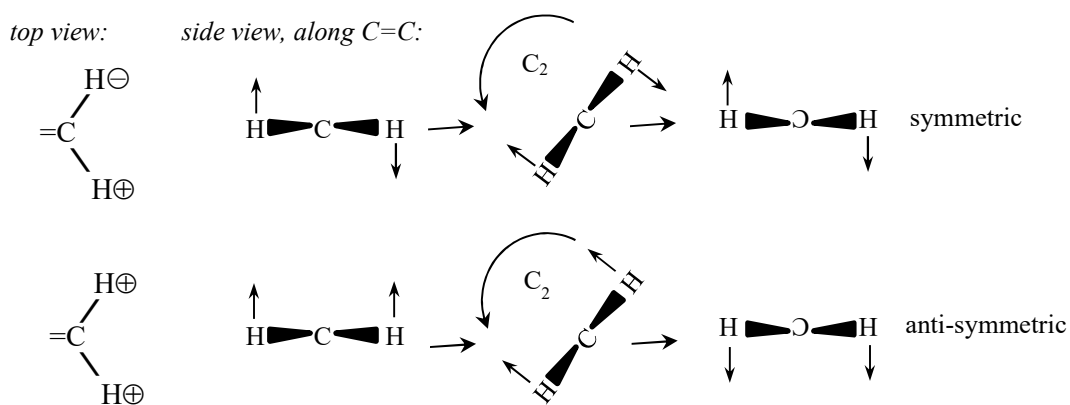
37. Determine the irreducible representations for the x, y, and z-components of the transition electric dipole moment in the point group whose character table is given below. The symmetry operations are three mutually perpendicular C_2 -axes, which are aligned along the x, y, and z-axes.

	E	$C_2(z)$	$C_2(y)$	$C_2(x)$
A	1	1	1	1
B_1	1	1	-1	-1
B_2	1	-1	1	-1
B_3	1	-1	-1	1

38. (a). Determine the symmetry species, which is the irreducible representation, of the following normal modes of ethylene, C_2H_4 . (b). Determine the IR and Raman activity of each mode.



The transformation properties of out-of-plane motions might require some clarification. The progress of the $C_2(x)$ rotation, viewed from the top and along the $\text{C}=\text{C}$ bond is shown below.



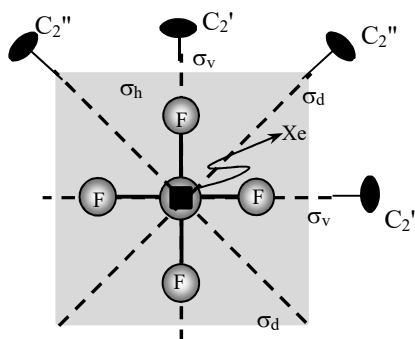
39. (a). Use group theory to determine the symmetry species of the normal modes of H_2O , using the corresponding approach to the all-mode vibrational analysis in Figure 27.8.10. The symmetry species are the irreducible representations of the normal modes. (b). Determine which irreducible representations correspond to stretches and which to bending vibrations. (c). Determine the modes that are IR and Raman active.

40. Use group theory to determine the symmetry species of the normal modes of BF_3 , using the corresponding approach to the all-mode vibrational analysis in Figure 27.8.10. The symmetry species are the irreducible representations of the normal modes. Determine which irreducible

representations correspond to stretches and which to bending vibrations. [Hint: for determining the symmetry of a trigonal planar molecule, the S_3 improper rotations act just like C_3 proper rotations, since all atoms lie in the σ_h -plane.]

41. (a). Use group theory to determine the symmetry species of the normal modes of T-shaped ClF_3 , using the corresponding approach to the all-mode vibrational analysis in Figure 27.8.10. The symmetry species are the irreducible representations of the normal modes. (b). Determine which irreducible representations correspond to stretches and which to bending vibrations. (c). Can the number of IR and Raman active bands distinguish between trigonal-planar and T-shaped geometries for ClF_3 ? [Hint: Use Table 27.7.1 for the symmetry species of a trigonal planar XY_3 molecule.]

42. (a). Use group theory to determine the symmetry species of the normal modes of square-planar XeF_4 , using the corresponding approach to the all-mode vibrational analysis in Figure 27.8.10. The symmetry species are the irreducible representations of the normal modes. (b). Determine which irreducible representations correspond to stretches and which to bending vibrations. (c). Determine the IR and Raman activity of the modes. The projection of the symmetry operations of the D_{4h} point group upon XeF_4 is shown below. [Hints: There are two C_4 axes, one for clockwise and one for counterclockwise rotation. The C_2 axis is coincident with the C_4 axis, while the C_2' and C_2'' are perpendicular to the C_4 axes. The C_2 axis is required for mathematical completeness and is equivalent to two successive C_4 rotations in the same direction. For determining the symmetry of a square-planar molecule, the S_4 improper rotations act just like C_4 proper rotations, since all atoms lie in the σ_h -plane.]



43. The normal mode vibrations of a square-planar XY_4 molecule transform as $\Gamma_{\text{vib}} = A_{1g} + B_{1g} + B_{2g} + A_{2u} + B_{2u} + 2E_u$. The normal mode vibrations of a tetrahedral XY_4 transform as $\Gamma_{\text{vib}} = A_1 + E + 2T_2$. For molecules such as CH_4 or XeF_4 , are square-planar XY_4 and tetrahedral XY_4 geometries distinguishable on the basis of the number of IR and Raman active modes?

44. *Challenge Problem:* Determine the equilibrium bond length R_e , dissociation energy \tilde{D}_e , Morse a -parameter, fundamental vibration frequency $\tilde{\nu}_e$, and anharmonicity for HF using molecular structure calculations at the CCSD(T)/cc-pVTZ level. Assume the potential energy surface is in the Morse form with Eq. 27.5.7 giving the fundamental vibration frequency and Eq. 27.5.19 giving the anharmonicity. Calculate the dissociation energy, \tilde{D}_e , using separate calculations of the atomic energies of H- and F-atoms. Compare the theoretical spectroscopic constants with experimental literature values. [Hint: you will need to do calculations for HF at

the geometry optimized bond length and two other values of the internuclear separation, use $R_e - 0.10 \text{ \AA}$ and $R_e + 0.15 \text{ \AA}$. Then fit your three data points to a Morse potential in a spreadsheet.]

45. Determine if the following statements are true or false. If the statement is false, describe the changes that are necessary to make the statement true, if possible. If the statement is true but too restrictive, give the more general statement.

- Doppler line broadening for UV transitions is greater than for microwave transitions.
- As molecules increase in size, rotational constants decrease.
- The wave number for vibrational transitions increases with temperature.
- In Raman scattering, the anti-Stokes lines are more intense than the Stokes lines.
- Two states with the same energy always mix and transitions to the two states can share intensity even if otherwise forbidden.

46. The “ABC Rotational Constant Calculator” applet determines the moments of inertia, spectroscopic rotational constants, symmetry point group, and the contributions of rotation to the entropy and Gibbs energy of a molecule. The applet is available on the textbook Web site or on the companion CD. Extensive collections of molecular coordinates are available on-line and from molecular mechanics or electronic structure calculations. While many electronic structure packages determine the point group of an input molecule, the “ABC” applet has an adjustable tolerance that allows the point group to be determined in cases where other programs fail. Use the following coordinates to determine the point group and rotational constants for ethane:

```

8
ethane
C      -0.7704  0.0003 -0.0010
C      0.7707  -0.0002 -0.0001
H     -1.1734  1.0280 -0.0004
H     -1.1725  -0.5129 -0.8919
H     -1.1740  -0.5148  0.8883
H      1.1736  -1.0279 -0.0013
H      1.1742  0.5154 -0.8891
H      1.1728  0.5124  0.8911

```

The input file is in xyz-format. The first line is the atom count. The second line is a comment. The subsequent lines list the atom and the coordinates.

47. Bending vibrations are characterized as one of four basic types of movements, Figure P27.2.

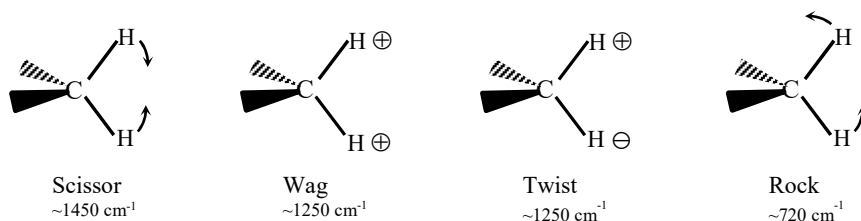


Figure P27.2: Bending vibrations of methylene. Typical frequencies for small hydrocarbons of normal modes dominated by the given type of bend are given.

Determine the normal modes of formaldehyde using an electronic structure calculation at the HF/6-31G* level (or equivalently HF/6-31G(d)). Display the “raw” numerical output files to find the symmetry designations. The experimental frequencies are given in Table P27.1.⁷

Formaldehyde has C_{2v} symmetry, the symmetry properties for which are given in Figure 26.6.4. The totally symmetric group, a_1 , contains the most symmetrical vibrations. The b_1 and b_2 -groups are less symmetrical in the atom movements, b_1 is symmetrical with respect to reflection across the vertical plane that runs through the C=O bond. The b_1 and b_2 designations may be switched in the calculation listing; some authors switch the symmetry labels. Compare the calculated and experimental frequencies, Table P27.1. Animate the normal modes to help compare the modes. Frequencies from *ab initio* calculations are normally multiplied by 0.9 to compare with experimental frequencies. This factor adjusts for anharmonicity. Multiply your frequencies by 0.9; does the scaling improve the agreement with the experimental values?

Table P27.1. Experimental Frequencies for the Normal Modes of Formaldehyde.⁷

Symmetry of mode	Type of mode	Frequency (cm^{-1})
a_1	CH ₂ symmetric stretch	2783 strong
	CO stretch	1746 very strong
	CH ₂ scissor	1500 strong
b_1	CH ₂ wag	1167 strong
b_2	CH ₂ asymmetric stretch	2843 very strong
	CH ₂ rock	1249 strong

48. The selection rule $\Delta v = \pm 1$ for harmonic vibrations can also be motivated by using the odd or even symmetry of the integrand in the transition dipole moment integrals, Eqs. 27.9.13. Note that the harmonic oscillator wave functions alternate between even or odd for increasing v , Table 24.1.1 and Figure 24.2.3b. (a). Assume v'' for the lower level is even, use the overall even/odd symmetry of the integrand to note if the transition dipole vanishes for $\Delta v = -2, -1, 0, +1, +2$. (b). Assume v'' for the lower level is odd, use the overall even/odd symmetry of the integrand to note if the transition dipole vanishes for $\Delta v = -2, -1, 0, +1, +2$.

49. *Time Dependent Perturbation Theory*: The next two problems derive the transition probability upon light absorption. A system in an eigenstate of the time independent Hamiltonian, \mathcal{H}^0 , with eigenfunction Ψ_k^0 and energy E_k is given by the solution of the time independent Schrödinger equation:

$$\mathcal{H}^0 \Psi_k^0 = E_k \Psi_k^0 \quad \text{P27.49.1}$$

Using Eq. 23.7.22, the full spatial and time dependent Schrödinger equation for the stationary state of the system is:

$$\mathcal{H}^0 \Psi_k^0(t) = i\hbar \frac{\partial \Psi_k^0(t)}{\partial t} \quad \text{with} \quad \Psi_k^0(t) = \Psi_k^0 e^{-iE_k t/\hbar} \quad \text{P27.49.2}$$

A time dependent perturbation $\mathcal{H}'(t)$ is applied to the system. For example, the time dependent perturbation is often caused by the oscillating electric field of light $E_x(t) = E_x^\circ \cos 2\pi\nu t$, where E_x° is the amplitude of the electric field of the incident light in the x-direction. The time evolution of the system with the perturbation present is also given by Eq. 23.7.22, which in terms of the unperturbed and perturbation Hamiltonians is:

$$\mathcal{H}^\circ \Psi(t) + \mathcal{H}'(t) \Psi(t) = i\hbar \frac{\partial \Psi(t)}{\partial t} \quad \text{P27.49.3}$$

If the perturbation is small compared to \mathcal{H}° , the resulting time dependent wave function, $\Psi(t)$, is a linear combination of the time independent, unperturbed wave functions: ⁸

$$\Psi(t) = \sum a_k(t) \Psi_k^\circ(t) \quad \text{P27.49.4}$$

where the time dependent coefficients $a_k(t)$ determine the time evolution of the system among the unperturbed eigenstates. These coefficients are only functions of time. The sum extends over all eigenstates of the unperturbed Hamiltonian. The probability of the system being found in eigenstate-n after the perturbation is $a_n^*(t) a_n(t)$.

(a). Consider a single proton in an applied magnetic field. How many eigenstates are available? Assume the spin starts in the lowest energy eigenstate at $t = 0$ and then an rf-field is applied for a sufficient time, t , that the spin is transferred to the highest energy state. Give the wave function coefficients in Eq. P27.49.4 at $t = 0$ and at time t .

(b). Show that substitution of Eq. P27.49.4 into Eq. P27.49.3 gives [Hint: Use Eq. P27.49.2]: ⁸

$$\sum a_k(t) \mathcal{H}'(t) \Psi_k^\circ = i\hbar \sum \frac{da_k(t)}{dt} \Psi_k^\circ(t) \quad \text{P27.49.5}$$

(c). Multiply both sides of Eq. P27.49.5 by $\Psi_n^\circ(t)$ and integrate over all spatial coordinates. Note that by orthogonality, $\int \Psi_n^{\circ*}(t) \Psi_k^\circ(t) d\tau = 0$ if $n \neq k$. Show that the result is: ⁸

$$\frac{da_n(t)}{dt} = \frac{1}{i\hbar} \sum a_k(t) \int \Psi_n^{\circ*}(t) \mathcal{H}'(t) \Psi_k^\circ(t) d\tau \quad \text{P27.49.6}$$

(d). Consider the transition from eigenstate-m to eigenstate-n. Derive the differential equation for the coefficient of eigenstate-n, $da_n(t)/dt$. Correspondingly, assume that at time $t = 0$ the system is in the eigenstate-m. Note that according to Eq. P27.49.2, $\Psi_k^\circ(t) = \Psi_k^\circ e^{-iE_k t/\hbar}$ with $k = n$ or m . For convenience define the **interaction integral**:

$$H_{nm} \equiv \int \Psi_n^{\circ*} \mathcal{H}'(t) \Psi_m^\circ d\tau \quad \text{P27.49.7}$$

where Ψ_n° and Ψ_m° are the time independent wave functions. For a short time after $t = 0$, all the terms in the sum in Eq. P27.49.6 may be neglected except for $a_m(t)$, which is approximately 1. Noting that the integral is over only the spatial coordinates, show that the result is: ⁸

$$\frac{da_n(t)}{dt} = -\frac{2\pi i}{\hbar} H_{nm}' e^{i(E_n - E_m)t/\hbar} \quad (\text{t short, m initial}) \quad \text{P27.49.8}$$

The probability of the system being found in eigenstate-n after the perturbation is $a_n^* a_n$ with the coefficients evaluated at time t .

50. Time Dependent Perturbation Theory: Absorption of Light: Determine the transition probability upon light absorption, based on Eq. P27.49.8. Consider the time dependent perturbation of a molecule, initially in eigenstate- m , by the oscillating electric field of light, $E_x(t) = E_x^0 \cos 2\pi\nu t$. The interaction between light and the molecule is given by the perturbation Hamiltonian:⁸

$$\mathcal{H}'(t) = -E_x(t)\mu_x \quad \text{P27.50.1}$$

where μ_x is the instantaneous dipole moment of the molecule in the x -direction, Eq. 27.1.5:

$$\mu_x = -\sum_{i=1}^n e x_i \quad \text{P27.50.2}$$

with the sum taken over the x -coordinates of each of the n -electrons. Correspondingly the interaction integral in Eq. P27.49.8 is then over all x . The corresponding expectation value of the **transition dipole moment** between the m^{th} and n^{th} quantum state is then:

$$\langle \mu_x \rangle_{nm} = \int \Psi_n^{0*} \mu_x \Psi_m^0 dx \quad \text{P27.50.3}$$

(a). Show that the interaction integral is given as: $H'_{nm} = -E_x(t) \langle \mu_x \rangle_{nm}$, using the definition in Eq. P27.49.7 and Eq. P27.50.2.

(b). Show that the oscillating electric field of the light can be expressed using the Euler formula as: $E_x(t) = E_x^0 \cos 2\pi\nu t = E_x^0 (e^{2\pi i\nu t} + e^{-2\pi i\nu t})/2$.

(c). Using Eq. P27.49.8 and the results of (a) and (b), show that:⁸

$$\frac{da_n(t)}{dt} = -\frac{\pi i}{h} E_x^0 \langle \mu_x \rangle_{nm} [e^{2\pi i(E_n - E_m + h\nu)t/h} + e^{2\pi i(E_n - E_m - h\nu)t/h}] \quad \text{P27.50.4}$$

(d). Eq. P27.50.4 looks scary but notice that after combining all the constants the right-side of the equation is in the form: $a(e^{bt} + e^{ct})$, with a , b , and c as constants. Eq. P27.50.4 assumes that the initial state is purely eigenstate- m , so that $a_n(0) = 0$. Separate variables in the time and integrate to show that:⁸

$$a_n(t) = \frac{1}{2} E_x^0 \langle \mu_x \rangle_{nm} \left[\frac{1 - e^{2\pi i(E_n - E_m + h\nu)t/h}}{E_n - E_m + h\nu} + \frac{1 - e^{2\pi i(E_n - E_m - h\nu)t/h}}{E_n - E_m - h\nu} \right] \quad \text{P27.50.5}$$

(e). For an absorption transition, $E_n > E_m$, and the frequency of the light must match the energy level difference between the two states, $\Delta E = E_n - E_m \cong h\nu$. Show that for an absorption transition, with the light frequency near the transition maximum that Eq. P27.50.5 reduces to:⁸

$$a_n(t) = \frac{1}{2} E_x^0 \langle \mu_x \rangle_{nm} \frac{1 - e^{2\pi i(E_n - E_m - h\nu)t/h}}{E_n - E_m - h\nu} \quad (\text{short } t, \text{absorption}) \quad \text{P27.50.6}$$

(f). Using Eq. P27.50.6, show that the probability that the state has changed to eigenstate- n is:⁸

$$a_n^*(t) a_n(t) = E_x^{\circ 2} \langle \mu_x \rangle_{nm}^2 \frac{\sin^2 \pi(E_n - E_m - h\nu)t/h}{(E_n - E_m - h\nu)^2} \quad (\text{short } t, \text{absorption}) \quad \text{P27.50.7}$$

Note the trigonometric identities: $\cos x = (e^{ix} + e^{-ix})/2$ and $\sin^2 x/2 = 1/2 - 1/2 \cos x$

(g). Eq. P27.50.7 is the transition probability from initial eigenstate-m to eigenstate-n for light absorption at a single frequency. Typical experiments use a range of frequencies instead of a narrowly monochromatic excitation source. Assume that the excitation bandwidth is broader than the transition width. Correspondingly, integrate Eq. P27.50.7 over a continuous range of frequencies. Because the integrand has a significant value only when the denominator is small, the integration limits can correspondingly be extended to ν ranging from $-\infty$ to $+\infty$. Show that the result is:⁸

$$a_n^*(t) a_n(t) = \frac{\pi^2}{h^2} E_x^{\circ 2} \langle \mu_x \rangle_{nm}^2 t \quad (\text{short } t, \text{absorption}) \quad \text{P27.50.8}$$

Comment on the nature of the time dependence. Note the standard integral: $\int_{-\infty}^{\infty} \frac{\sin^2 x}{x^2} dx = \pi$

Literature Cited:

1. Computational Chemistry Comparison and Benchmark Database, National Institute Of Standards and Technology, *NIST Standard Reference Database 101*, **2013**, <http://cccbdb.nist.gov/>, Table II.A.1.(XV.A.).
2. K. S. Pitzer, *Quantum Chemistry*, Prentice-Hall, Englewood Cliffs, NJ, 1953. Section 9c.
3. B. deB. Darwent, "Bond Dissociation Energies in Simple Molecules," *Nat. Stand. Ref. Data Ser.*, NSRDS-NBS 31, Washington, DC, 1970.
4. G. Herzberg, *Molecular Spectra and Molecular Structure, v. 2, Infrared and Raman Spectra of Polyatomic Molecules*, Van Nostrand, Toronto, Canada, 1945. p. 178
5. D. C. Harris, *Symmetry and Spectroscopy: An Introduction to Vibrational and Electronic Spectroscopy*, Oxford, New York, NY, 1978. pp. 147, 159
6. J. Noggle, "Flow Chart for Identification of Schoenflies Point Groups," and also: D. Quane, "Systematic Procedures for the Classification of Molecules into Point Groups: The Problem of the D_{nd} Group," *J. Chem. Ed.*, **1976**, 53, 178.
7. W. J. Hehre, L. D. Burke, A. J. Shusterman, *A PC Spartan Pro Tutorial*, Wavefunction, Inc., Irvine, CA., 1999, pp. 23-24.
- 8 K. S. Pitzer, *Quantum Chemistry*, Prentice-Hall, Englewood Cliffs, NJ, 1953. Chap. 6, pp. 90-99.